"COMPARISON BETWEEN LOW-DOSE AND STANDARD-DOSE COMPUTED TOMOGRAPHY FOR DIAGNOSIS OF UROLITHIASIS"

By

Dr. SHIVAPRASAD GANGADHAR SAVAGAVE

DISSERTATION SUBMITTED TO SRI DEVARAJ URS ACADEMY OF HIGHER EDUCATION AND RESEARCH, KOLAR, KARNATAKA

In partial fulfilment of the requirements for the degree of

DOCTOR OF MEDICINE
IN
RADIODIAGNOSIS

Under the Guidance of

Dr. PURNIMA HEGDE, MD,
PROFESSOR & HOD

DEPARTMENT OF RADIODIAGNOSIS,
SRI DEVARAJ URS MEDICAL COLLEGE,
TAMAKA, KOLAR-563101

MAY 2017

SRI DEVARAJ URS ACADEMY OF HIGHER EDUCATION AND RESEARCH, TAMAKA, KOLAR, KARNATAKA

DECLARATION BY THE CANDIDATE

I hereby declare that this dissertation entitled **"COMPARISON BETWEEN LOW-DOSE AND STANDARD-DOSE COMPUTED TOMOGRAPHY FOR DIAGNOSIS OF UROLITHIASIS"** is a bonafide and genuine research work carried out by me under the guidance of **Dr. PURNIMA HEGDE**, Professor & Head, Department of Radiodiagnosis, Sri Devaraj Urs Medical College, Kolar, in partial fulfilment of University regulation for the award "**M. D. DEGREE IN RADIODIAGNOSIS**", the examination to be held in May 2017 by SDUAHER. This has not been submitted by me previously for the award of any degree or diploma from the university or any other university.

Dr. SHIVAPRASAD GANGADHAR SAVAGAVE
Postgraduate in Radiodiagnosis
Sri Devaraj Urs Medical College
Tamaka, Kolar

Date:

Place: Kolar

SRI DEVARAJ URS ACADEMY OF HIGHER EDUCATION

AND RESEARCH, TAMAKA, KOLAR, KARNATAKA

CERTIFICATE BY THE GUIDE & HOD

This is to certify that the dissertation entitled "**COMPARISON BETWEEN LOW-DOSE AND STANDARD-DOSE COMPUTED TOMOGRAPHY FOR DIAGNOSIS OF UROLITHIASIS"** is a bonafide research work done by **Dr. SHIVAPRASAD GANGADHAR SAVAGAVE,** under my direct guidance and supervision at Sri Devaraj Urs Medical College, Kolar**,** in partial fulfilment of the requirement for the degree of "**M.D. IN RADIODIAGNOSIS"**.

Dr. PURNIMA HEGDE, MD

Professor & HOD

Department Of Radiodiagnosis

Sri Devaraj Urs Medical College

Tamaka, Kolar

Date:

Place: Kolar

SRI DEVARAJ URS ACADEMY OF HIGHER EDUCATION AND RESEARCH, TAMAKA, KOLAR, KARNATAKA

ENDORSEMENT BY THE HEAD OF THE DEPARTMENT AND PRINCIPAL

This is to certify that the dissertation entitled **"COMPARISON BETWEEN LOW-DOSE AND STANDARD-DOSE COMPUTED TOMOGRAPHY FOR DIAGNOSIS OF UROLITHIASIS"** is a bonafide research work done by **Dr. SHIVAPRASAD GANGADHAR SAVAGAVE** under the direct guidance and supervision of **Dr. PURNIMA HEGDE,** Professor & Head, Department of Radiodiagnosis, Sri Devaraj Urs Medical College, Kolar, in partial fulfilment of University regulation for the award "**M.D. DEGREE IN RADIODIAGNOSIS**"**.**

Dr. PURNIMA HEGDE,
Professor & HOD
Department Of Radiodiagnosis,
Sri Devaraj Urs Medical College,
Tamaka, Kolar

Date:
Place: Kolar

Dr. M. L. HARENDRA KUMAR
Principal,
Sri Devaraj Urs Medical College
Tamaka, Kolar

Date:
Place: Kolar

SRI DEVARAJ URS ACADEMY OF HIGHER EDUCATION AND RESEARCH TAMAKA, KOLAR, KARNATAKA

ETHICAL COMMITTEE CERTIFICATE

This is to certify that the Ethical committee of Sri Devaraj Urs Medical College, Tamaka, and Kolar has unanimously approved

Dr. SHIVAPRASAD GANGADHAR SAVAGAVE

Post-Graduate student in the subject of

RADIODIAGNOSIS at Sri Devaraj Urs Medical College, Kolar

to take up the Dissertation work entitled

"COMPARISON BETWEEN LOW-DOSE AND STANDARD-DOSE COMPUTED TOMOGRAPHY FOR DIAGNOSIS OF UROLITHIASIS"

to be submitted to the

SRI DEVARAJ URS ACADEMY OF HIGHER EDUCATION AND RESEARCH, TAMAKA, KOLAR, KARNATAKA,

Member Secretary

Sri Devaraj Urs Medical College,

Kolar–563101

SRI DEVARAJ URS ACADEMY OF HIGHER EDUCATION

AND RESEARCH TAMAKA, KOLAR, KARNATAKA

COPY RIGHT

I hereby declare that Sri Devaraj Urs Academy of Higher Education and Research, Kolar, Karnataka shall have the rights to preserve, use and disseminate this dissertation/thesis in print or electronic format for academic/research purpose.

Dr. SHIVAPRASAD GANGADHAR SAVAGAVE.

Date:

Place: Kolar

ACKNOWLEDGEMENT

I owe debt and gratitude to my parents ***Sri. GANGADHAR C. SAVAGAVE and Prof. Smt PRABHAVATHI G. SAVAGAVE****, along with my sister* ***Miss SHWETASHREE SAVAGAVE*** *for their moral support and constant encouragement during the study.*

With humble gratitude and great respect, I would like to thank my teacher, mentor and guide, ***Dr. PURNIMA HEGDE,*** *Professor and Head, Department of Radiodiagnosis, Sri Devaraj Urs Medical College, Kolar, for her able guidance, constant encouragement, immense help and valuable advices which went a long way in moulding and enabling me to complete this work successfully. Without her initiative and constant encouragement this study would not have been possible. Her vast experience, knowledge, able supervision and valuable advices have served as a constant source of inspiration during the entire course of my study. I would like to express my sincere thanks to* ***Dr. PATTABHIRAMAN V. and Dr. ANIL KUMAR SAKALECHA,*** *Professors, Department of Radiodiagnosis, Sri Devaraj Urs Medical College for their valuable support, guidance and encouragement throughout the study. I would also like to thank* ***Dr. GIRISH H,*** *Department of Urology, Sri Devaraj Urs Medical College for his wholehearted support, constant encouragement and guidance.*

I would like to thank ***Dr. RACHEGOWDA N., Dr. A. NABAKUMAR SINGH, Dr. ASHWATHNARAYANA, Dr. NAVEEN G NAIK, Dr. JAGADISH, Dr. VINAY, Dr. KUKU MARIAM SURESH*** *and* ***Dr. ANIL KUMAR T. R.*** *and all my teachers of Department of Radio diagnosis, Sri Devaraj Urs Medical College and Research Institute, Kolar, for their constant guidance and encouragement during the study period.*

I am extremely grateful to the patients who volunteered to this study, without them this study would just be a dream.

I am thankful to my fellow ***postgraduates, especially Dr. Sujata and Dr. Varun S.****, for having rendered all their co-operation and help to me during my study.*

My sincere thanks to ***Mrs. Veena*** *along with rest of the computer operators.*

I am also thankful to ***Mr. Aleem, Mr. Mateen, Mr. Ravi, Mr. Chandrasekhar,*** *and* ***Mr. Gurumurthy*** *with other* ***technicians*** *of Department of Radiodiagnosis, R.L Jalappa Hospital & Research Centre, Tamaka, Kolar for their help.*

Dr. SHIVAPRASAD GANGADHAR SAVAGAVE

LIST OF ABBREVIATIONS

3D -	*3 dimension*
AAPM	*American Association of Physicists in Medicine*
AEC	*Automated exposure control*
a.k.a	*also known as*
ALARA	*As low as reasonably achievable*
AP	*Anteroposterior*
AUA	*American Urology Association*
BMI -	*Body mass index*
C	*Coulomb*
CR	*Central ray*
COLA -	*Cystine, ornithine, lysine and arginine*
CT	*Computed tomography*
CTA	*Computed tomography angiography*
$CTDI_{vol}$	*Computed tomography dose index volume*
DLP	*Dose length product*
EAU	*European Association of Urology*
EBCT	*Electron beam computed tomography*
FOV	*Field of view*
Gy	*Gray*
HIV	*Human immunodeficiency virus*
HN	*Hydronephrosis*
HU	*Hounsfield Unit*

LIST OF ABBREVIATIONS

HUN	*Hydroureteronephrosis*
IR	*Incident ray*
IVU	*Intravenous urography*
KUB	*Kidney, ureter and bladder*
kVp	*kilo Volt peak*
mAs	*milli Ampere second*
MDCT	*Multidetector computed tomography*
mSv	*milli Sievert*
NCCT	*Non-contrast computed tomography*
PH	*Primary hyperoxaluria*
PET	*Position emission tomography*
PUJ	*Pelviureteric junction*
R	*Röntgen or Roentgen*
RAD	*Radiation absorbed dose*
REM	*Roentgen equivalent*
RTA	*Renal tubular acidosis*
SD	*Standard deviation*
SID	*Source-to-image distance*
STP	*Standard temperature and pressure*
SWL	*Shockwave lithotripsy*
VUJ	*Vesicoureteric junction*

ABSTRACT

Background: Patients who present with renal calculi often undergo multiple imaging studies before, during, and after treatment. Additionally, these patients are at high risk of recurrence, with recurrence rates as high as 75% in 20 years. CT is currently the investigation of choice in the diagnosis of urolithiasis, but is associated with risk of radiation. There is need to use low-dose CT study whenever feasible.

Aims and Objectives: To evaluate the efficacy of low-dose CT when compared with standard-dose CT for detection of urolithiasis, to understand the potential limitations of using low-dose CT when compared with standard-dose CT for detection of urolithiasis and to help formulate appropriate strategies for diagnosis and follow-up of urolithiasis.

Methodology: The study was conducted for a period of 18 months from January 2015 to June 2016. All the patients underwent standard-dose CT before entering the study. The study was conducted in two stages. During the first stage, individuals underwent NCCT scan with standard dose protocol as per current management strategy (130 kVp along with mAs as per CARE Dose 4D). Individuals with CT evidence of urolithiasis were included in the second stage where an additional NCCT with low-dose protocol was performed (110 kVp along with mAs as per CARE Dose 4D). Both the scans were performed in a single scan setting. Two experienced radiologists reviewed the scans. The radiologists were blinded to the type of the scans (130 kVp and 110 kVp) and assessed the studies independently. The number and size of calculi detected by each scan was recorded along with tube current (in mAs) and radiation dose data (in mSv). The data was analyzed and compared in patients of different BMI.

Results: Majority of the patients were in the BMI category of 25 to 30 kg/m^2 (n = 42; 40.4%) and 18 to 25 kg/m^2 (n = 38; 36.5%) followed by BMI category 30-35 kg/m^2 (n = 13; 12.5%) and lastly in BMI category 18 to 25 kg/m^2 (n = 11; 10.6%). A total of 428 calculi were observed in 104 patients. All the calculi detected on standard-dose CT were detected on low-dose CT. The sensitivity of both standard and low dose CT in detection of calculi was excellent. There was a statistically significant reduction (*P*<.0001) in mean effective radiation dose in the low-dose group (4.16 ± 1.47 mSv; mean ± SD) (range: 1.84 to 9.86 mSv) compared with the standard-dose group (6.04 ± 2.11 mSv; mean ± SD) (range: 2.63 to 15.39 mSv) with a mean difference of 1.88 ± 0.69 mSv (mean ± SD) (range: 0.71 to 5.53 mSv). There was an overall non-significant increase (P = .08) in mean mAs delivered by about 8.83 ± 5.48% (mean ± SD) (range: 3.28% to 53.46%) in the low-dose group (141.9 ± 55.95 mAs; mean ± SD) (range: 63 to 310 mAs) compared with the standard-dose group (129.4 ± 47.15 mAs; mean ± SD) (range: 61 to 244 mAs). A reduction in tube potential by about 15.4% resulted in mean reduction in radiation dose by 31.21 ± 3.15% (mean ± SD) (range: 22.45% to 41.4%). The dose reduction was similar across all the subgroups studies, irrespective of the BMI status.

Conclusion: Reduction of tube voltage by 15% significantly reduced radiation dose by approximately 31% in patients undergoing CT for evaluation of urolithiasis, irrespective of their BMI. A combination of reduced tube potential and AEC helps to achieve optimum results for diagnosis of urolithiasis. We strongly support the use of low-dose CT for diagnosis and follow-up of urolithiasis.

TABLE OF CONTENTS

LIST OF TABLES

LIST OF FIGURES

INTRODUCTION

Urolithiasis can be defined as occurrence of calculi in the urinary tract, which include kidneys, ureters, bladder and urethra[1,2]. Patients who present with renal calculi often undergo multiple imaging studies before, during, and after treatment[3]. Additionally, these patients are at high risk of recurrence, with recurrence rates as high as 75% in 20 years[3,4].

Conventional radiography and sonography do not have a high diagnostic yield[5]. Alternatively, excretory urography, although an excellent investigation, is invasive, sometimes painful, and potentially time consuming. It does not have high sensitivity and specificity as compared with computed tomography (CT) scan[5,6]. In comparison, CT has shown high sensitivity of 94-100% and specificity of 97%[4]. However, among its disadvantages, the risk of ionizing radiation is perhaps the most significant.

CT is a major contributor towards medical radiation and barring natural background sources, it is the largest source of radiation to mankind[7,8]. Standard-dose CT for urolithiasis is associated with radiation exposure ranging from 8 to 16 mSv. A significant dose reduction is plausible due to the high contrast difference between majority of urinary tract calculi and the surrounding soft tissues[4].

Various studies have compared the efficacy of low dose CT with standard dose CT for evaluation of urolithiasis. The results from all these studies have shown that low-dose CT is effective for detection of urolithiasis and these studies recommend use of low-dose CT for detection of urolithiasis considering the reduced risk of radiation without affecting specificity and sensitivity as compared with standard-dose CT scan[9,10,11,12,13,14,15,16,17].

However, to our knowledge, there are very few studies conducted in Indian subcontinent comparing standard-dose and low-dose CT. It is therefore necessary to obtain data on usefulness of low-dose CT when compared with standard-dose CT in this population.

Hence, the current study has been planned to assess the efficacy of low-dose CT with standard-dose CT for detection of urolithiasis in Indian population.

AIMS AND OBJECTIVES

The objectives of the study are as follows:

1. To evaluate the efficacy of low-dose CT when compared with standard-dose CT for detection of urolithiasis
2. To understand the potential limitations of using low-dose CT when compared with standard-dose CT for detection of urolithiasis
3. To help formulate appropriate strategies for diagnosis and follow-up of urolithiasis

REVIEW OF LITERATURE

ANATOMY OF URINARY TRACT

Kidneys

The kidneys are associated with excretion of water and metabolic waste products thus playing an important role in maintaining water and electrolyte balance[18,19]. Apart from this the kidneys also have endocrine functions such as production and release of erythropoietin (involved in red blood cell formation), renin (blood pressure control) and 1,25-di-hydroxycholecalciferol (active form of vitamin D involved in calcium metabolism), etc[18].

The kidneys are located posteriorly behind the peritoneum on each side of the vertebral column and are surrounded by adipose tissue (Figure 1). Superiorly they border the upper border of the 12th thoracic vertebra and inferiorly with the third lumbar vertebra. The right kidney is generally situated slightly inferior to the left, due to its relationship to the liver, which is situated superiorly. The left is a little longer and narrower than the right and lies nearer the median plane. The long axis of each kidney is directed anterolaterally and the transverse axis posteromedially, which means that the anterior and posterior aspects described are anterolateral and posteromedial (Figure 2, Figure 3, Figure 4). An appreciation of this orientation is important in percutaneous and endo-urologic renal surgery[18].

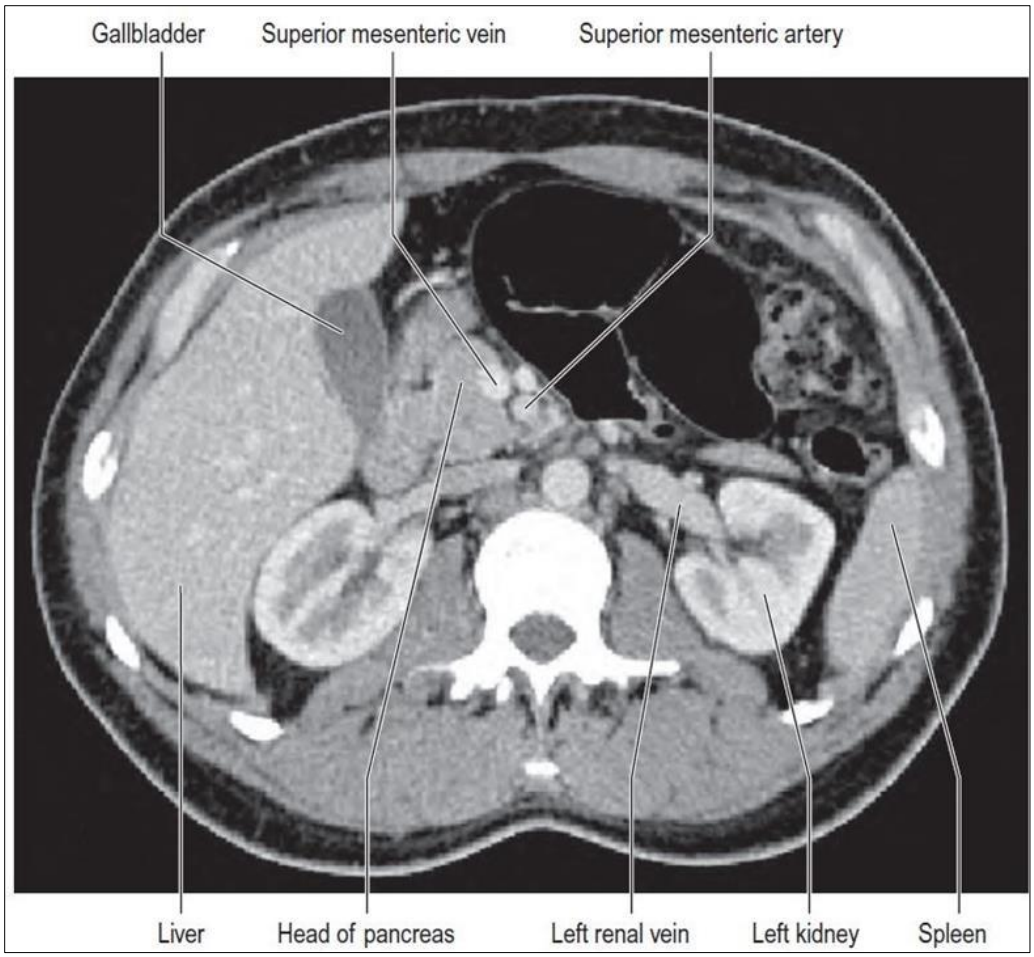

Figure 1. Axial contrast enhanced CT of the kidneys showing anatomical relationships of the kidneys at the renal hilum.

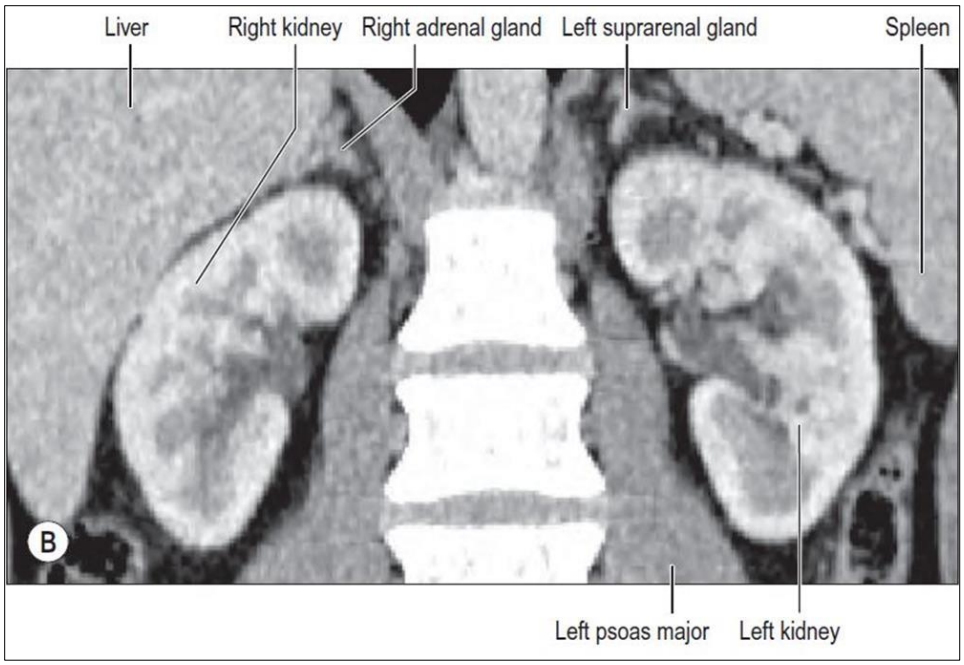

Figure 2. Coronal reformat of contrast enhanced CT showing both kidneys and the suprarenal glands.

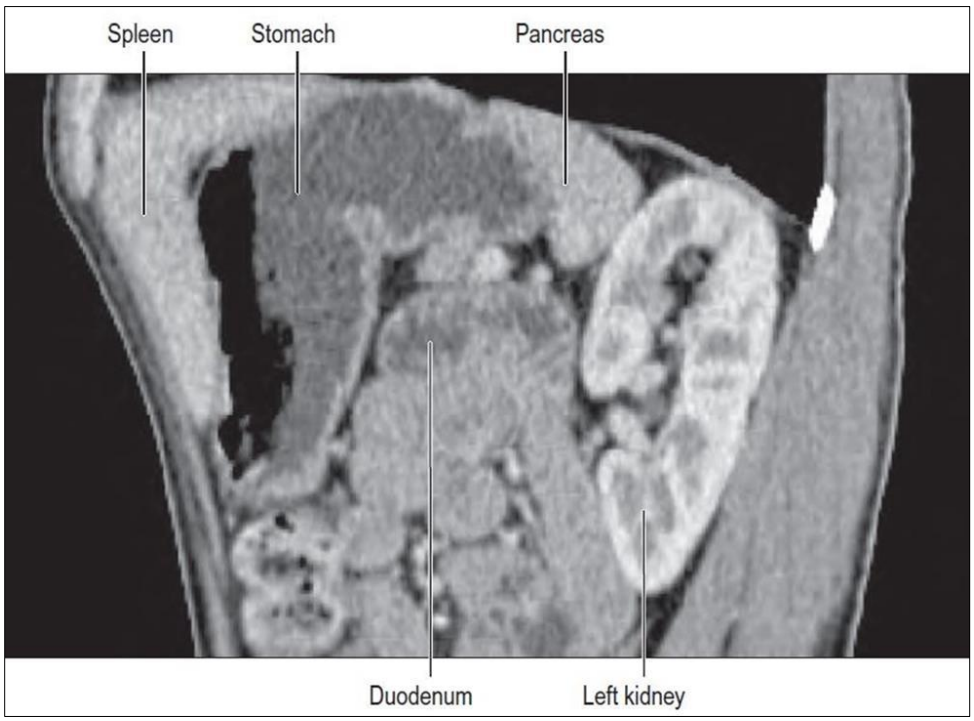

Figure 3. Sagittal reformat of contrast enhanced CT of the left kidney lying posterior to the stomach, spleen and pancreas.

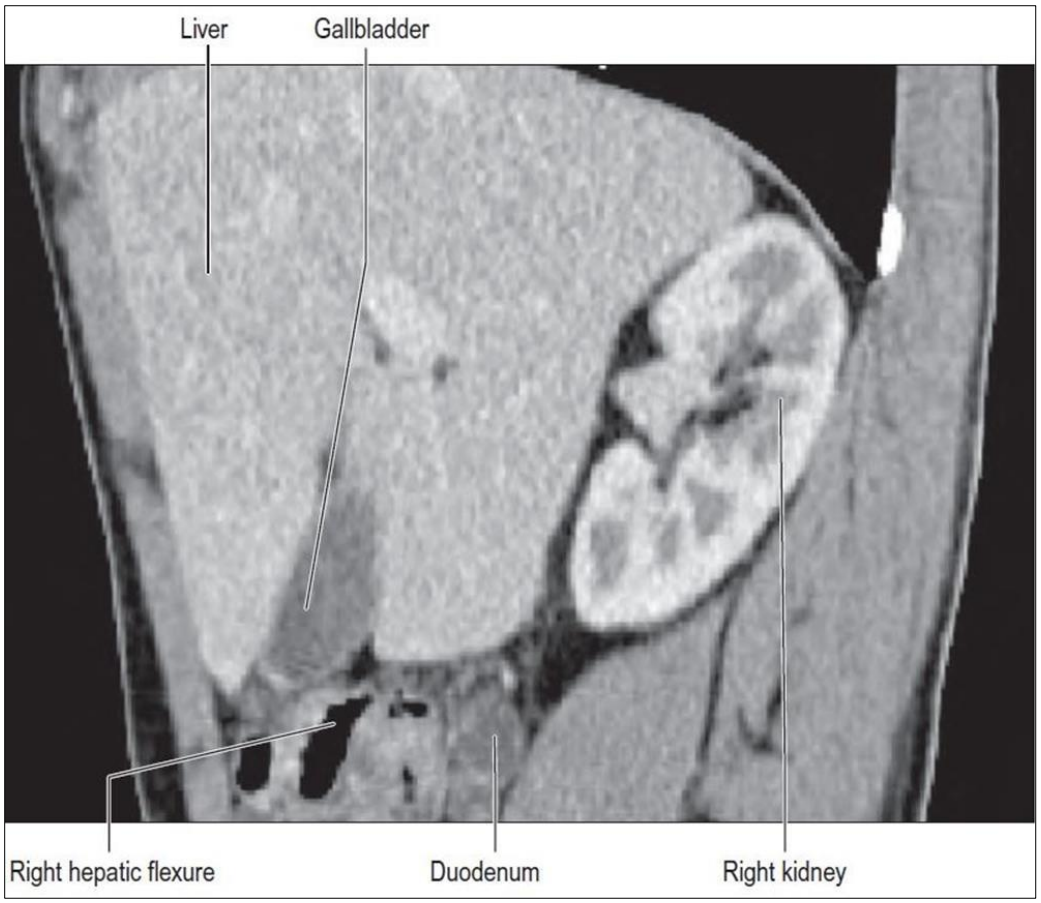

Figure 4. Sagittal reformat of contrast enhanced CT of right kidney lying posterior to the right lobe of liver, hepatic flexure and duodenum.

Each kidney typically measures approximately 11 to 12 cm in length, 6 cm in breadth and 2.5 to 3 cm in anteroposterior (AP) dimension. The left kidney may be about 1.5 cm longer than the right; however, it is rare for the right kidney to be greater than one cm long compared with the left. The average weight is approximately 125-170 g in men and 115-155 g in women[18,20]. It is subdivided into 8–10 lobes, each of which is composed of around one cm thick overlying cortex and a renal pyramid, the apex of which (papilla) opens into a minor calyx (Figure 5)[20]. In thin individuals with a lax abdominal wall the lower pole of the lower right kidney may just be felt in full inspiration by bimanual lumbar examination, however it is uncommon[18].

In the fetus and newborn, the kidney normally has 12 lobules. These lobules get fused in adults and therefore adult kidneys have a smooth surface (although traces of lobulations may remain)[18,20].

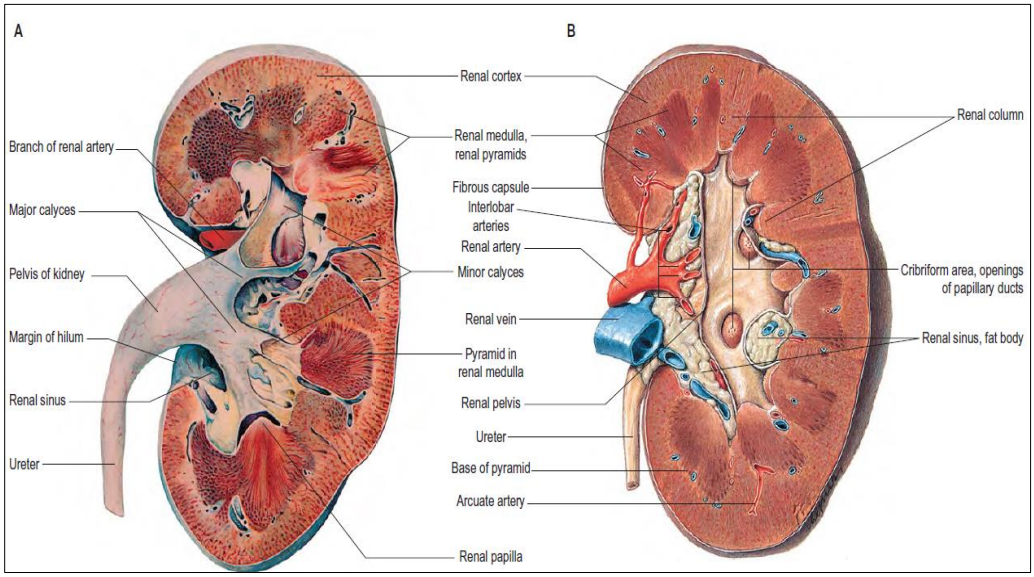

Figure 5.Left kidney, oblique vertical hemisection: normal macroscopic appearance of the renal cortex and renal medulla and the major structures at the hilum of the kidney. (Left) the fat body of the renal sinus and most of the major vessels at the hilum have been removed, and the renal pelvis has not been opened. (Right), the renal pelvis has been opened to reveal the interlobar arteries.

The kidneys are surrounded by a fibrous capsule which demarcates it from surrounding perirenal fat. The cortex forms the outer part of the renal parenchyma surrounding the medulla, which is made up of the renal pyramids arranged around the

renal sinus. Projections of the cortex extend down to the renal sinus between the pyramids; these are called septa (or columns) of Bertin[21].

The renal sinus contains the collecting system, major arteries and veins, all of which are surrounded by renal sinus fat. The tips of the pyramids project into the calyces of the collecting system, and the calyces ultimately coalesce to form the renal pelvis. The renal sinus opens on the medial aspect of the kidney; most of the renal pelvis is usually within the renal sinus but it can project outside the kidney to some extent, producing an extrarenal pelvis[21].

Renal Pelvis and Calyces

The hilum of the kidney leads to central renal sinus, which is lined by the renal capsule and occupied by renal pelvis, vessels, and fat. Understanding the anatomy of this plane is important in surgery on the renal pelvis, particularly open stone surgery. Within the renal sinus, the collecting tubules of the nephrons of the kidney open onto the summits of the renal papillae to drain into minor calyces, which are funnel-shaped expansions of the upper urinary tract. The renal capsule covers the external surface of the kidney and continues through the hilum to line the sinus and fuse with the adventitial coverings of the minor calyces. Each minor calyx surrounds either a single papilla or, more rarely, groups of two or three papillae. The minor calyces unite with their neighbors to form two or possibly three larger chambers, the major calyces[18].

There is wide variation in the arrangement of the calyces. As the posterior aspect of the kidney rotates laterally during its ascent in utero, the calyces are

positioned anteriorly, and the medial calyces move more posteriorly. The calyces drain into the infundibula. The renal pelvis is normally formed from the junction of two infundibula, one from the upper and one from the lower pole calyces, but there may be a third, which drains the calyces in the mid-portion of the kidney. The calyces are usually grouped so that three pairs drain into the upper pole infundibulum and four pairs into the lower pole infundibulum. If there is a middle infundibulum, the distribution is normally three pairs at the upper pole, two in the middle, and two at the lower pole. There is considerable variation in the arrangement of the infundibula and in the extent to which the pelvis is intrarenal or extrarenal. The funnel-shaped renal pelvis tapers as it passes inferomedially, traversing the renal hilum to become continuous with the ureter (Figure 5). It is rarely possible to determine precisely where the renal pelvis ceases and the ureter begins: the region is usually extrahilar and normally lies adjacent to the lower part of the medial border of the kidney. Rarely, the entire renal pelvis has been found to lie inside the sinus of the kidney so that the pelviureteric region occurs either in the vicinity of the renal hilum or completely within the renal sinus[18].

The calyces, renal pelvis and ureter are well-demonstrated radiologically following an intravenous injection of radio-opaque contrast, which is excreted in the urine (as in intravenous urography (IVU) study);or after the introduction of radio-opaque contrast into the ureter by catheterization through a cystoscope (ascending pyelography). Normal cupping of the minor calyces by projecting renal papillae may be obliterated by conditions that cause hydronephrosis, chronic distension of the ureter and renal pelvis due to upper or lower urinary tract obstruction resulting in elevated intrapelvic pressure. An appreciation of the rotation of the kidneys which

results in the posterior calyces lying relatively medially and the anterior calyces lying laterally is essential when interpreting contrast imaging of the collecting system of the kidneys[19].

The wall of the proximal part of the urinary tract is composed of three layers, an outer connective tissue adventitia, an intermediate layer of smooth muscle and an inner mucosa. The mucosal lining of the renal calyces and pelvis is identical in structure to that of the ureter. The adventitia consists of loose fibroelastic connective tissue which merges with retroperitoneal areolar tissue. Proximally the coat fuses with the fibrous capsule of the kidney lining the renal sinus[18].

The smooth muscle of the renal calyces and pelvis is composed of two distinct types of smooth muscle cell. One type of muscle cell is identical to that described for the ureter and can be traced proximally through the pelviureteric region and renal pelvis as far as the minor calyces. The other type of cell forms the muscle coat of each minor calyx and continues into the major calyces and pelvis where it forms a distinct inner layer. The cells also form a thin sheet of muscle which covers each minor calyx and extends across the renal parenchyma between the attachments of neighboring minor calyces, thereby linking each minor calyx to its neighbors. This discrete inner layer of atypical smooth muscle ceases in the pelviureteric region so that the proximal ureter lacks such an inner layer. Pacemaker cells that initiate renal pelvic and ureteric peristalsis are sited within the calyces. These allow coordinated peristalsis of the ureter (frequency of about six times a minute)[18].

Ureters

The ureters are two muscular tubes measuring 25–30 cm in length which transport urine from the kidneys to the urinary bladder through peristaltic contractions. Ureters are thick-walled and narrow and continuous superiorly with renal pelvis. Ureters descend slightly medially, anterior to psoas major, and enter the pelvic cavity where they the initially curve laterally, then medially, to open into the base of the urinary bladder. The diameter of the ureter is normally 3 mm, but is slightly less at its junction with the renal pelvis, at the brim of the lesser pelvis near the medial border of psoas major, and where it runs within the wall of the urinary bladder, which is its narrowest part. These are the commonest sites for renal stone impaction[18].

Relations

In the abdomen ureters descend posterior to the peritoneum on the medial part of psoas major, which separates it from the tips of the lumbar transverse processes. During surgery on intraperitoneal structures, the ureter can be tented up as the peritoneum is drawn anteriorly, resulting in inadvertent ureteric injury. Anterior to psoas major the ureters cross in front of the genitofemoral nerve and are obliquely crossed by the gonadal vessels (Figure 6). The ureters enter the lesser pelvis anterior to either the end of the common iliac vessels or at the origin of the external iliac vessels[18].

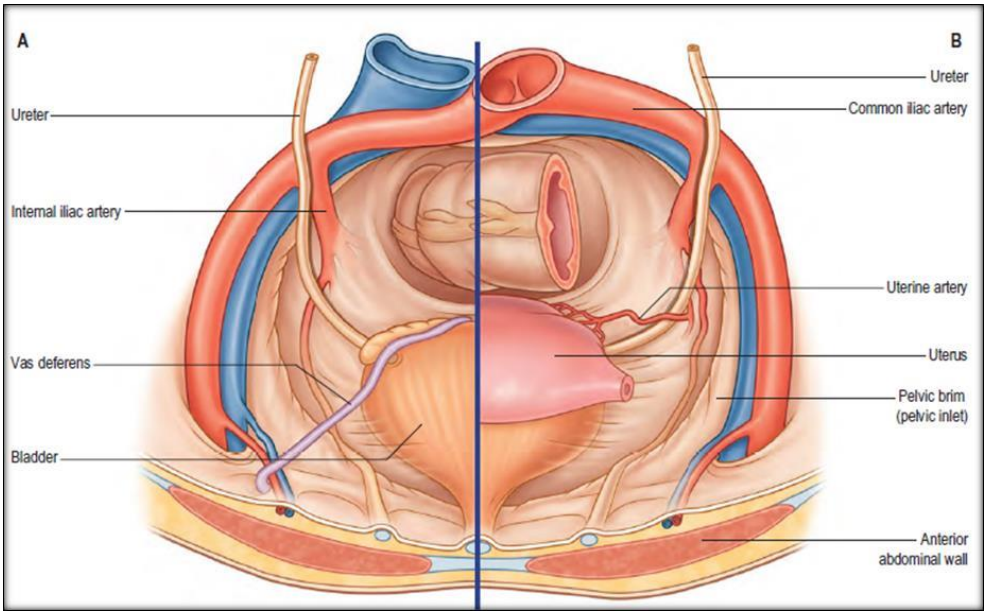

Figure 6.Relations of lower ureter. A. Male pelvis. B. Female pelvis.

The inferior vena cava is medial to the right ureter while the left ureter is lateral to the aorta. The inferior mesenteric vein has a long retroperitoneal course lying close to the medial aspect of the left ureter. The right ureter is usually overlapped by the descending part of the duodenum at its origin. It descends lateral to the inferior vena cava, and is crossed anteriorly by the right colic and ileocolic vessels. Near the superior aperture of the lesser pelvis it passes behind the lower part of the mesentery and terminal ileum[18].

The gonadal and left colic vessels cross the left ureter (Figure 7). The left ureter passes behind jejunal loops and sigmoid colon and its mesentery in the posterior wall of the intersigmoid recess. The left ureter lies in extraperitoneal areolar tissue in the pelvis. Initially, it descends posterolaterally on the lateral wall of the lesser pelvis along the anterior border of the greater sciatic notch. Opposite the ischial spine it turns anteromedially into fibrous adipose tissue above levator ani to reach the

base of the bladder. On the pelvic side-wall it is anterior to the internal iliac artery and the beginning of its anterior trunk, posterior to which are the internal iliac vein, lumbosacral nerve and sacroiliac joint. Laterally it lies on the fascia of obturator internus. It progressively crosses to become medial to the umbilical, inferior vesical, and middle rectal arteries[18].

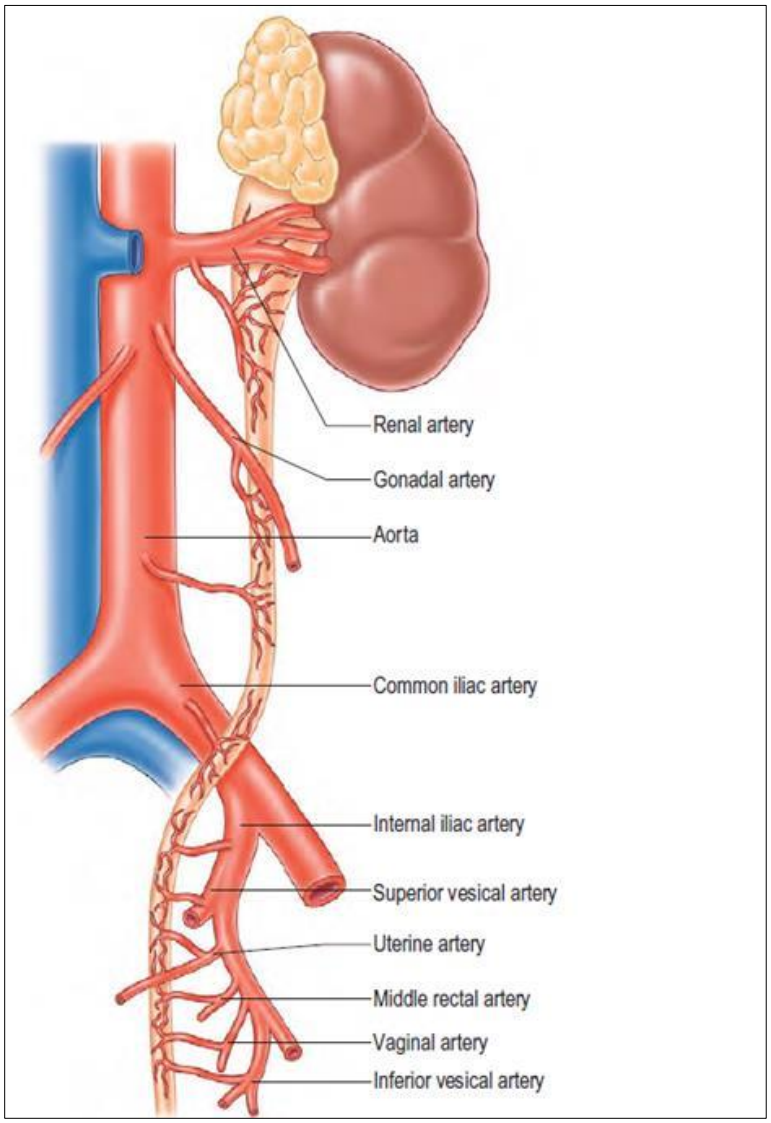

Figure 7.Arterial supply of the left ureter. The proximal part takes its blood supply medially, and the distal part is supplied laterally.

In males, the pelvic ureter hooks under the vas deferens (Figure 8), then passes in front of and slightly above the upper pole of the seminal vesicle to traverse the bladder wall obliquely before opening at the ipsilateral trigonal angle. Its terminal part is surrounded by tributaries of the vesical veins. In females, the pelvic part at first has the same relations as in males, but anterior to the internal iliac artery it is immediately behind the ovary, forming the posterior boundary of the ovarian fossa. In the anteromedial part of its course to the bladder it is related to the uterine artery, uterine cervix and vaginal fornices. It is in extraperitoneal connective tissue in the inferomedial part of the broad ligament of the uterus where it may be damaged during hysterectomy. In the broad ligament, the uterine artery is anterosuperior to the ureter for 2.5 cm and then crosses to its medial side to ascend alongside the uterus. The ureter turns forwards slightly above the lateral vaginal fornix and is generally two cm lateral to the supravaginal part of the uterine cervix in this location. It then turns medially to reach the bladder, maintaining a variable relation to the anterior aspect of vagina. As the uterus is commonly deviated to one side, one ureter (commonly the left), may be more extensively apposed to the vagina, and may cross the midline[18].

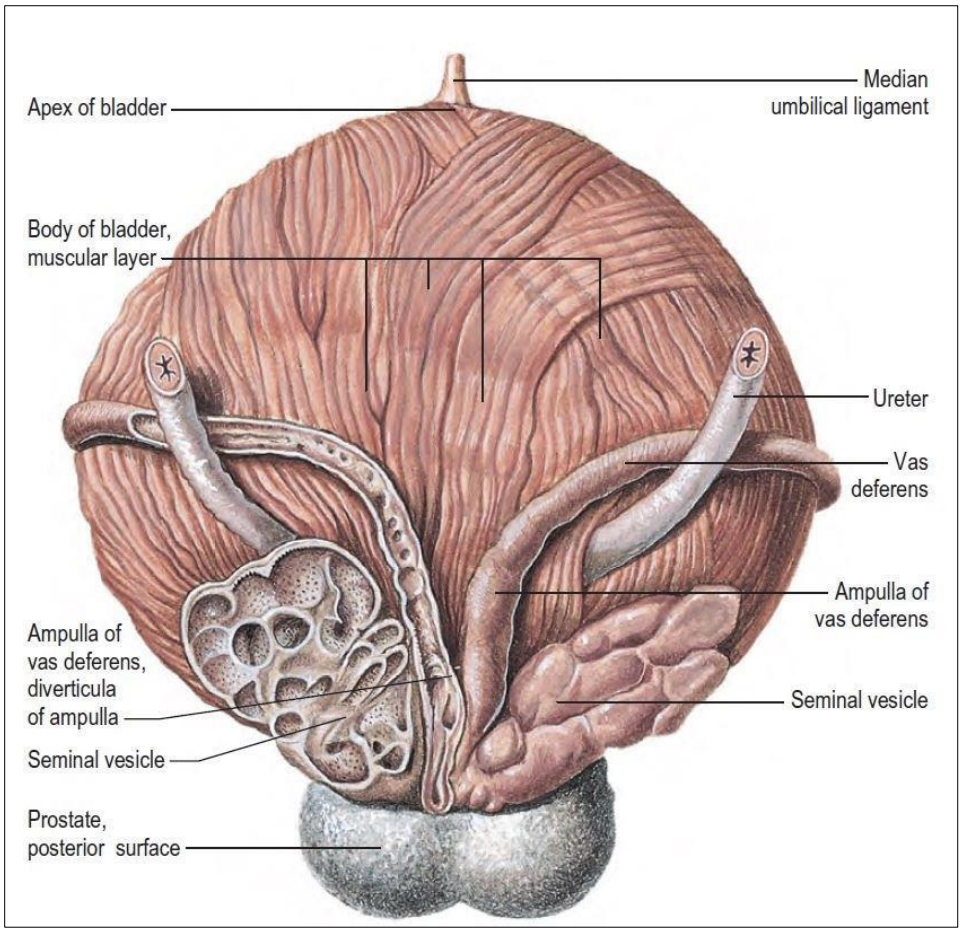

Figure 8. Posterior aspect of the male urogenital organs, showing relationship of the lower ureter to the vas deferens and seminal vesicles.

The distal 1–2 cm of each ureter is surrounded by an incomplete collar of non-striated muscle, which forms a sheath (of Waldeyer). The ureters pierce the posterior aspect of the bladder and run obliquely through its wall for a distance of 1.5–2.0 cm before terminating at the ureteric orifices (Figure 6). This arrangement is believed to assist in the prevention of reflux of urine into the ureter, since the intramural ureters are thought to be occluded during increases in bladder pressure at the time of micturition. There is no evidence of a classic ureteral sphincter mechanism in man. The longitudinally oriented muscle bundles of the terminal ureter continue into the

bladder wall and at the ureteric orifices become continuous with the superficial trigonal muscle. In the distended bladder, in both sexes, the ureteric openings are usually 5 cm apart and 2.5 cm apart when the bladder is empty[18].

Urinary Bladder

The urinary bladder is an expansile reservoir to hold urine and hence its size, shape, position and relations all vary according to its content and the state of neighboring viscera. When the bladder is empty, it lies entirely in the lesser pelvis, but as it distends it expands anterosuperiorly into the abdominal cavity. An empty bladder is somewhat tetrahedral and has a base (fundus), neck, apex, a superior and two inferolateral surfaces[22].

Relations

The bladder base is triangular and located posteroinferiorly. It is closely related to the anterior vaginal wall in females (Figure 9); and to rectum in males, although it is separated from rectum by rectovesical pouch superiorly, seminal vesicle inferiorly and laterally by vas deferens and Denonvillier's fascia (Figure 10). The bladder neck, the most fixed part lies most inferiorly, about 3–4 cm behind the lower part of the symphysis pubis and just above the plane of the inferior aperture of the lesser pelvis[22].

The bladder neck lies in a constant position and acts as an internal urethral orifice. In males it is in direct continuity with the base of the prostate; and in females

it is related to the pelvic fascia, surrounding the upper urethra. The apex of urinary bladder faces towards the upper part of the symphysis pubis in both males and females. The median umbilical ligament (urachus) ascends behind the anterior abdominal wall from the apex to the umbilicus. It is covered by peritoneum, which forms the median umbilical fold[22].

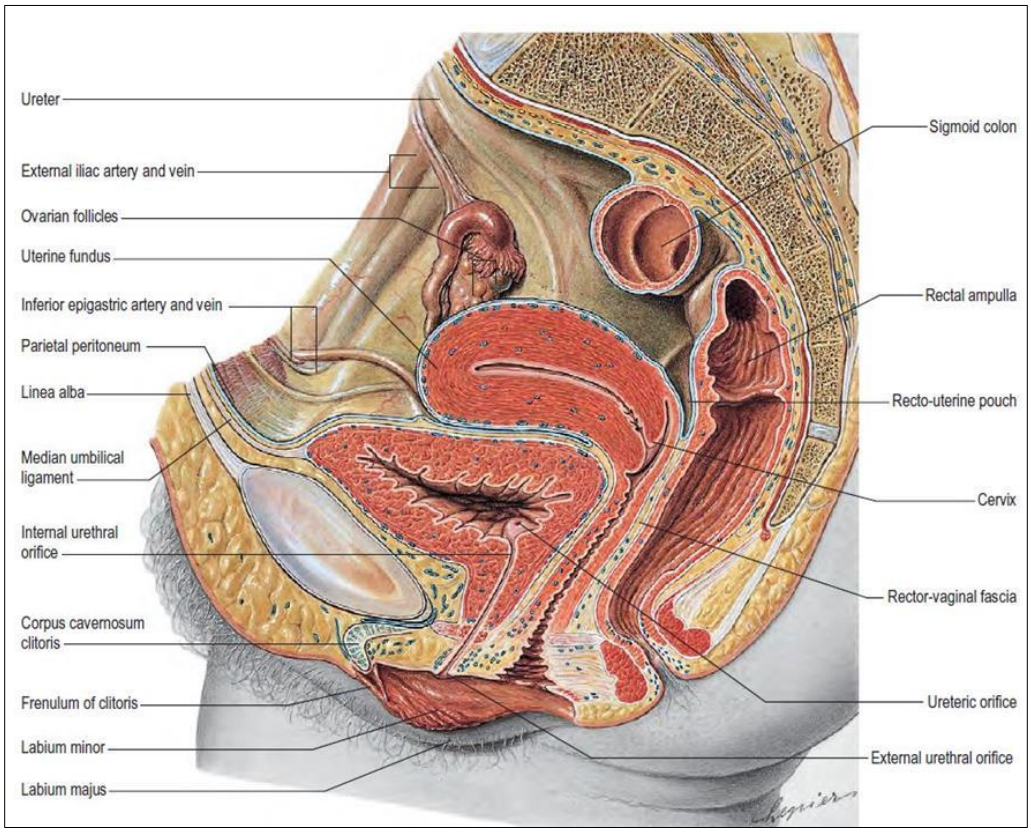

Figure 9.Relations of the female bladder, sagittal section of the pelvis.

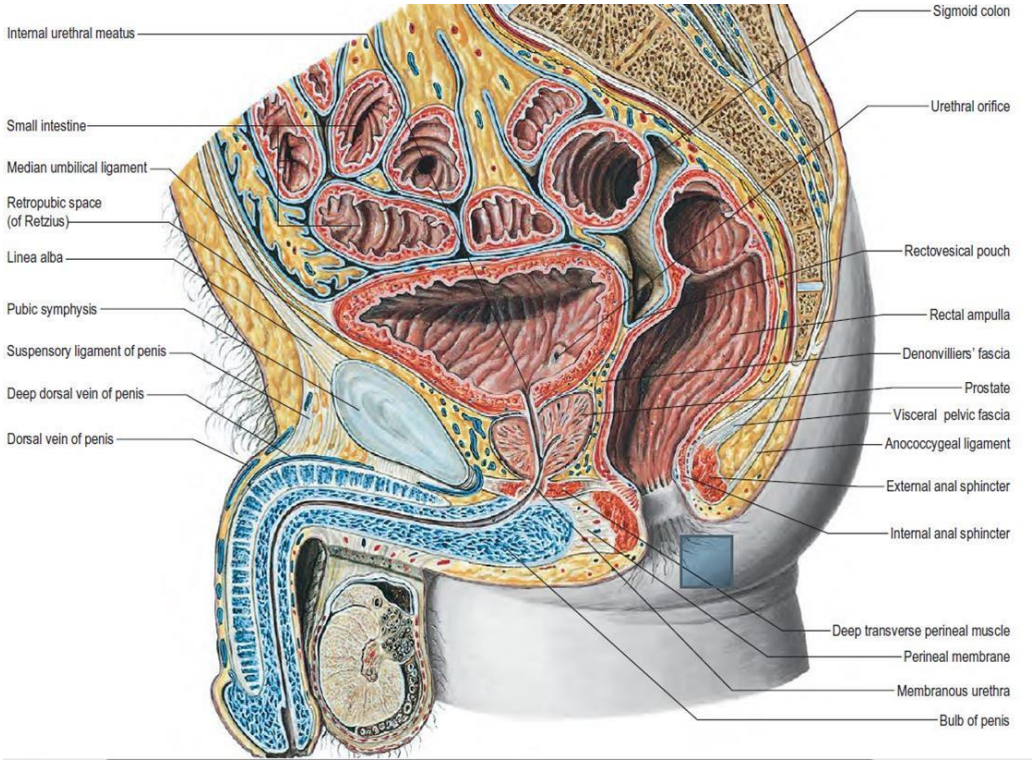

Figure 10.The relationship of the bladder and prostate, sagittal section, male pelvis.

The fat in the potential retropubic space (of Retzius) separates the anterior surface of bladder from the transversalis fascia. Inferolateral surface is related anteriorly to the pubis and puboprostatic ligaments in males and in females the pubovesical ligaments replace the puboprostatic ligaments, whereas the rest of the relations are similar in males and females. The inferolateral surfaces are not covered by peritoneum. The triangular superior surface is bounded by lateral borders from the apex to the ureteric entrances, and by a posterior border which joins them. In males the superior surface is completely covered by peritoneum, which extends slightly onto the base and continues posteriorly into the rectovesical pouch and anteriorly into the median umbilical fold: it is in contact with the sigmoid colon and the terminal coils of the ileum (Figure 9 and Figure 10). In females the superior surface is largely covered

by peritoneum, which is reflected posteriorly onto the uterus at the level of the internal os (the junction of the uterine body and cervix), to form the vesicouterine pouch. The posterior part of the superior surface, devoid of peritoneum, is separated from the supra vaginal cervix by fibroareolar tissue. As the bladder fills it becomes ovoid. Anteriorly, it displaces the parietal peritoneum from the suprapubic region of the abdominal wall[22].

UROLITHIASIS

Classification of Calculi

Urinary calculi can be classified based on the cause of stone formation – infectious or non-infectious causes. Non-infectious causes include genetic defects or adverse drug effects (Table 1)[23].

Table 1. Classification of Urinary Calculi Based on Etiology[23].

Cause	**Examples**
Non-infection stones	Calcium oxalate
	Calcium phosphate,
	Uric acid
Infection stones	Magnesium ammonium phosphate
	Carbonate apatite
	Ammonium urate
Genetic causes	Cystine
	Xanthine
	2,8-dihydroxyadenine
Drug stones	Allopurinol, amoxicillin/ampicillin, quinolones, ephedrine, indinavir, triamterene, acetazolamide, calcium

Stone Composition

Urinary calculi are composed of various compounds, which is the basis for further diagnostic and management decisions. Calculi are usually formed from mixtures, which are described in Table 2. The substance comprising the largest part(s) of the stone is considered to be the most important[23].

Table 2. Relevant Chemicals and Mineral Components Involved in Stone Formation[23]

Chemical name	Mineral name
Calcium oxalate monohydrate	Whewellite
Calcium oxalate dihydrate	Wheddelite
Basic calcium phosphate	Apatite
Calcium hydroxyl phosphate	Carbonite apatite
b-tricalcium phosphate	Whitlockite
Carbonate apatite phosphate	Dahllite
Calcium hydrogen phosphate	Brushite
Calcium carbonate	Aragonite
Octacalcium phosphate	
Uric acid	Uricite
Uric acid dihydrate	Uricite
Ammonium urate	
Sodium acid urate monohydrate	
Magnesium ammonium phosphate	Struvite
Magnesium acid phosphate trihydrate	Newberyite
Magnesium ammonium phosphate monohydrate	Dittmarite
Cystine	
Gypsum	Calcium sulphate dehydrate Zinc phosphate tetrahydrate
Xanthine	
2,8- Dihydroxyadenine	
Proteins	
Cholesterol	
Calcite	
Potassium urate	
Trimagnesium phosphate	
Drug stones	Active compounds crystallising in urine or Substances impairing urine composition
Foreign body calculi	

Additionally, urinary calculi are classified according to size, location, X-ray characteristics, composition and risk of recurrence[23].

Stone size

Urinary calculus size is generally measured in one or two dimensions and can be stratified into the following groups: < 5 mm, 5 to 10 mm, 10 to 20 mm and > 20 mm in greatest dimension[23]. Any calculus less than 3 mm is unlikely to cause symptoms and therefore may not be considered significant[17].

Stone Location

Urinary calculi can also be classified based on the anatomical location: upper, middle or lower calyx, renal pelvis, upper, middle or distal ureter and urinary bladder. Management of location plays a role in the management of patients with urinary calculi[23].

X-ray Characteristics

Urinary calculi can be stratified based on the plain radiograph appearance in kidney, ureter, and bladder (KUB) radiography. The radiograph characteristic is based on the mineral composition (Table 3). Non-contrast enhanced computed tomography (NCCT) can be useful to classify stones based on density, inner structure and composition[23].

Table 3. X-ray Characteristics of Various Minerals Forming Calculi[23]

Radiopaque	**Poor radiopacity**	**Radiolucent**
Calcium oxalate dihydrate	Magnesium ammonium phosphate	Uric acid
Calcium oxalate monohydrate	Apatite	Ammonium urate
Calcium phosphates	Cystine	Xanthine
		2,8-Dihydroxyadenine
		Drug-stones (such as allopurinol, amoxicillin/ampicillin, quinolones, ephedrine, indinavir, triamterene, acetazolamide, calcium)

Individuals at Risk for Stone Formation

Some individuals are more prone for developing urinary calculi, called as stone formers (Table 4). The risk of stone formation helps in determining pharmacological treatment. The stone type and underlying pathology helps to determine the risk of recurrence in individuals prone to stone formation[23].

Table 4. High Risk Stone Formers

General factors	Early onset of urolithiasis
	Familial stone formation
	Brushite-containing stones
	Uric acid and urate-containing stones
	Infection stones
Diseases associated with stone formation	Hyperparathyroidism
	Metabolic syndrome
	Nephrocalcinosis
	Gastrointestinal diseases (i.e., jejuno-ileal bypass, intestinal resection, Crohn's disease, malabsorptive conditions, enteric hyperoxaluria after urinary diversion) and bariatric surgery
	Sarcoidosis
Genetically determined stone formation	Cystinuria (type A, B and AB)
	Primary hyperoxaluria (PH)
	Renal tubular acidosis (RTA) type I
	2,8-Dihydroxyadeninuria
	Xanthinuria
	Lesch-Nyhan syndrome
	Cystic fibrosis
Drugs associated with stone formation	Allopurinol, amoxicillin/ampicillin, quinolones, ephedrine, indinavir, triamterene, acetazolamide, calcium
Anatomical abnormalities associated with stone formation	Medullary sponge kidney (tubular ectasia)
	Ureteropelvic junction (UPJ) obstruction
	Calyceal diverticulum, calyceal cyst
	Ureteral stricture
	Vesico-uretero-renal reflux
	Horseshoe kidney
	Ureterocele

Renal calculi

Four types of renal calculi are commonly observed[32]:

1. Calcium stones. Commonest and are associated with abnormal calcium metabolism.

2. Struvite (triple phosphate) stones. Usually form staghorn calculus and are associated with urinary tract infections.

3. Uric acid stones. Usually associated with gout.
4. Cystine stones. Rarest and are associated with abnormal amino acid metabolism.

Most of the renal calculi are located within the collecting system. However, calculi may sometimes be seen within renal sinus dilated pelvicalyceal collecting system or apparently within the parenchyma in non-dilated calyx[32].

Calcium Oxalate Stones

It is believed that the majority of calcium oxalate stones form from an initial calcium phosphate concretion that originates near the renal calyx epithelium in the highly concentrated environment of the terminal collecting duct, also referred to as Randall's plaque. This Randall's plaque erodes through the urothelium and on exposure to urine is thought to form a nidus for calcium oxalate deposition with time ultimately resulting in calculi[24,25].

Struvite Stones

As mentioned earlier (Table 1 and Table 2) struvite stones are formed as a result of urinary tract infections with urease producing organisms, *Proteus mirabilis,* being the most common. Other less common pathogens include *Klebsiella, Enterobacter,* or *Pseudomonas*. It is hypothesized that urease enzymes cleaves each mole of (soluble) urea into two moles of (relatively insoluble) ammonium. As this cleavage occurs, free H^+(proton) is bound to NH_3 to produce NH_4^+ and OH^-(hydroxyl) from water, making urine more alkaline. Phosphate is less soluble at alkaline pH (compared to acidic pH), so phosphate precipitates onto the insoluble ammonium

products, yielding magnesium ammonium phosphate. As long as urease producing bacteria remain in urine and within the stone, they continue to produce urease, and continue to cleave urea. This explains the reason why struvite calculi are so large (staghorn shaped) and develop quite rapidly and fill the calyceal spaces of the kidney[24].

Uric Acid Stones

Uric acid, a byproduct of purine metabolism is 100 times more soluble at a pH > 6 compared to a pH <5.5. Apart from dehydration, the most common risk factor for uric acid stone formation is persistently acidic urine including the lack of a normal postprandial alkaline tide. Similarly, patients with persistent acidosis (e.g., distal renal tubular acidosis) are also at risk for developing uric acid stones. Less commonly, gout (hyperuricemia) is associated in approximately 20% of cases with hyperuricosuria and uric acid lithiasis. Hyperuricosuria is also associated diseases such as lymphoma or leukemia that are treated with chemotherapy. With such treatment, the sudden lysis of millions of cells releases a large quantity of purines into the circulation and urine that may precipitate in the renal tubules and cause uric acid stones[24].

Cystine Stones

Cystine stones are formed in patients with a homozygous recessive gene for cystine transport, producing excess urinary cystine. Cystine is an amino acid of cysteine-S-S-cysteine. (The four dibasic amino acids are cystine, ornithine, lysine, and arginine, hence the mnemonic: COLA.) Normal individuals generally excrete <100 mg cystine/day in urine whereas the majority of homozygous cytinurics excrete > 200 mg/day. There are no known inhibitors of cystine. Cystine is more soluble at a

pH of 9.6 and higher compared to lower pH's, but it is practically impossible to achieve such a high urine pH by oral alkali agents (and not without risk of calcium phosphate stone formation)[24].

Ureteral stones

Calculi may be seen upper ureter, the distal ureter or around the vesico-ureteric junction portion of the ureter behind a filled bladder. In these patients unenhanced CT KUB is the preferred modality of investigation[32].

Role of CT in differentiating radiopaque and radiolucent calculi

Table 3 lists the x-ray characteristics with respect to their radiopacity or radiolucency. Calculi composed of cysteine, xanthine and uric acid are radiolucent, which limits role of KUB radiograph and intravenous urography for evaluation of calculi. In contrast, CT is able to detect virtually all types of calculi, owing to their high Hounsfield Unit (HU) (usually > 200 HU) values compared to surrounding tissue. The only calculi that are difficult to detect on NCCT are pure matrix calculi (which account for <1% of all calculi) and stones composed of pure indinavir (protease inhibitor) as these have soft tissue attenuation (15 to 30 HU). Indinavir is currently used in the treatment of human immunodeficiency virus (HIV) infection. Indinavir is excreted unchanged in urine and may precipitate to form pure indinavir calculi or may serve as a nidus for formation of other calculi. However, a clinical history of renal colic in a patient on indinavir therapy for treatment of HIV infection helps to clinch the diagnosis[26,27]. Secondary signs of obstruction due to calculi such as

ureteric dilatation, inflammatory changes in perinephric and periureteric fat, pelvicalyceal system dilatation and renal enlargement can provide additional information to diagnose/exclude calculi[26]. Many studies have evaluated the relationship between type of calculi and the mean HU values. The results among these studies vary in terms of HU values for the stone composition; however, uric acid and cysteine stones have the lowest HU values compared to other calculi. Due to a wide range of HU values between studies a meaningful comparison may not be possible[28,29,30,31].

PELVIURETERIC DILATATION

Pelviureteric dilatation can be physiological, secondary to urinary tract reflux disease and is sometimes seen in a nonobstructed system when the bladder is too full. Pelviureteric dilatation on imaging, suggests that there may be urinary tract obstruction distal to the dilatation in patients presenting with clinical symptoms. Although, ultrasound has been routinely used to assess patients with normal or abnormal renal function, there has been increasing usage of unenhanced computed tomographic examination of the kidneys, ureter and bladder (CT KUB) as a first-line examination from acute admission or accident and emergency referral to assess patients with loin pain. This is because obstructing stones within the ureter may or may not cause pelviureteric dilatation in the early stage and CT KUB is the most sensitive modality in assessing these patients[32].

Causes of pelviureteric dilatation

Causes of pelviureteric dilatation can be divided into physiological and pathological. Physiological causes include pregnancy and in a full/overdistended urinary bladder. Following voiding, pelviureteric dilatation resolves in case of a full/overdistended urinary bladder. During normal pregnancy at around six–10 weeks onwards, it is common to present with non-obstructing mild pelviureteric dilatation. This is partly due to extrinsic compression from the gravid uterus on the ureters and partly from hormonal factors. This can involve both ureters, but is commoner and more marked on the right than the left, with increasing severity throughout the pregnancy. Following delivery, the appearances resolve rapidly but may persist for up to three months postpartum[32].

There are numerous causes for obstructive uropathy of which calculi are the commoner cause. In the context of pelviureteric dilatation, stones may lie anywhere along the urinary tract system causing proximal obstruction. Patients usually present with acute loin pain and have complete or partial obstructive uropathy on the symptomatic side. They may also present in association with urinary tract infections or haematuria. Occasionally, presentation may be with a staghorn calculus which occupies and obstructs the whole of the renal pelvicalyceal system[32].

HISTORICAL BACKGROUND

Role of X-rays in Evaluation of Urolithiasis

The utility of conventional abdominal KUB radiograph for evaluation of urolithiasis is limited by various factors including bowel gas, extra-renal calcification, and patient's body habitus. Therefore, the overall diagnostic accuracy of KUB radiography is limited[27]. The sensitivity of KUB radiography is low and ranges from 45 to 60%. Additionally, presence of fecoliths and abdominal or pelvic calcifications (phleboliths) makes it challenging to confidently diagnose urolithiasis. About 10 to 20% of radiolucent calculi are also not diagnosed by radiograph. However, it still helps in localizing large calculi[33].

Positioning of patient for KUB radiography

The technical factors are: minimum source to image-receptor distance (SID) should be about 40 inches (102 cm) the image receptor (IR) should be of size 14 x 17 inches (35 x 43 cm), lengthwise. The patient is positioned supine with midsagittal plane centered to midline of table or IR with arms placed at the sides away from body and legs extended with support under knees. The IR is centered to the level of iliac crests, with bottom margin at the symphysis. There should be no rotation of pelvis or shoulders. The central ray (CR) should be perpendicular to and directed to centre of IR (to the level of iliac crest). The recommended collimation is a 35 x 53 cm (14 x 17"), field of view (FoV) or collimation on four sides to anatomy of interest.

Exposure should be made at end of expiration (about one second delay following expiration to allow involuntary motion of bowel to cease)[34].

Role of Intravenous Urography for diagnosis of Urolithiasis

IVU was traditionally considered as "gold standard" investigation for evaluation of ureteric colic. IVU has the advantage of providing structural and functional information regarding the site, degree and the nature of obstruction[33]. It will also help to assess renal function. However, the sensitivity of IVU varies widely from about just a little more than 50% (~52%) to about 80%[27,33]. IVU is an invasive technique and involves use of iodinated intravenous contrast medium[27]. Use of contrast carries possible risk of nephrotoxicity and contrast reaction, which may make the procedure undesirable. Additionally, the time taken to acquire delayed films further increases the time taken to complete the study and therefore increases time taken to complete the study[33]. Interestingly, a study by Sameh conducted in 200 patients to evaluate impact of preprocedure IVU on outcome of shockwave lithotripsy (SWL) did not show any significant different in terms of clinical outcome with IVU procedure, hence it is questionable if IVU really needs to be performed as pre-evaluation of SWL[35].

Role of Ultrasonography in Evaluation of Urolithiasis

Calculi appear as highly reflective focus with posterior acoustic shadowing on ultrasound. When calculi have a rougher surface or are smaller they tend to absorb all the transmitted incident sound waves, but if they are smaller than the beam width of sound waves, they cannot be assessed with ultrasound. Most of the renal calculi are commonly located in the renal pelvis. However visualization of calculi may be

complicated by the presence of highly reflective renal sinus, dilated pelvicalyceal system or within parenchyma in non-dilated calyx[32].

Composition of renal calculi usually does not influence the ability of ultrasound to detect as both radiolucent and radio-opaque calculi are visualized on ultrasound. The larger the calculus, more easy it is to detect on ultrasound; however, very large calculi such as stag-horn calculus or large matrix calculi may not have associated posterior acoustic shadowing due to presence of proteinaceous content and therefore may be difficult to be demonstrable on ultrasound. These calculi are usually less obvious on ultrasound compared to plain radiograph as dense shadows within pelvicalyceal system can sometimes obscure collecting system dilatation and may be represented as bowel gas shadowing. Also, a lobulated shape of calculus within the collecting system may be easily mistaken for numerous separate calculi within collecting system. Therefore, in cases with suspected stag horn calculi, scanning from a coronal plane is more helpful compared with sagittal scanning. Additionally, a plain radiograph or unenhanced CT should be recommended in these cases[32].

Overall, majority of calculi greater than 5 mm are easily diagnosed on ultrasound. However, for calculi less than 5 mm not many can be diagnosed easily on ultrasonography. It has also been observed that ultrasonography tends to overestimate the calculus size and therefore in instances when exact calculus size is needed for determining management, then CT study is preferred[32].

The visibility of calculus also depends on location as calculi within renal sinus are usually difficult to visualize due to presence of heterogeneous echogenicity of surrounding structures that can defocus ultrasound beam. Other issues such as posterior acoustic shadowing produced by renal sinus structure can mimic calculus. Calculi impacted within pelviureteric system may not be visible on ultrasonography. Finally, increased echogenicity in chronic renal failure makes it difficult to visualize calculus[32].

Although ultrasonography is usually a good modality for detection of calculi, sometimes it may not be able to distinguish exact location or part of collecting system in which the calculus resides. Ultrasonography may not be able to differentiate parenchyma or papillary calcification from calyceal stone, or vascular calcification from small calculus. Whenever, there is a doubt regarding calculus, further investigation such as KUB radiograph or CT is recommended[32].

Ultrasound is also helpful in detecting calculi in upper ureter, distal ureter and around the vesicoureteric junction (VUJ) in an adequately distended urinary bladder. Mid ureteric calculi may sometimes be seen adjacent to iliac vessel crossing, however, more often than not they are not visualized. Presence of hydroureteronephrosis (HUN) is an indirect indicator for ureteric calculus. However, a ureteric calculus without HUN is difficult to suspect on ultrasound. Currently, NCCT is the best modality for assessing individuals with loin pain and suspected ureteric colic[32].

Role of CT KUB in evaluation of urolithiasis

In a patient presenting with renal/ureteric calculus, the clinical history should guide the physician towards most appropriate first line imaging modality. Usually, ultrasound is the initial imaging modality that is considered, as it is safe, quick, and inexpensive, with no risk of radiation. However, ultrasonography has sensitivity of <50% for diagnosis of renal/ureteric calculi, thereby necessitating need to employ other investigations. Currently, NCCT KUB is considered as the standard investigation for diagnosis of acute flank pain, replacing IVU. NCCT can be performed quickly and can help in determining location, size and attenuation value of calculi, all of which help in appropriate treatment planning. NCCT has high sensitivity and specificity in diagnosis of urolithiasis compared to any other imaging techniques. The introduction of low-dose protocol has significantly contributed in making NCCT the standard imaging of choice in patients presenting with renal colic[3,23].

The latest European Association of Urology (EAU)[23] and the American Urology Association (AUA)[3] guidelines recommend low-dose NCCT following ultrasonography in evaluation of urolithiasis in patients with body mass index (BMI) $\leq$ 30 kg/sq. m[3,23]. However, in patients with BMI of >30 kg/m^2 standard-dose CT study is recommended due to low sensitivity and specificity of low-dose CT in this patient population[3].

CT IMAGING: BACKGROUND

There has been a significant improvement in the field of medical imaging in both the technologic and clinical areas following the discovery of X-ray in 1895 by Wilhelm Conrad Roentgen, a German Physicist. Innovations in technology are a norm in the Radiology Department, with introduction of new ideas and methods and refinements in existing techniques happening continuously. One such evolution is the invention of computed tomography (CT)[36].

The first idea of a computed tomography machine was conceived by Sir Godfrey Hounsfield in 1967 and the first patient was scanned for brain cyst in 1971[36].

Sir Godfrey Hounsfield, an electronic engineer working at the Central Research Laboratories of EMI in England commenced work on image reconstruction in 1968.His original apparatus consisted of a collimated isotope source mounted on a lathe bed. The objects examined were phantoms contained within a ten-inch water. The scan took nine days to complete because of the low intensity of the X-ray radiation source, and a further two and half hours to process the reading through a computer. The resulting image though of poor quality proved that the system worked. To provide sufficient intensity the equipment was modified by replacing the isotope with an industrial X-ray tube[36].

A prototype scanner was then developed and installed in Atkinson Morley Hospital in Wimbledon, England on 1st October 1971. The first patient scan was a 41 year old female with suspected frontal lobe tumor, the tumor was clearly demonstrated on the scan[36].

Hounsfield and Ambrose presented their paper on CT to the annual congress of the British Institute of Radiology on 20th April 1972 to great acclaim. The first CT papers, by these authors appeared in British Journal of Radiology in 1973. The invention of this technique resulted in the award of 1979 Nobel Prize in physiology and medicine to Sir G. N. Hounsfield, Central Research Lab., England (EMI), and A. N. Cormack of Physics Department, Tufts University, Massachusetts, U.S.A. Advanced Technological Developments. Over the last ten years, four different generations of CT scan equipment were produced. The most important improvements have been in the reduction in the single image generation time from five minutes to 2.5 seconds in the third and fourth generations scanners and an increase in spatial resolution and contrast[36]. The introduction of second generation CT scanners further reduced the scan time from about six minutes to about two minutes. Late second generation CT scanners with $\geq$ 20 detectors further reduced scanning time to about $\leq$ 20 seconds. This dramatically improved quality of body scans, which could not be performed previously within a breath hold. The third generation scanners further reduced the scan time to 5 seconds or less, which has now further improved to about 0.33 seconds[37].

Slip Ring Scanners

There was no significant improvement in CT technology following 4th generation CT scanners in late 1980's. The only limitation at that time was interscan delays. Following one 360^0 rotation, the cables connecting rotating components (x-ray tube and detectors) to the rest of the gantry required rotation to be stopped and reversed for next slice, all of which added time of scan. All this changed with application of low-voltage slip rings. Slip rings provide electricity to the rotating components without fixed connections (Figure 11). Slip rings made it possible for continuous rotation, thereby reducing scan time. This technology also paved the way for introduction of spiral/helical CT scans[37].

In the mid-1980s, another high speed CT scanner was introduced, which was referred to as the Electron Beam CT (EBCT) scanner used for imaging cardiovascular system. In 1989, Dr. Willi Kalender introduced volume scanning by using spiral / helical CT scanners. In spiral/helical CT Scanners, a thin X-ray beam traces a path around the patient and scans a volume of the tissue. Recently, dual slice spiral /helical CT scanner and multislice CT scanners were introduced which mainly increase the speed and volume of scan. Volume CT scanning has resulted in a wide range of applications such as CT fluoroscopy, CT angiography, 3D Imaging and virtual reality imaging[36].

Figure 11. Slip-ring technology in Siemens Somatom Emotion CT scanner

RADIATION DOSE MEASURES: GENERAL DEFINITIONS

Exposure:

The term exposure describes the ability of x-rays to ionize air. It is measured in roentgens (R); this unit is defined as the quantity of x rays that produces 2.580 $x10^{4}$ C of charge collected per unit mass (kilograms) of air at standard temperature and pressure (STP): 1 R = 0.000258 C/kg air. This term refers to the concentration, in air, of radiation at a specific point and is the ionization produced in a specific volume of air. It is typically measured with an ionization chamber and an electrometer. It essentially describes how much ionization is present in the volume of air, but it does not tell how much energy is absorbed by the tissues being irradiated[38].

Absorbed Radiation Dose:

Absorbed radiation dose, often referred to as radiation dose describes the amount of energy absorbed per unit mass at a specific point. It is measured in Grays (1 Gy = 1 J/kg) or rads (1 rad = 100 erg/g). The conversion between rads and grays is 100 rad = 1 Gy. Absorbed dose essentially describes how much energy from ionizing radiation has been absorbed in a small volume centered at a point; it does not describe where that radiation dose is absorbed or reflect the relative radiosensitivity or risk of detriment to those tissues being irradiated[38].

Effective Dose:

Effective dose (formerly referred to as the effective dose equivalent) takes into account where the radiation dose is being absorbed (eg, which tissue has absorbed that radiation dose) and attempts to reflect the equivalent whole-body dose that results in a stochastic risk that is equivalent to the stochastic risk from the actual absorbed dose to those tissues irradiated in a non-uniform, partial-body irradiation such as a CT scan[38].

Effective dose is measured in Sieverts (Sv) or rems. The conversion between Sieverts and rems is 100 rem = 1 Sv[38].

RADIATION DOSE OPTIMIZATION

All CT scanners have a gantry, an x-ray source, and an array of detectors. On passage through the body part, the incident beam is attenuated in a manner dependent on the local tissue composition (greater attenuation for bones, lesser for soft tissues)[39].

Principle of ALARA

As low as reasonably achievable (ALARA) is a concept designated for ensuring that any radiological investigation should use optimal radiation dose to provide images, which are adequate for diagnosis and treatment. This is possible by identifying imaging parameters and protocols, which can provide clinically required information while maintaining radiation doses as low as possible[40].

FACTORS THAT INFLUENCE RADIATION DOSE FROM CT

In general, there are some factors that have a direct influence on radiation dose, such as the x-ray beam energy (kilovolt peak), tube current (in milliampere), rotation or exposure time, section thickness, object thickness or attenuation, pitch and/or spacing, dose reduction techniques such as tube current variation or modulation, and distance from the x-ray tube to isocenter[39]. The principles of ALARA suggest that the right radiation dose should be given to the right patient and a one-size-fits-all approach should be abandoned. The various techniques through dose-optimization can be achieved is by using tube current modulation a.k.a. automated

exposure control (AEC), use of lower tube potential and use of advanced reconstructive techniques such as iterative reconstruction methods[41].

Beam Energy

Tube potential (peak voltage) determines the incident x-ray beam energy, and therefore variation in tube potential substantially changes CT radiation dose. However, the effect of tube voltage on image quality is more complex as it affects both image noise and tissue contrast. It is important to note that decreased tube voltage is associated with a notable increase in image noise. Specially, this occurs if the patient is too large or the tube current is not appropriately increased to compensate for the lower tube voltage. The dose variation is approximately proportional to the square of the tube voltage change (i.e., square of the ratio of final and initial peak voltage), and the noise change is approximately inversely proportional to the tube voltage change[42].

However, it is essential that the relationship between reduction in tube voltage and reduction in radiation exposure be carefully evaluated owing to the complex relationship between tissue contrast, image noise and radiation dose depending on patient size. For example by reducing kVp from 140 kV to 120 kV in an abdominal CT a 20 to 40% reduction in radiation dose can be obtained. However, there is need for further research into this area so as to assess the feasibility of reduction in kV as part of dose reduction measures[39].

Tube current

Reduction in tube current is a simple means of reducing CT radiation dose as it follows a linear relationship. For example, a 50% reduction in tube current reduces radiation dose by half. The beam energy and photon fluence of an x-ray beam varies with the tube potential and the current used during the particular examination. Tube current–time product settings are proportional to the number of photons in the defined exposure time (photon fluence)[39].

The radiation dose is directly proportional to the milliampere-seconds value. When all other technical parameters are kept constant, the effective dose values increase linearly with milli Ampere-seconds (mAs). Any decrease in tube current should be considered carefully, because such reduction causes an increase in image noise, which may affect the diagnostic outcome of the examination. This is especially true in abdominal studies, where low-contrast areas are severely affected by an increase in image noise[39].

Automatic exposure control

Automatic tube current modulation or AEC is a program designed to modulate radiation dose to the patient based on patient's size and attenuation. This ensures optimal radiation dose by either increased radiation to body parts, which have greater attenuation (such as hips or shoulders) or decreased radiation to body parts, which

have lesser attenuation (such as abdomen and thorax). AEC therefore helps in providing optimal radiation dose without affecting image quality[43].

Currently there are four types of AEC models, which are as follows:

1. Patient-size AEC: These programs optimize radiation based on overall size of patient and adjusting mAs as determined by topographic image.
2. Z-axis AEC: These programs optimize mAs along the length of patient based on scout image to equalize image quality throughout the study.
3. Angular AEC: These programs modulate radiation dose as the X-ray tube in the gantry moves 360^0 around the patient and makes adjustment based on the fact that attenuation can vary from different projections (example there is more attenuation when the X-rays pass laterally compared to anteroposteriorly.
4. X-axis, Y-axis and Z-axis AEC: These programs combine angular and z-axis modulation throughout the length of the scan and optimize mAs delivered

Collimation, Table Speed, and Pitch

For helical CT scanners, pitch is defined as the ratio of table feed per gantry rotation to the nominal width of the x-ray beam. An increase in the pitch decreases the duration of radiation exposure to the anatomic part being scanned. With helical CT scanners, beam collimation, table speed, and pitch are interlinked parameters that affect the diagnostic quality of an imaging study[39].

Faster table speed for a given collimation, resulting in higher pitch, is associated with a reduced radiation dose (especially if other scanning parameters, including tube current, are held constant) because of a shorter exposure time, whereas narrow collimation with slow table speed, resulting in a longer exposure time, is associated with a higher radiation dose. This is not true for scanners that use an effective milliampere-second setting (defined as milliampere seconds divided by pitch) and maintain a constant value for effective milliampere seconds[39].

In such scanners, the effective milliampere-second level is held constant irrespective of pitch value, so that radiation dose does not vary as pitch is changed[39]. For a given collimation, an increase in table speed increases the pitch and reduces the radiation dose by 1 divided by the pitch[44].

Modern multi–detector row scanners may automatically recommend the appropriate tube current adjustment to maintain a given image noise level when pitch is changed. Although scanning at a higher pitch is generally more dose efficient, it also tends to cause helical artifacts, degradation of the section-sensitivity profile (section broadening), and decrease in spatial resolution. Hence, alterations in pitch can have varying effects on image quality in different situations[39].

Scanning Modes

Use of a multi–detector row CT scanner results in some amount of unused radiation extending beyond the beginning and end of the imaging region[45].This occurs because, at the start of the acquisition, only the first detector row is contributing to the image. As the acquisition proceeds, additional detector rows enter the imaging region until all rows are contributing. A similar effect occurs in reverse at the end of the acquisition. As a result, it is generally more dose efficient to use a single helical scan rather than multiple helical scans if there are no overriding clinical considerations, such as breath holding, for the patient. The need to prescribe multiple contiguous helical scans should be infrequent with modern high-speed multi–detector row scanners[39].

Gantry Rotation Time

There has been a dramatic decrease in tube rotation times with recent technologic innovations, most notably with the development of four–, eight–, and 16–detector row CT scanners. A four-row scanner with a 0.8 second rotation time requires a 16-second breath hold to scan the entire abdomen; an eight-row scanner covers this length in 8 seconds. If the tube rotation time is decreased (faster gantry rotation), the radiation exposure decreases, and tube current may thus have to be increased to maintain constant image quality[39].

Modern 16-row scanners are capable of high scanning speeds and submillimeter section thicknesses. Thin collimation can lead to a higher dose,

especially if tube current is increased to maintain image noise at a level similar to that of thicker sections. The contrast resolution of small lesions improves because of reduced partial volume effects; hence, greater noise on thinner sections may often be acceptable[46]. In addition, submillimeter- collimation scans can usually be reconstructed as thicker sections, which reduce inherent noise. Thus, it is important to optimize beam collimation for different multi–detector row scanners on the basis of the clinical situation in question[39].

RADIATION PROTECTION

The triad of radiation protection actions comprise of "time-distance-shielding". Reduction of exposure time, increasing distance from source, and shielding of patients and occupational workers have proven to be of great importance in protecting patients, personnel, and members of the public from the potential risks of radiation. It has been recommended that the thyroid, breast and gonads of the patients be shielded, to protect these organs especially in children and young adults. In gonadal shielding, a lead apron is placed appropriately on the patient to protect the gonads from primary beam radiation exposure. A lead bib and collar worn over the patient's neck and thorax have been documented to effectively shield radiosensitive organs like the thyroid and the breast, and are therefore recommended for routine use in head CT examinations[47].

ESTIMATING EFFECTIVE DOSE FROM CT

The definition of effective dose was given earlier as the weighted sum of organ doses resulting from the examination, where the radiosensitive organs were defined along with their tissue-weighting factors. Although it appears straightforward to estimate effective dose, it is actually difficult to accurately estimate the dose to an individual organ from a CT scan. This is even more difficult when attempting to estimate the effective dose for each patient when each one has unique characteristics of height, weight, age, gender, and composition. Many methods are in practice for calculating the effective dose[38].

One of the widely used methods to estimate the effective dose involves conversion factors for a general anatomic region as described by the European Guidelines on Quality Criteria for Computed Tomography, which are based on the work of Jessen et al. In this approach, the $CTDI_{vol}$ and distance are used to estimate the dose length product (DLP), which is then multiplied by a region-specific conversion factor to estimate the effective dose. These conversion factors range from 0.0023 mSv/mGy X cm for the head region to 0.017 mSv/ mGy X cm for the chest region and 0.019 mSv/ mGy X cm for the pelvis. This approach obviously does not take into account any patient-specific or even examination-specific factors but provides an easily estimated value of effective dose[38]. The conversion factor for CT abdomen and pelvis is 0.015 mSv/mGy cm[48].

The effective dose is calculated as product of DLP X f (conversion)[48].

RADIATION DOSES WITH CURRENT CT PROCEDURES

The concern with any studies evaluating efficacy of low-dose vs standard-dose CT for evaluation of urolithiasis is the risk of additional radiation with low-dose protocol. In fact one might argue for the need of additional radiation dose. To address this question, it is important to review the additional risk of radiation and how it fares with current CT studies and recommendations on limitations of radiation dose.

An average person receives somewhere up to 3 mSv radiation per year from background sources[49,50]. The risk of a person contracting fatal cancer with use of CT is somewhere about 1:2000, which is in contrast to lifetime natural risk of 1:5[51]. Table 5 shows the average radiation exposure for different radiological techniques. It can be seen from the table that average radiation exposure of CT abdomen and pelvis can be up to 10 mSv. Additionally a contrast enhanced abdominal scan can result in radiation exposure of up to 20 mSv. Radiation exposure of 10-12 mSv is classified as low lifetime risk for fatal cancer from examination[49].

Table 5. Average Radiation Exposure for Different Radiological Techniques

For this procedure:	*** Your approximate effective radiation dose is:**	**Comparable to natural background radiation for:**	****Additional lifetime risk of fatal cancer from examination:**
ABDOMINAL REGION:			
Computed Tomography (CT)-Abdomen and Pelvis	10 mSv	3 years	Low
Computed Tomography (CT)-Abdomen and Pelvis, repeated with and without contrast material	20 mSv	7 years	Moderate
Computed Tomography (CT)-Colonography	10 mSv	3 years	Low
Intravenous Pyelogram (IVP)	3 mSv	1 year	Low
Radiography (X-ray)-Lower GI Tract	8 mSv	3 years	Low
Radiography (X-ray)-Upper GI Tract	6 mSv	2 years	Low
BONE:			
Radiography (X-ray)-Spine	1.5 mSv	6 months	Very Low
Radiography (X-ray)-Extremity	0.001 mSv	3 hours	Negligible
CENTRAL NERVOUS SYSTEM:			
Computed Tomography (CT)-Head	2 mSv	8 months	Very Low
Computed Tomography (CT)-Head. repeated with and without contrast material	4 mSv	16 months	Low
Computed Tomography (CT)-Spine	6 mSv	2 years	Low
CHEST:			
Computed Tomography (CT)-Chest	7 mSv	2 years	Low
Computed Tomography (CT)-Chest Low Dose	1.5 mSv	6 months	Very Low
Radiography-Chest	0.1 mSv	10 days	Minimal
HEART:			
Coronary Computed Tomography Angiography (CTA)	12 mSv	4 years	Low
Cardiac CT for Calcium Scoring	3 mSv	1 year	Low
NUCLEAR MEDICINE:			
Positron Emission Tomography - Computed Tomography (PET/CT)	25 mSv	8 years	Moderate

*The effective doses are typical values for an average-sized adult. The actual dose can vary substantially, depending on a person's size as well as on differences in imaging practices.

**Legend

Risk Level	Approximate additional risk of fatal cancer for an adult from examination:
Negligible:	less than 1 in 1,000,000
Minimal:	1 in 1,000,000 to 1 in 100,000
Very Low:	1 in 100,000 to 1 in 10,000
Low:	1 in 10,000 to 1 in 1000
Moderate:	1 in 1000 to 1 in 500

Note: These risk levels represent very small additions to the 1 in 5 chance we all have of dying from cancer.

Additionally, the American Association of Physicists in Medicine (AAPM), a scientific body that ensures safety and quality in use of radiation in medical procedures has stated that "Risks of medical imaging at effective doses below 50 mSv for single procedures or 100 mSv for multiple procedures over short time periods are too low to be detectable and may be non-existent. Predictions of hypothetical cancer incidence and deaths in patient populations exposed to such low doses are highly speculative and should be discouraged. These predictions are harmful because they lead to sensationalistic articles in the public media that cause some patients and parents to refuse medical imaging procedures, placing them at substantial risk by not receiving the clinical benefits of the prescribed procedures"[52].

Low-dose CT Techniques in Evaluation of Sinusitis

Computerized tomography (CT) is the gold standard for visualization of anatomy of paranasal sinuses and to determine the extent of disease, both of which are important for endoscopic sinus surgery. CT helps in providing important structural landmarks, which are critical to help avoid complications such as absent uncinate process or asymmetry of cribriform niche[53]. Imaging of paranasal sinuses has undergone tremendous change with the availability of CT scans. The anatomy of paranasal sinuses can be visualized with greater details, which was not available before. This has made the radiologist a key member of the patient management team[54]. CT is currently the standard test for evaluation of sinusitis; however this technique is associated with risk of radiation to sensitive structures such as lens and thyroid gland and may cause complications such as cataract[55]. Various studies have shown that it is possible to evaluate paranasal sinuses for sinusitis with low-dose CT compared with standard-dose CT[56,57,58,59].

Low-Dose CT Techniques in Evaluation of Appendicitis

CT has been increasingly used for diagnosis of acute appendicitis owning to its high diagnostic accuracy. CT is easy to perform, highly sensitive and specific in the diagnosis of appendicitis. Non-contrast CT studies have been shown to have diagnostic performance of > 95% for diagnosis of acute appendicitis[60].The preferential use of CT for diagnosis of appendicitis also stems in part from the increasing trend of practicing defensive medicine and dependency of imaging tests[61]. Acute appendicitis is more common among adolescents and young adults, both of who are susceptible to risks of radiation compared to middle aged individuals. It is therefore necessary to determine if radiation dose can be lowered, without affecting the diagnostic quality of the study[61,62]. The use of CT study for assessment of appendicitis has also reduced the need for unnecessary appendectomies without increasing risk of appendicular perforation, both of which are considered as important parameters for determining quality of care. In these instances CT study would help to confirm/exclude diagnosis of appendicitis in a patient with pain abdomen[63]. Various studies have compared the accuracy of low-dose CT for diagnosis of acute appendicitis compared to standard-dose CT. All the studies have shown that low-dose CT should be preferred over standard-dose CT for diagnosis of acute appendicitis[60,61,62,63]. These studies reduced radiation dose from >500 mGy X cm to <130 mGy X cm[61,62,63].

CLINICAL STUDIES

The efficacy of low-dose vs standard-dose CT for diagnosis of ureteral stones has been studied using different study designs, such as comparison with same patients[10], different patient groups[15] and with low-dose simulation techniques[10].

Studies have been conducted by performing standard-dose CT in patients with suspected/clinically diagnosed urolithiasis following which noise was artificially introduced to simulate low-dose CT scan. Results have shown an excellent agreement with both standard-dose CT and simulated low-dose CT results and the results from these studies prompted suggestions for considering low-dose CT protocol for diagnosis of urolithiasis. However, as these were simulation studies reduction in mA was assessed, but changes in other CT scan parameters could not be assessed. Additionally increase in noise may inadvertently have introduced bias/inter-observer variability in reporting, limiting accurate reporting in these studies[10,13,17,64,65].

Low-dose and standard-dose CT scan results in patients with similar clinical and demographic profile has shown excellent correlation. However, the results may not be ideal considering that scans were performed in different groups of patients. Nonetheless, it suggests that low-dose CT protocol be followed wherever possible[15]. Data from studies conducted in same patient population helps in better understanding the efficacy of low-dose CT compared with standard-dose CT.

It is possible that body mass index (BMI) may play a role in detection of calculi, as efficacy of low-dose CT in detection of calculi of <3 mm may be limited with increasing BMI, however, there is mixed evidence for the same[12,16].

Kim et al compared the efficacy of low-dose vs standard-dose CT for diagnosis of ureteral stones in 121 patients with suspected acute renal colic. In the study, standard dose CT was performed with 260 mAs (at 120 kVp), pitch 1.5 and low dose CT was performed at 50 mAs with other parameters unchanged. The two studies were independently and prospectively interpreted for presence and location of ureteral stones and for secondary signs of urolithiasis. The study showed very high sensitivity for detection of urolithiasis with standard-dose CT (99%) and low-dose CT (93-95%). The study was limited in its ability to accurately depict small-sized calculi (< 2 mm). It was concluded from the study that low-dose CT is comparable to standard-dose CT for detection of urolithiasis[9].

A study was conducted by Paulson et al to compare the efficacy of conventional and reduced dose CT for evaluation of nephroureterolithiasis using dose reduction simulation technique. In the study, unenhanced 16-MDCT was conducted with at least 160 mA. Noise was then artificially introduced to simulate levels of 130, 100 and 70 mA. The results showed no significant reduction in detection or exclusion of renal collecting system calculi with simulated reduction of dose when compared with standard dose. However, in case of ureteral calcifications, a reduction in confidence for detection/exclusion or ureterolithiasis was noted for mA of 70

(35 mAs). It was concluded from the study that low mA (90; mAs 35) is acceptable for evaluation of nephrolithiasis, however, evaluation of ureterolithiasis may be compromised[11].

Licheng et al conducted a study in 28 patients to compare efficacy of low-dose unenhanced spiral CT with standard-dose spiral CT in patients with upper urinary tract calculi. The patients underwent CT with both standard-dose protocol (100 mAs) and low-dose protocol (25 mAs) and the scans were independently reviewed. The study showed 100% sensitivity and specificity for detection of renal and ureteral calculus, renal enlargement, and pyeloureteral dilatation. It was concluded from the study that unenhanced low-dose CT may have specificity and sensitivity similar to standard-dose CT for assessment of renal calculi[10].

El-Ghar et al conducted a study in 50 patients to evaluate the detectability, location, size and density of urinary calculi with low-dose technique (half-dose) compared with standard-dose CT in obese patients. All the patients had low-dose CT during follow-up and standard-dose CT was used as reference for comparison. The results showed that baring calculi measuring <3 mm, larger calculi had same appearance on both scans. All the calculi were detected with low-dose CT. It was concluded from the study that in obese patients with renal calculi, low-dose CT is as accurate as standard-dose CT, thereby avoiding high-dose radiation[12].

A study was conducted in 62 patients to evaluate the usefulness of low dose NCCT for diagnosis of urolithiasis. In this study, CT was performed with a tube current of 160 mA following which images were modified with introduction of image

noise to simulate tube currents of 70, 100 and 130 mA. The studies were interpreted by three different radiologists. The study showed no statistically significant differences in interobserver and intra-observer variability for detection of calculi. There was increased likelihood of calculi detection with increasing calculus size. The authors concluded that low dose CT is effective in diagnosis of urolithiasis. However, with significant reduction in tube current, the diagnostic accuracy was also lowered especially for calculi < 2 mm in size[13].

A study was conducted in 50 patients (weight < 90 kg) to determine the accuracy of low-dose NCCT in diagnosis of nephrolithiasis/urolithiasis compared with standard-dose NCCT. The patients underwent standard dose CT with 140 kVp, 135-208 mAs (mean of 160 mAs) followed by low-dose CT study with tube current reduced to 100 mA (mean of 76 mAs), while rest of the parameters remained unchanged. The studies were reviewed independently by three radiologists who were blinded to the study. Calculi were observed in 66% of patients (n = 33) of whom 25 patients (50% of total n) had renal calculi and 19 patients (n = 38%) had ureteral calculus. The accuracy rates with low-dose CT study were 91% for nephrolithiasis, 94% for ureteral calculi, 91% for obstruction, and 92% for normal finings. There was no significant difference between the readers. There was 25% reduction in radiation dose in patients who underwent CT with multidetector CT and 42% reduction in patients who underwent CT with single detector CT. The study concluded that reduction in tube current reduces radiation dose without any significant reduction in detection rate[14].

A prospective study was conducted to compare the performance of standard-dose CT with low-dose CT following tube current modulation in renal colic. A total of 150 patients underwent standard-dose CT at 95 mAs at 130 kV (6-slice MDCT) or 120 mAs at 120 kV (16-slice MDCT) and another 150 patients underwent low-dose CT at 51 mAs at 110 kV (6-slice MDCT) or 70 mAs at 120 kV (16-slice MDCT) performed with 4D tube current modulation. The reports were reviewed with two radiologists blinded to the study. Additionally, 100 studies with standard-dose CT and low-dose CT each were randomly reported by one experienced radiologist and two first-year residents. The studies showed average dose reduction of about 51.2 to 64.3% with low dose studies compared to standard dose studies. There was excellent correlation with experienced with both standard- and low-dose studies, reaching sensitivity, specificity and accuracy of 97.3% to 98.6%, 93.5%, 95.3% respectively with low-dose protocol and 97 to 100%, 100% and 98-100% respectively for standard dose protocol. There was excellent interobserver agreement. However, one of the study limitations was that standard-dose and low-dose study were performed in different patients and not in same patients. The authors concluded that low-dose CT can be used as standard procedure for evaluation of patients with suspected acute renal colic[15].

A study was conducted by Poletti et al in 125 patients to compare low-dose abdominal CT with standard-dose CT in patients with suspected renal colic. The patients underwent standard dose CT at 180 mAs and low-dose CT at 30 mAs. The studies were evaluated by independent radiologists, blinded to the study. In patients with BMI <30 kg/m^2, low-dose CT achieved 96% sensitivity and 100% specificity for detection of indirect signs of renal colic and sensitivity of 95% and specificity of 97%

for detecting ureteral calculi. However, sensitivity in diagnosis of ureteral calculi with low-dose CT was 86% for calculi < 3 mm and 100% for calculi > 3 mm. The study depicted excellent sensitivity and specificity for diagnosis of urolithiasis for calculi > 3 mm in patients with BMI < 30kg/sq. m[16].

A retrospective dose-simulation study was performed by Ciaschini et al in 47 patients with urinary calculi. Reconstruction of raw-CT data was performed at 100%, 50%, and 25% of original tube current by using dose-simulation software with tube currents averaged at 177, 88, and 44 mA respectively. All the reconstructed examination were randomized and evaluated by two radiologists, blinded to the study. A total of 108 calculi (85 renal, 21 ureteral and 2 vesical) calculi were present in 32 or 47 patients with diameter ranging from 1.4 mm to 13.2 mm (mean size 3.4 mm). For all calculi, combined sensitivities for 100%, 50%, and 25% tube current reconstructions were 83.3%, and 67.1%, respectively. For calculi > 3 mm, combined sensitivities reached values of 97.7%, 93.0%, and 91.9%, respectively, for the 100%, 50%, and 25% reconstructions. There was no significant difference between the three groups for detection of stones greater than 3 mm[17].

A study was conducted by Jin et al to evaluate effect of radiation dose reduction on sensitivity and specificity of MDCT in the diagnosis of renal calculi. The study was conducted in 14 human cadaveric kidneys in which three to five renal stones (ranging from 2.0 to 4.0 mm) were randomly placed and scanned with 16-detector CT scanner at 100, 60 and 30 mAs. The results were evaluated by two reviewers who were blinded to the study. The results showed a significant agreement between the readers

in detection of calculi of size ≥ 3 mm. There was poor detection of calculi of size 2 mm among all the tube current setting. The authors concluded that low-dose should be considered to minimize radiation exposure in diagnosis of urolithiasis[66].

A study was conducted by Karmazyn in 45 pediatric patients (age < 20 years) to evaluate the performance of low-dose CT compared to standard-dose CT for diagnosis of urolithiasis. The study included 45 children who underwent CT with standard dose (120 kVp) and effective mAs of 70 to 208 with few children having effective mAs of up to 340 mAs. Computer simulation techniques were then used to produce additional 80- and 40 mA images and the study were reviewed by three radiologists blinded to the study. There was significant reduction in radiation dose with 80 mA (mean dose reduction 67%) without any significant reduction in detection of calculi. However, at 40 mA setting, no significant reduction in detection of calculi was seen only in children weighing < 50 kg. The authors concluded that low-dose setting is helpful in diagnosing urolithiasis without significant reduction in diagnostic quality[64].

MATERIALS AND METHODS

Source of data:

Individuals with clinically/sonographically suspected urolithiasis and referred for CT evaluation at Department of Radiology, R. L. Jalappa Hospital and Research Centre attached to Sri Devaraj Urs Medical College, were screened for the study. An informed consent was taken from individuals for their willingness to participate in the study. Individuals who met the inclusion/exclusion criteria were included in the study. The study was conducted over a period of 18 months from January 2015 to June 2016.

All the patients underwent standard-dose CT before entering the study.

Inclusion Criteria:

1. Individuals aged 18 years and above.
2. Patients in whom renal/ureteric calculi are seen on standard-dose CT

Exclusion Criteria:

1. Pregnancy.
2. Women of child bearing age, unless they have undergone appropriate sterilization.
3. BMI >35 $kg.m^{-2}$.
4. Presence of suspected co-morbidities such as acute appendicitis.
5. Moribund patients.

The concern with this study evaluating efficacy of low-dose vs standard-dose CT for evaluation of urolithiasis is the risk of additional radiation with low-dose protocol. The American Association of Physicists in Medicine (AAPM) has stated that "Risks of medical imaging at effective doses below 50 mSv for single procedures or 100 mSv for multiple procedures over short time periods are too low to be detectable and may be non-existent"[52]. Hence this study is well within acceptable limits for risks associated with radiation exposure.

Additionally, patients with BMI > 35 $kg.m^{-2}$ were not included as current guidelines do not recommend low-dose CT in morbidly obese patients[23]. Few studies have shown that low-dose CT may be effective in patients with BMI > 35 $kg.m^{-2}$ however there is sparse data regarding the same[12].

Method of collection of data:

This study was approved by the institutional review board and informed consent was taken from all the individuals prior to inclusion in the study. The study was conducted in two stages.

During the first stage, individuals underwent NCCT scan (SIEMENS® SOMATOM EMOTION® 16) with standard dose protocol as per current management strategy. Individuals with CT evidence of urolithiasis were included in the second stage of the study. Individuals, who did not demonstrate urolithiasis on standard-dose CT were excluded from Stage 2 and not included in the study.

During Stage 2, individuals in whom the standard-dose CT showed presence of urolithiasis, an additional NCCT with low-dose protocol was performed (Figure 12). Both the scans were performed in a single setting.

The mAs delivered to the patient and the dose received by the patient was accurately provided by the CT equipment after the completion of each protocol and this data was recorded.

Baseline demographic data was collected, which included the gender and BMI status and the patients were grouped based on the BMI to evaluate whether BMI has any impact on detection of calculi with low-dose CT protocol[16].

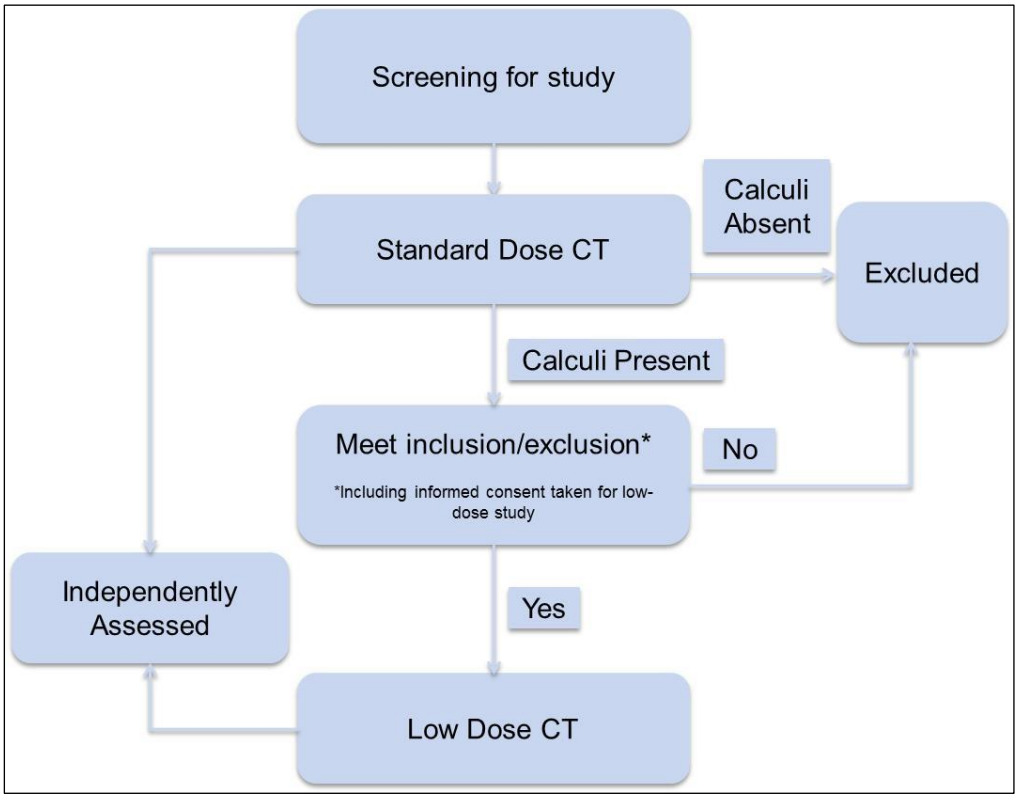

Figure 12. Study Design Schematic

CT Protocol

The following were the parameters for standard-dose and low-dose CT protocol.

Standard Dose CT

- kV – 130 kV
- Tube current – Based on the BMI the tube current varied as per the CARE Dose 4D®, the AEC software present in our current CT scanner.
- Slice thickness – 5 mm acquisition reconstructed to 1.2 mm slice thickness
- Multiplanar reconstruction using standard algorithm as and when required

Low Dose CT

- kV – 110 kV
- Tube current – Based on the BMI the tube current varied as per the CARE Dose 4D®, the AEC software present in our current CT scanner
- Slice thickness – 5 mm acquisition reconstructed to 1.2 mm slice thickness
- Multiplanar reconstruction using standard algorithm as and when required

Calculation of Effective Dose:

The effective dose was calculated as product of DLP X f (conversion factor). The CT scanner provided the DLP data. The conversion factor for CT abdomen and pelvis is 0.015 mSv/mGy cm. Hence the effective dose was calculated using Microsoft Excel® based on the following formula[48]:

Effective dose (in mSv) = DLP (in mGy cm) X 0.015 mSv/mGy cm.

Image Assessment

Two experienced radiologists reviewed the scans. The radiologists were blinded to the type of the scans (130 kVp and 110 kVp) and they assessed the studies independently. The radiologists were however aware of the clinical history and probable diagnosis in all the patients. Each study was evaluated by both the radiologists in random order and the results were compared (Figure 12). The confidence level of each radiologist was also evaluated on 3-point scale (1 = no confidence, 2 = confidence with reservation and 3 = highly confident). The radiologists evaluated the studies with respect to number, location and size of urolithiasis, and presence of hydronephrosis/hydroureteronephrosis independently in each datasets.

Statistical Analysis

Data was recorded into Microsoft® Excel® and was analyzed using OpenEpi® software. All the data were presented as mean ± SD. For radiation dose and mean mAs delivered, a paired t-test was performed to compare both the groups. Since each patient served as his/her own control, the results obtained in the standard-dose group was considered as standard and findings from low-dose group were compared with standard-dose group. Sensitivity and specificity for low-dose group was compared with results obtained from standard-dose group. A *P* value of <.05 was considered as statistically significant. The interobserver agreement among both the radiologists was evaluated for both the groups using kappa (κ) statistics: $\kappa \leq 0.2$ indicated poor agreement; κ of 0.21 to 0.40 indicated fair agreement, κ of 0.41 to 0.60 indicated moderate agreement, κ 0.61 to 0.80 indicated good agreement and κ of 0.81 to 1.00 indicated excellent agreement.

Figure 13. SIEMENS® SOMATOM EMOTION 16® CT scanner used in the study.

RESULTS

A total of 837 individuals with clinically suspected urolithiasis who underwent ultrasonography were screened for the study. Among these, 1) 603 patients were excluded from the study due to absence of ultrasonography features of renal and/or ureteral/vesicoureteral junction calculus (evidenced by absence of renal calculus, hydronephrosis/hydroureteronephrosis), and were treated symptomatically; 2) 35 patients had ureteric/vesicoureteric junction calculus or renal calculus, which was diagnostic and therefore they were not referred for CT and underwent further management for calculi; 3) 51 patients who had ultrasonography features suggestive of calculus, refused for CT scan and were therefore treated conservatively. Thus a total of 689 patients did not undergo CT evaluation.

A total of 148 patients underwent standard-dose CT for evaluation of urolithiasis. Additionally, there were 23 patients who were referred directly for CT due to high clinical suspicion of urolithiasis, constituting a total of 171 patients who underwent NCCT KUB. Among patients who underwent CT scan 16 patients were excluded from study as no calculus was detected on NCCT. Urolithiasis was seen in 155 patients who met the inclusion criteria. Among these, 26 patients declined for low-dose CT, nine patients had BMI > 35 kg/m^2 and 16 patients were of age <18 years and hence were excluded from the study. Finally there were 104 patients who underwent low-dose CT and were included in the final analysis (Figure 14).

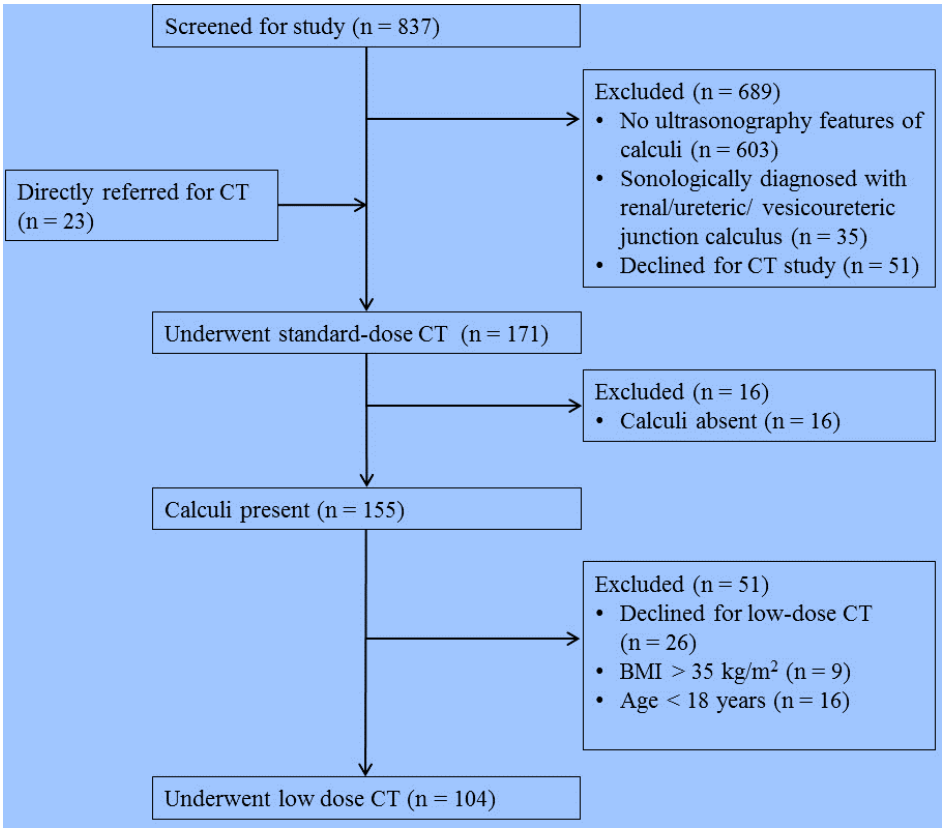

Figure 14. Flow chart showing screening of individuals for the study

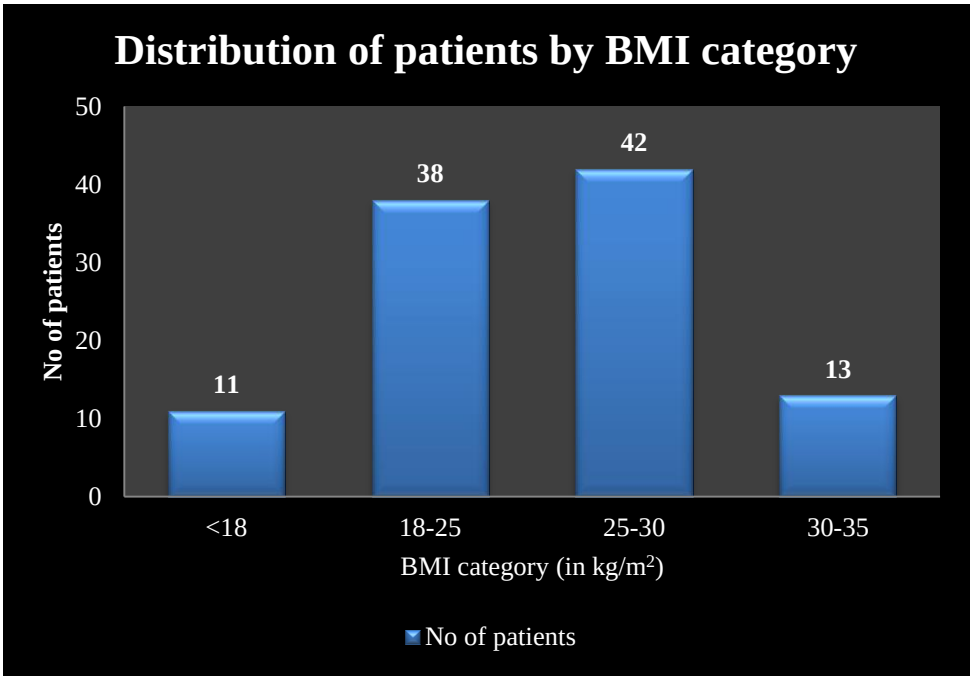

Figure 15. Distribution of patients based on BMI category

A total of 104 patients were included in this study (Figure 15). In our study, most of the patients were in the BMI category of 25-30 kg/m^2 (n = 42; 40.4%) and 18-25 kg/m^2 (n = 38; 36.5%). This was followed by BMI category 30-35 kg/m^2 (n = 13; 12.5%) (Table 6). There were only 11 patients in the BMI category <18 kg/m^2 (10.6%).

Table 6. Distribution of Patients Based on BMI Category

BMI Category (kg/m^2)	No of patients	%
<18	11	10.6
18-25	38	36.5
25-30	42	40.4
30-35	13	12.5
Total	104	100

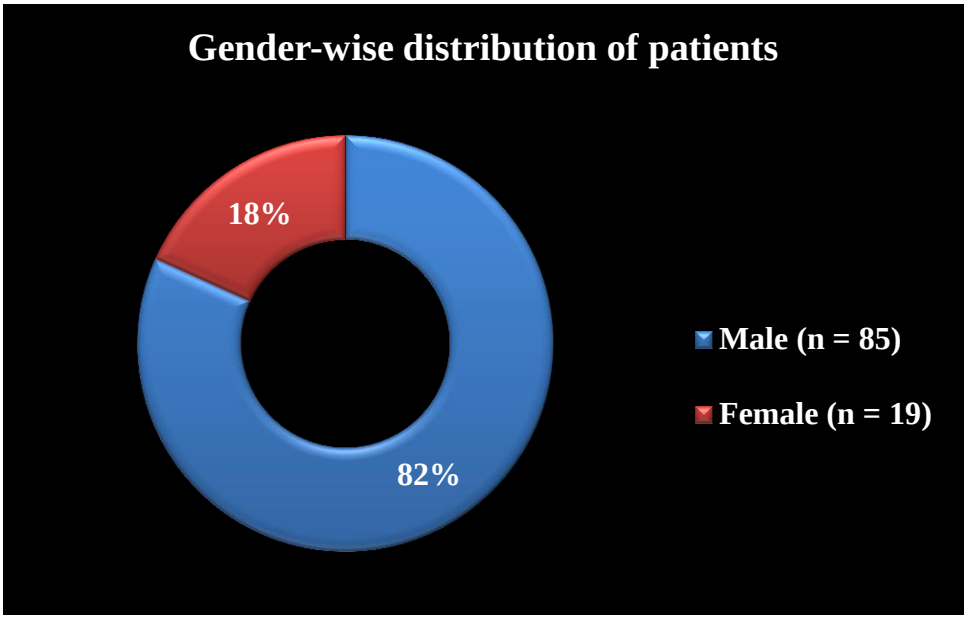

Figure 16. Gender-wise distribution of patients

In our study more than 80% of the patients were males (n = 85; 81.7%) (Figure 16) (Table 7).

Table 7. Gender-wise Distribution of Patients

Gender	No of patients	%
Male (n = 85)	85	81.7
Female (n = 19)	19	18.3

A total of 428 calculi were observed across 104 patients in both the standard- and low-dose groups (range: 1 to 19 calculi/patient). None of the calculi seen in standard-dose CT scan was missed by the low-dose CT scan (Figure 24, Figure 25, Figure 26, Figure 27, and Figure 28). A size correlation for calculi was performed on the basis that any calculus less than 3 mm is unlikely to cause symptoms and therefore is not significant. Therefore, calculi of size 2 mm or more have been considered for comparison[17]. There was an excellent correlation with respect to size of calculus in both the groups (Table 8) (Figure 29). Calculi size ranged from 2 mm to 23 mm, largest was a staghorn calculus.

Table 8.Interobserver Sensitivity for Detection of Calculi in Standard- and Low-Dose Groups

Reader	**Standard-dose CT (sensitivity)**	**Low-dose CT (sensitivity)**	**% difference in sensitivity**	***P* value**
1	428/428 (100%)	428/428 (100%)	nil	NS
2	428/428 (100%)	428/428 (100%)	nil	NS
1 and 2	856/856 (100%)	856/856 (100%)	nil	NS
NS = not significant				

The sensitivity for detection of calculi in both the standard- and low-dose groups was considered to be 100% as none of the calculi seen on standard-dose CT were missed on low-dose CT. Similarly there was an excellent inter-observer agreement with a κ value of 0.99. None of the calculus seen by radiologist 1 was missed by radiologist 2 and vice versa (Table 8).

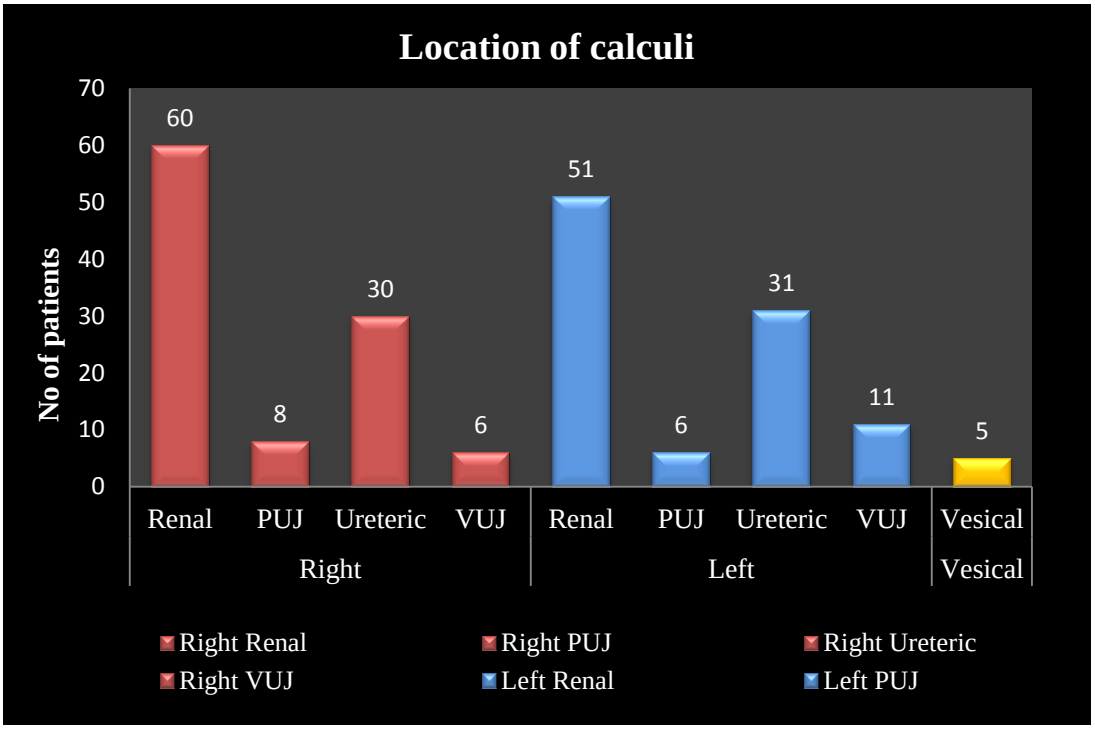

Figure 17. Location and distribution of calculi

Figure 17 shows the location and distribution of calculi seen at different locations. Majority of the calculi were in kidneys (111 of 208; 53.4%) followed by ureters (61 of 208; 29.3%), vesicoureteric junction (VUJ) (17 of 208; 8.2%), pelviureteric junction (PUJ) (14 of 208; 6.7%) and lastly urinary bladder (5 of 208; 2.4%) (Table 9). All the cases with PUJ calculus demonstrated hydronephrosis and all the cases with ureteric and VUJ calculus demonstrated hydroureteronephrosis. Hydronephrosis was seen in seven patients on right side and six patients on left side and hydroureteronephrosis was seen in 35 patients on right side and 41 patients on left side. One patient had both right PUJ and right ureteric calculus and one patient had both ureteric and VUJ calculus on right side. One patient had both ureteric and VUJ calculus on left side (Figure 18). There were eight patients who had bilateral hydroureteronephrosis and one patient had bilateral hydronephrosis.

Table 9. Location and Distribution of Calculi

Location of calculus		Number of patients	%
Right	Renal	60	28.8
	PUJ	8	3.8
	Ureteric	30	14.4
	VUJ	6	2.9
Left	Renal	51	24.5
	PUJ	6	2.9
	Ureteric	31	14.9
	VUJ	11	5.3
Vesical	Vesical	5	2.4

PUJ = pelviureteric junction; VUJ = vesicoureteric junction

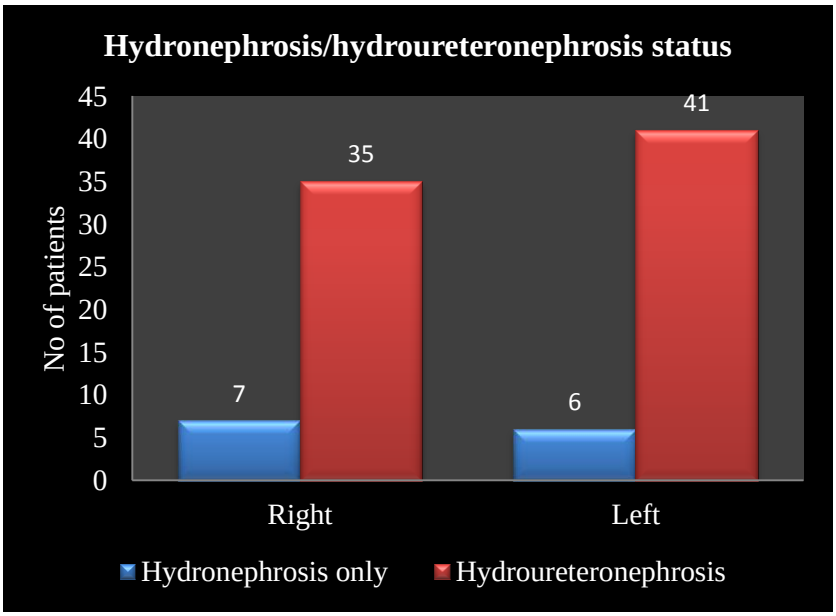

Figure 18. Status of hydronephrosis and hydroureteronephrosis

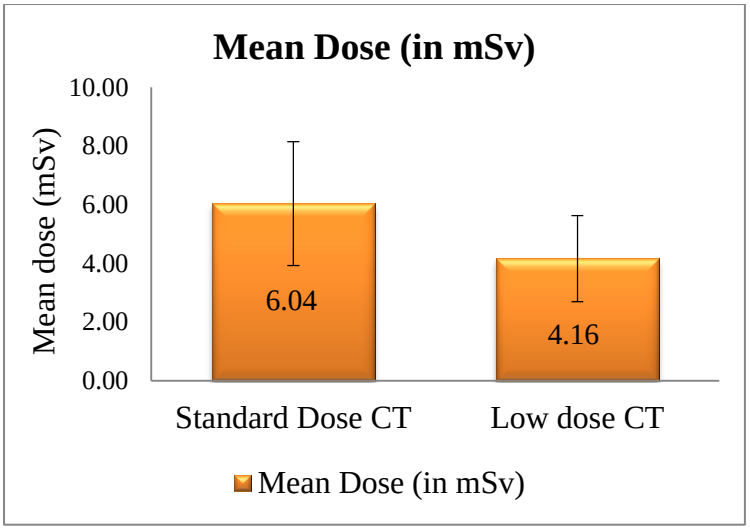

Figure 19. Mean CT radiation dose (in mSv) across standard-dose and low-dose groups. mSv = milli Sieverts

The mean effective radiation dose in the standard-dose group was 6.04 ± 2.11 mSv (mean ± SD) (range: 2.63 to 15.39 mSv) and in the low-dose group was 4.16 ± 1.47 mSv (mean ± SD) (range: 1.84 to 9.86 mSv) with a mean difference of 1.88 ± 0.69 mSv (mean ± SD) (range: 0.71 to 5.53 mSv) between the groups (Figure 19). There was an overall reduction of radiation dose by 31.21 ± 3.15% (mean ± SD) (range: 22.45% to 41.4%) in the low-dose group compared with standard-dose group, which was statistically significant (p<.0001) (Table 10).

Table 10. Mean Dose (in mSv) Across Standard-Dose and Low-Dose Groups

Group	**Mean Dose (in mSv)***	**SD**
Standard Dose CT	6.04	2.11
Low dose CT	4.16	1.47
Dose Reduction (mean %)	1.88 (31.21%)	0.69 (3.15%)

*P<.0001
mSv = milli Sievert; CT = Computed tomography; SD = Standard deviation

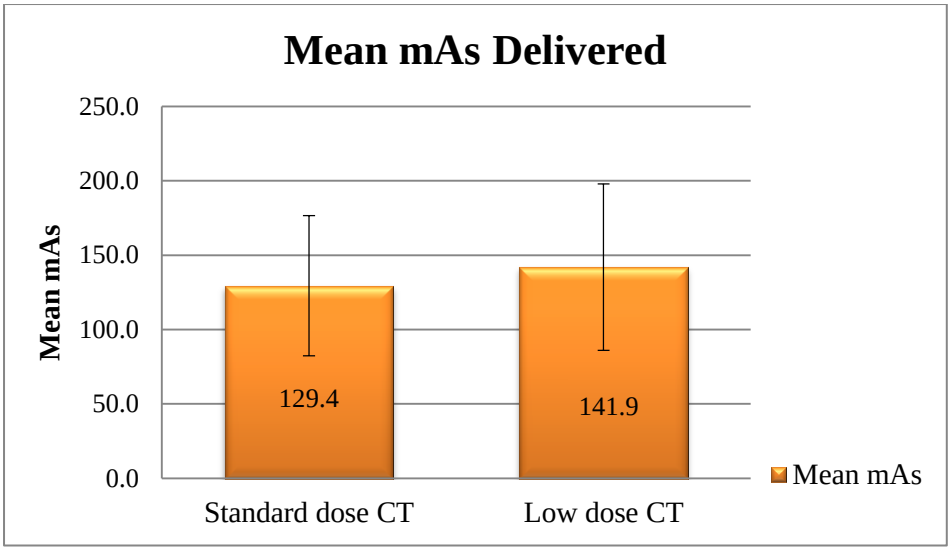

Figure 20. Mean mAs delivered across standard-dose and low-dose groups.

mAs = milli Ampere second.

The mean mAs delivered in the standard-dose group was 129.4 ± 47.15 mAs (mean ± SD) (range: 61 to 244 mAs) and across the low-dose group was 141.9 ± 55.95 mAs (mean ± SD) (range: 63 to 310 mAs). There was an increase in the mean mAs in the low-dose group by about 8.83 ± 5.48% (mean ± SD) (range: 3.28% to 53.46%); however, this difference was not statistically significant (p = .08) across the study.

Table 11. Mean mAs Delivered Across Standard-Dose and Low-Dose Groups

Group	Mean mAs*	SD
Standard dose CT	129.4	47.15
Low dose CT	141.9	55.95
Difference (in %)	8.83	5.48

*P = .08 (not significant)
mAs = milli Ampere second; CT = computed tomography; SD = standard deviation

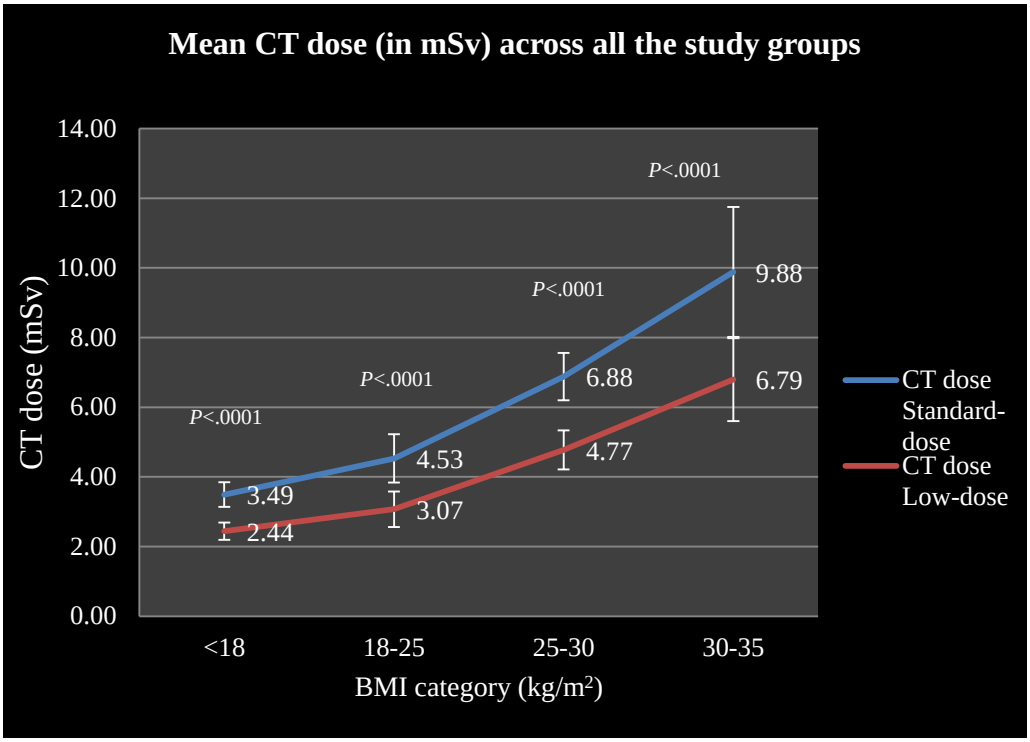

Figure 21. Mean radiation dose (in mSv) across all the BMI category groups.

A subgroup analysis was performed to evaluate if the reduction in radiation dose was consistent across all BMI categories. Figure 21 shows the mean CT dose across all the study groups. There was significant reduction in radiation dose received with low-dose CT across all the BMI categories (Table 12) with *P*<.0001. Additionally, the quantum of dose reduction across the various BMI groups was also evaluated (Figure 22). There was similar dose reduction across all the groups, which was comparable to overall dose reduction observed in our study. This suggests that irrespective of BMI status the dose reduction was consistent (Table 13). The mean reduction in radiation dose in the BMI category <18 kg/m^2 was 29.94 ± 2.98% (mean ± SD) (range 22.45 to 33.09%). The mean radiation dose reduction in BMI category 18 to 25 kg/m^2 was 32.26 ± 3.2% (mean ± SD) (range: 24.24 to 39.91%). The mean reduction in radiation dose in BMI category 25 to 30 kg/m^2 was 30.66 ± 2.35% (mean ± SD) (range: 26.92 to 38.29%) and the mean radiation dose

reduction in the BMI category 30 to 35 kg/m^2 was 31.03 ± 4.29% (mean ± SD) (range: 26.3 to 41.4%) (Table 13).

Table 12. Mean radiation dose (mSv) across all BMI category groups

BMI Category (kg/m^2)	Standard dose		Low dose		*P* value
	Mean dose	Standard deviation	Mean dose	Standard deviation	
<18	3.49	0.36	2.44	0.25	<.0001
18-25	4.53	0.69	3.07	0.51	<.0001
25-30	6.88	0.68	4.77	0.56	<.0001
30-35	9.88	1.86	6.79	1.19	<.0001
BMI = body mass index; mSv = milli Sievert					

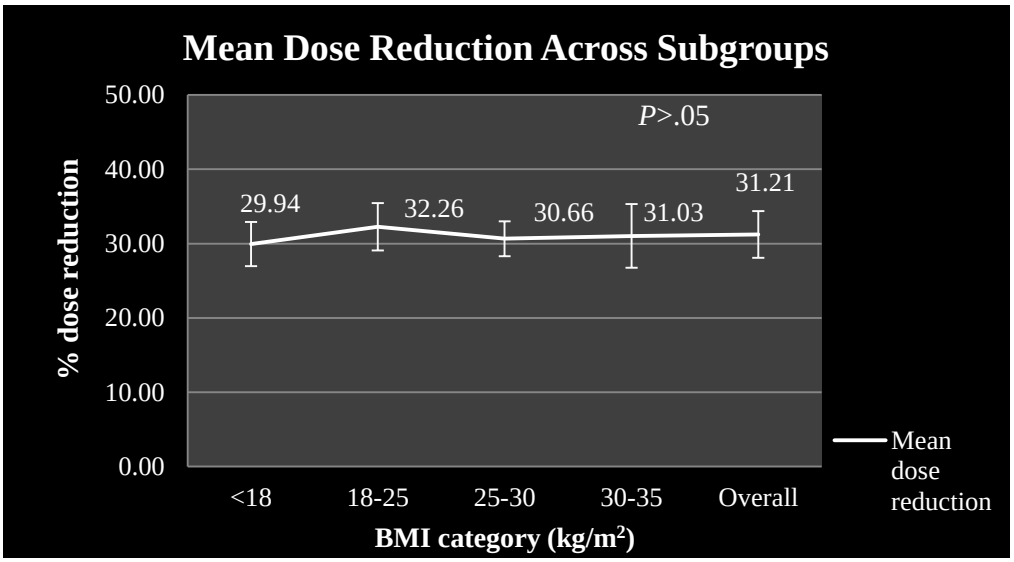

Figure 22. Mean dose reduction across subgroups

Table 13. Mean Dose Reduction Across Subgroups vs Overall Study

BMI Category (kg/m^2)	Mean dose reduction	SD
<18	29.94	2.98
18-25	32.26	3.20
25-30	30.66	2.35
30-35	31.03	4.29
Overall*	31.21	3.15
*P>.05 BMI = body mass index; SD = standard deviation		

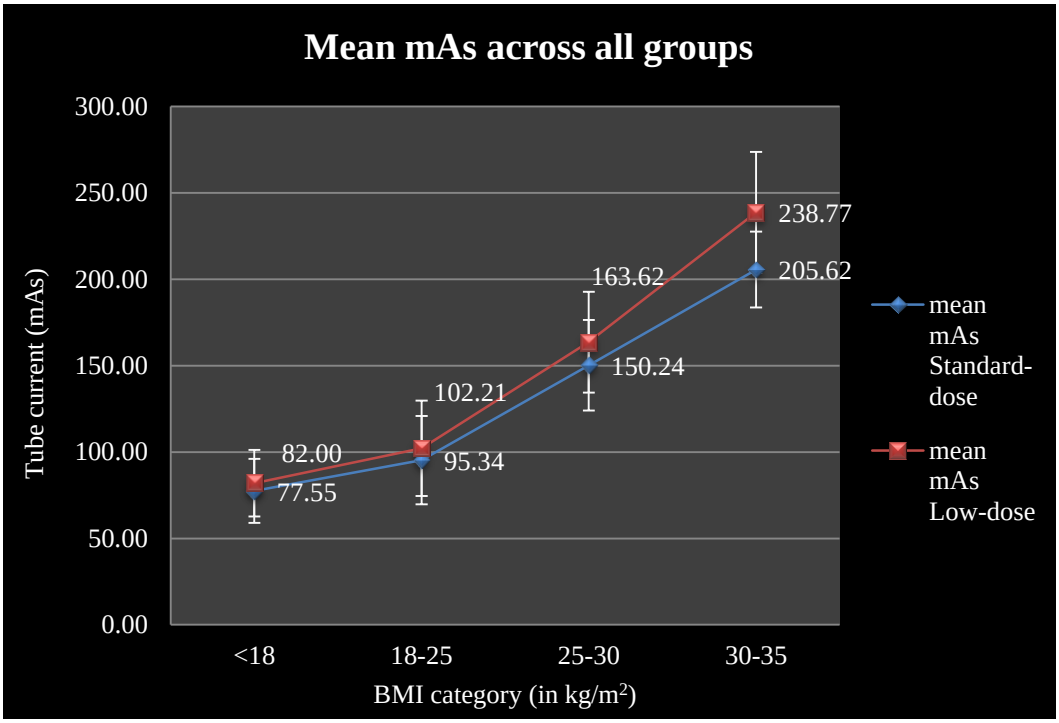

Figure 23.mean mAs across all BMI groups

Similarly a comparison between increase in tube current with both standard and low dose CT was evaluated across BMI groups. Figure 23 shows the mean mAs delivered across the BMI categories. There was a non-significant increase in tube current with low-dose CT protocol in the BMI categories <18 and 18-25 group, whereas the difference in tube current in BMI categories 25-30 and 30-35 group assumed statistical significance (*P* = .03 and *P* = .008 respectively) (Table 14).

Table 14.Mean mAs Across all BMI Category Groups

BMI Category (kg/m^2)	**Standard dose**		**Low dose**		***P* value**
	Mean mAs	Standard deviation	Mean mAs	Standard deviation	
<18	77.55	18.57	82.00	19.32	0.59
18-25	95.34	25.59	102.21	27.56	0.26
25-30	150.24	26.18	163.62	29.11	0.03
30-35	205.62	21.99	238.77	34.98	0.008
BMI = body mass index					

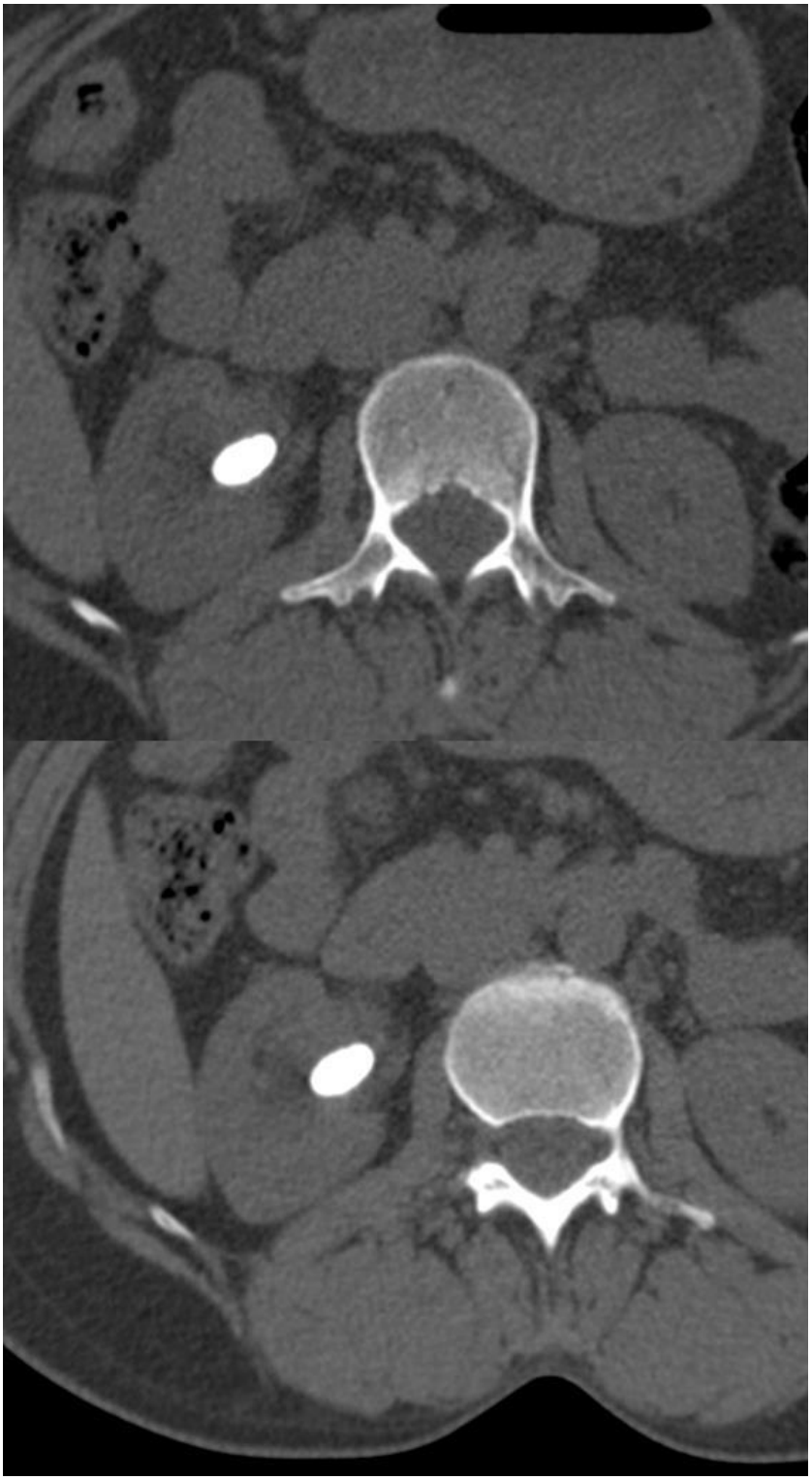

Figure 24. Comparison of standard-dose (top) and low-dose CT (bottom) image quality in a patient with right renal pelvis calculus. Note the slight increase in noise in the low-dose CT study; however there is no change in calculus size.

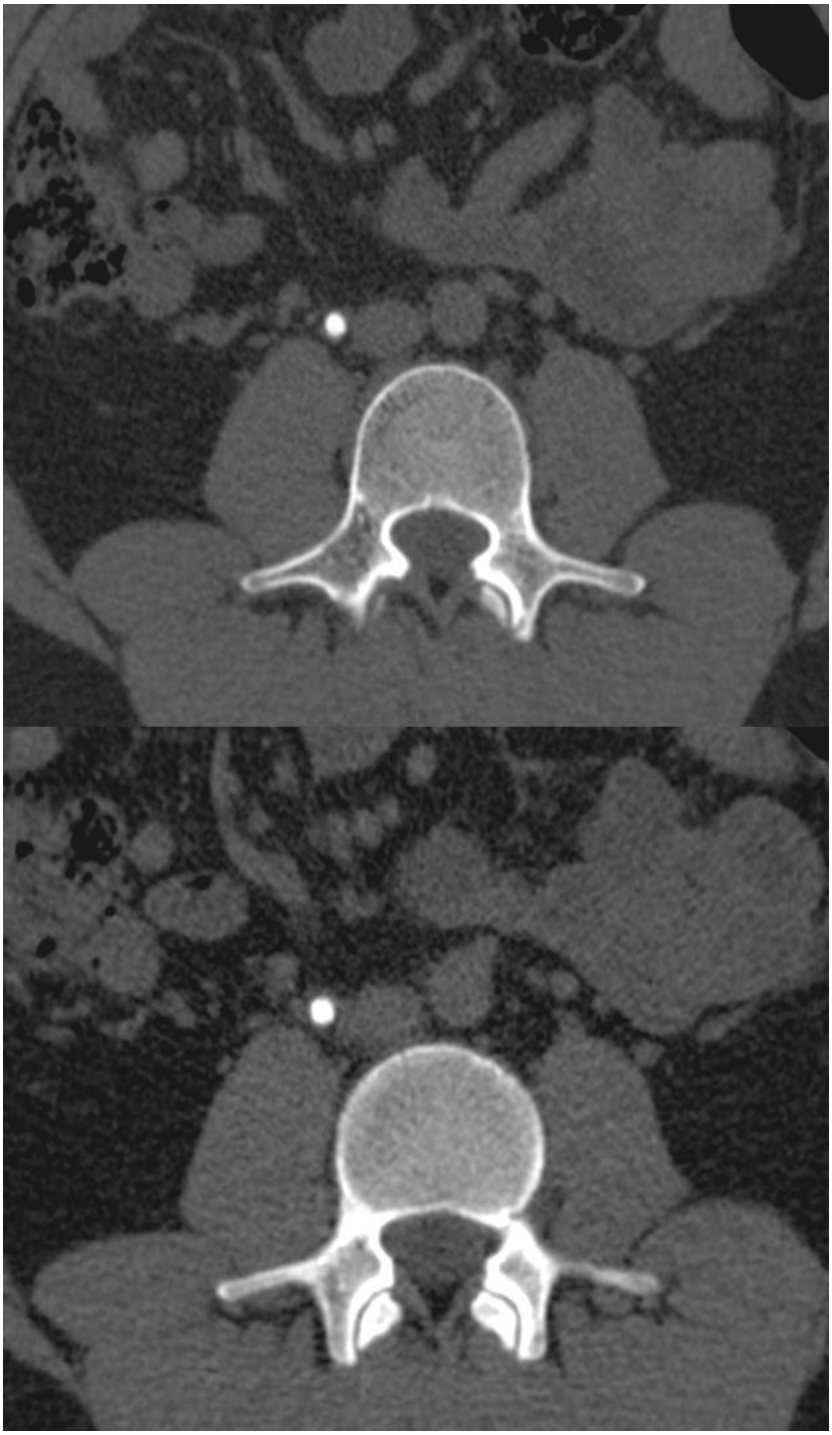

Figure 25. Comparison of standard-dose (top) and low-dose CT (bottom) image quality in a patient with right mid-ureteric calculus. As shown in the previous image, there is slight increase in noise in the low-dose CT study; however there is no change in calculus size.

Figure 26. Comparison of standard-dose (top) and low-dose CT (bottom) image quality in a patient with left terminal ureteric calculus. There is ureteric wall thickening. Note the slight increase in noise in the low-dose CT study, however there is no effect on visualization of surrounding changes such as periureteric edema.

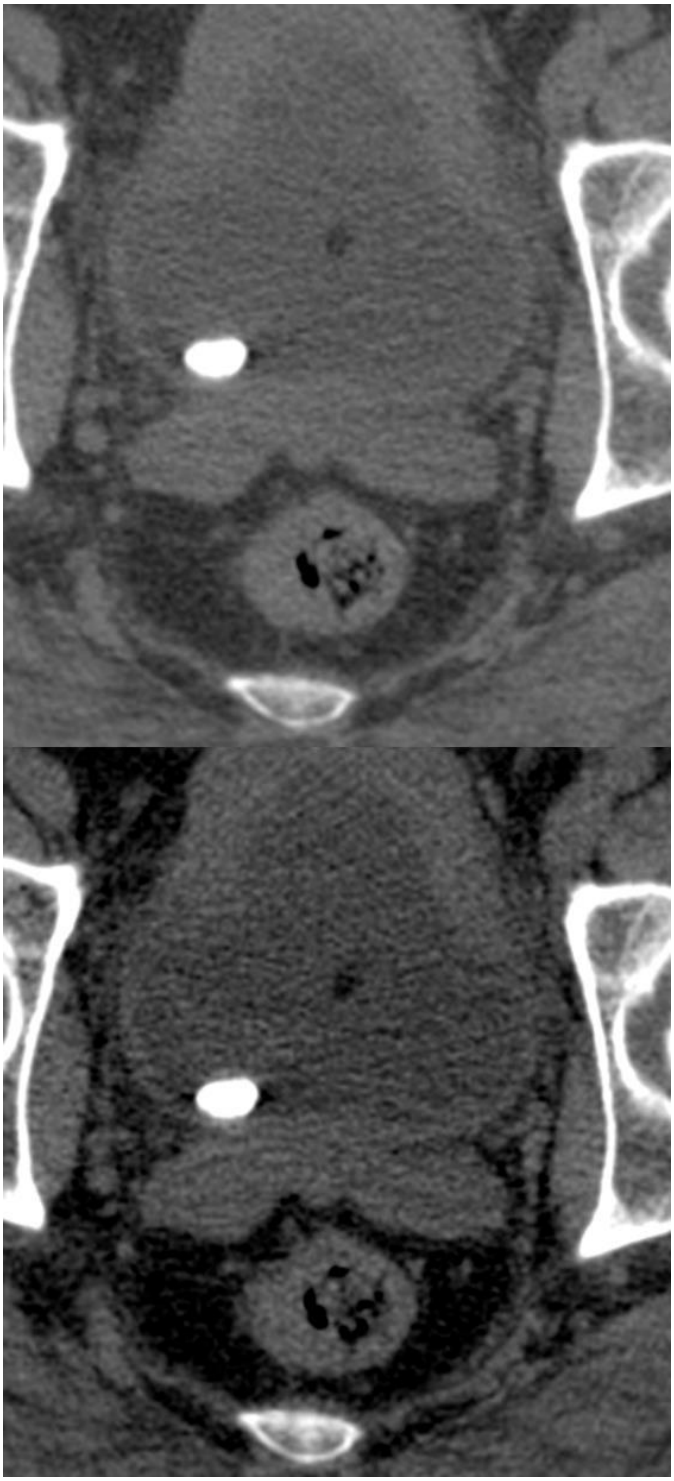

Figure 27. Comparison of standard-dose (top) and low-dose CT (bottom) image quality in a patient with vesical calculus. Note the slight increase in noise in the low-dose CT study. Beam hardening artifact caused by the calculus is seen in both the studies.

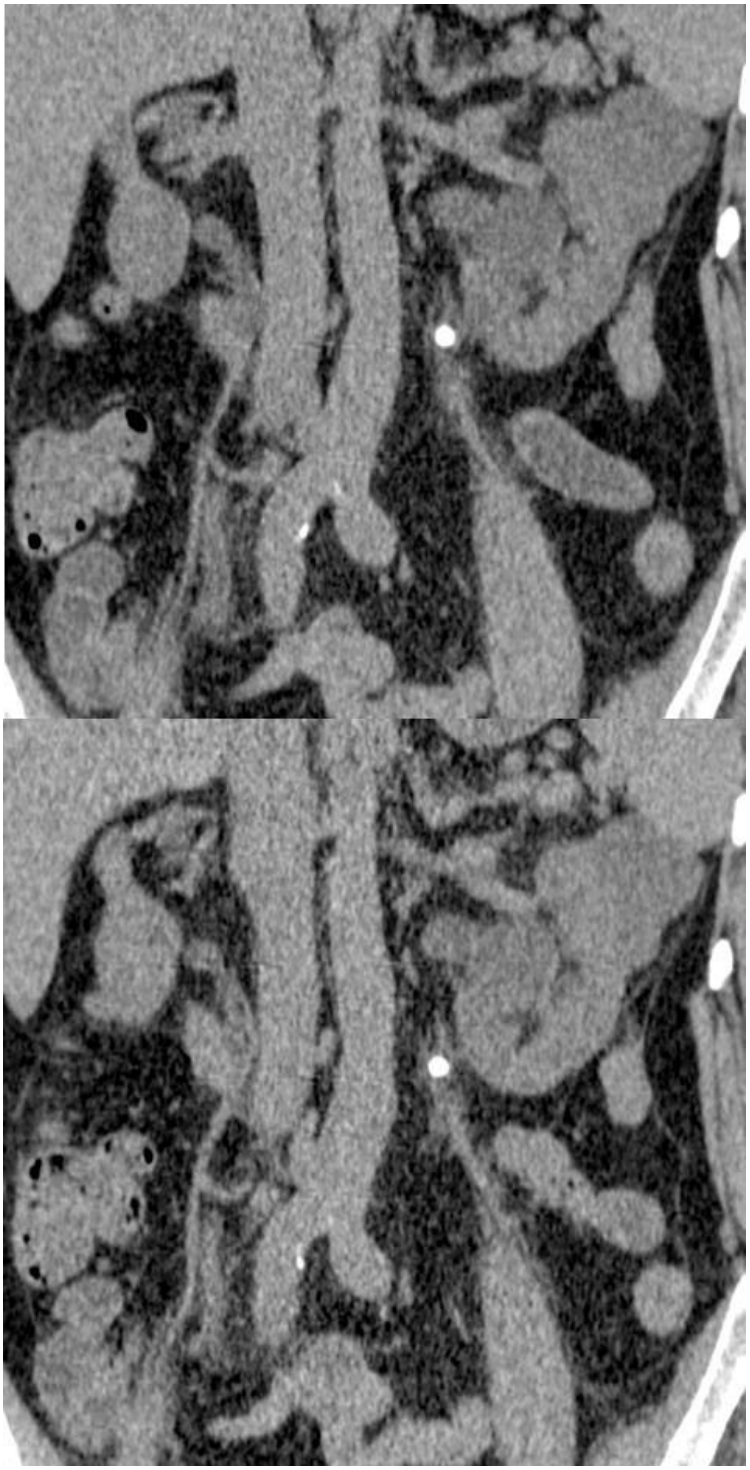

Figure 28. Coronal reformatted images comparing standard-dose (top) and low-dose CT (bottom) image quality in a patient with left upper ureteric calculus and left hydroureteronephrosis. There is increase in noise with low-dose CT study; however, there is no effect on visualization of surrounding changes such as periureteric fat stranding.

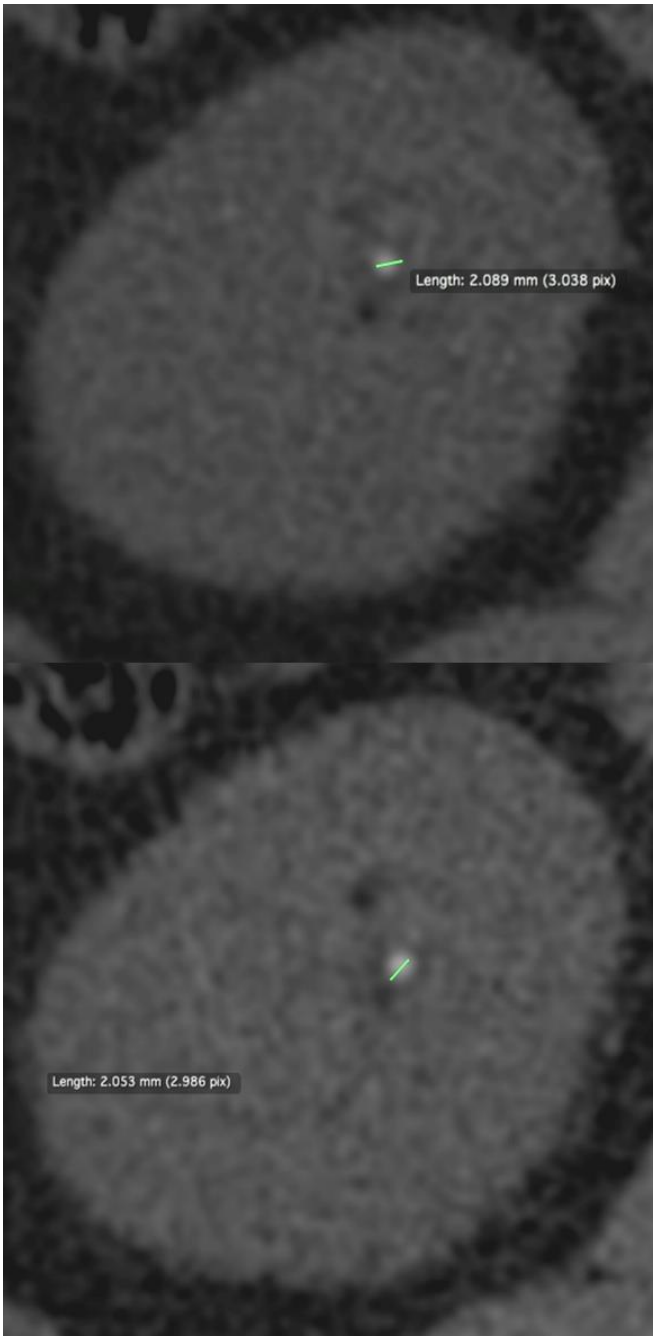

Figure 29. Comparison of standard-dose (top) and low-dose CT (bottom) magnified images in a patient with left lower pole calculus for size of calculi. There is increase in noise with low-dose CT study. There is excellent agreement in terms of calculus size with standard- and low-dose CT.

DISCUSSION

In urology practice, diagnostic evaluation and management of renal calculi accounts for a sizeable portion of day-to-day practice. Patients with renal calculi have high risk of recurrence and often need to undergo multiple imaging studies before, during, and after treatment[2,3]. Increasing use of CT has made it the commonest cause of medical radiation[7,8]. The increase in number of CT studies being conducted every day indicates that the background radiation from CT studies is going to increase. It is therefore necessary to reduce radiation from CT wherever possible.

A multicentric study by Ferrandino et al evaluated the effective radiation dose received due to CT studies in individuals with acute renal calculi episodes and short-term follow-up. They observed that up to 20% of patients received radiation dose of > 50 mSv, which is the recommended annual dose limit for short term studies[52,67]. Similarly another study by Manohar and McCahy in patients in Australia with renal calculi showed that up to 44% of patients were exposed to radiation dose of at least 50 mGy and at least 14% of patients were exposed to radiation of 100 mGy due to CT scans alone over short period of time. The authors concluded that there is a need to reduce radiation dose in patients with renal calculi and recommended low-dose CT whenever feasible[68].

Various studies have shown efficacy of low-dose CT protocol for diagnosis of urolithiasis[9,13,14]. There are very few studies, which have systematically compared

low-dose CT protocol with standard-dose CT protocol in the same patient population – these studies have shown high sensitivity and specificity (up to 100%) for diagnosis of urolithiasis with low-dose CT. All the studies recommend use of low-dose CT for diagnosis of urolithiasis[10,12,14,16].

In our study we have compared the diagnostic yield with low-dose CT scan when compared with standard-dose CT scan in the same patient population. We consider this model better compared with randomizing patients to either standard-dose or low-dose study as was performed in the study of Mulkens et al[15]. Our study also has certain advantages over other evaluation models, which have employed artificial introduction of noise to mimic low-dose CT images. In those studies it is possible that other factors that influence scan quality such as kVp, pitch, manufacturer, and importantly effect of tube current modulation may not be evaluated[11].

We utilized automated tube current setting based on CARE Dose 4D software (Siemens®), which modulated tube current based on patient's body habitus both in standard-dose and low-dose studies[48]. Although, this model has not been explored fully for diagnosis of urolithiasis it holds significant promise.

Our study consisted of 104 patients. Although there is a wide variability among sample size in various studies, our patient population was comparable to other similar studies, where sample size ranged from 28 to 125 patients[10,14,16,69]. Most of the

studies had a predominance of males[14,16,69], which is similar to observations seen in our study.

In our study of 104 patients with 428 calculi, none of the calculi seen in the standard-dose CT were missed on low-dose CT. There was excellent calculus size agreement. There was a statistically significant reduction (p<.0001) in mean effective radiation dose in the low-dose group (4.16 ± 1.47 mSv; mean ± SD) compared with the standard-dose group (6.04 ± 2.11 mSv; mean ± SD) with a mean difference of 1.88 ± 0.69 mSv (mean ± SD) (Figure 19). There was an overall increase in mean mAs delivered by about 8.83 ± 5.48% (mean ± SD) in the low-dose group (141.9 ± 55.95 mAs; mean ± SD) compared with the standard-dose group (129.4 ± 47.15 mAs; mean ± SD). However, this difference was not statistically significant (p = .08) across the study. We reduced the tube potential by about 15.4% and achieved a mean reduction in radiation dose by 31.21 ± 3.15% (mean ± SD).The dose reduction was similar across all the subgroups studied, irrespective of the BMI status. These results are comparable to the theoretical dose reduction, which states that the dose reduction is approximately proportional to square of tube voltage change. In our study, the tube voltage reduction would have resulted in approximately 28.4% reduction in radiation dose[42,43]. There are seen several studies, which have shown higher reduction in radiation dose compared to our study. However, these studies have employed fixed kV and mAs protocols for standard-dose and low-dose CT[9,11,13,16]. Other studies which employed fixed kV with variable mAs have also reported dose reduction, proportionate to decrease in tube current (approximately 25% to 42% reduction in radiation dose)[14].

Reduction in tube voltage (kVp) is considered as an extremely effective means for decreasing radiation exposure. However, all things unchanged, reduction in tube voltage results in non-linear increase in image noise, possibly due to reduced tissue penetration of photons. This reduces the contrast-to-noise ratio, which can be compensated by increase in mAs to preserve image quality. Use of automated tube current modulation or AEC in our study resulted in increase in mAs in the low-dose group with preserved image quality. There is however no guideline on the quantum of increase in mAs required to reduce contrast-to-noise ratio[43]. The current CT scanners support the use of low kV setting as they can operate at lower tube potential setting since the X-ray tubes are capable of achieving higher tube current. Most of the CT equipments in use offer adjustment of tube potential in steps of 20 kV, which was the case in our study. Additionally, the availability of iterative image reconstruction techniques helps in reducing image noise while preserving contrast among tissues[70].

Dose reduction with lower tube potential has been evaluated in many studies involving conventional thoracoabdominal CT, coronary and carotid CT angiography, and pulmonary angiography[71,72,73]. A study by Funama et al evaluated reduction in radiation dose in abdominal CT when performed at 120 kV and 90kV using a phantom model. In their study they observed that low-dose CT results in approximately 35% reduction in radiation dose compared to standard-dose CT[74]. Similarly, Tang et al investigated effect of low tube voltage (80 kV) on image quality, radiation dose and low-contrast detectability on abdominal CT in a phantom study. In that study, the tube current was set at 150 to 650 mAs at 80 kV and 300 mAs at

120 kV. Their study showed no statistically significant difference in contrast-to-noise ratio and low-contrast detectability with low-dose CT protocol. The authors concluded that a reduction of tube voltage from 120 kV to 80 kV results in radiation dose reduction by 32% to 42% without worsening of contrast-to-noise ratio and low-contrast detectability[75]. In another study evaluating efficacy of low tube voltage by Nakayama et al, 40 patients underwent initial abdominal CT at 120 kV followed by CT at 90 kV with a constant tube current at 300 mAs. Although the mAs was higher than the standard used, it was still well within the safe range. The authors reported radiation reduction ranging from 46.2% to 56.8% with lower kV setting[76]. All these study results have shown radiation dose reduction comparable to that obtained in our study, which is based on reduction in tube potential together with AEC.

The other techniques in which dose reduction can be achieved in the modern CT scanners include tube current modulation and using iterative reconstruction models. Currently, almost all of the CT scanner vendors have automatic tube current modulation or AEC. This allows the machine to modulate the radiation dose by changing tube current-time product (mAs) depending on the patient's size and attenuation. This helps to optimize attenuation in various organs, such as abdomen, which requires lower attenuation compared to other body parts such as shoulders[43]. The AEC used in our study is the CARE Dose 4D® (Siemens®). This technique makes use of effective mA and compensates helical pitch for given tube mA. It assesses the size and shape of patient and automatically adapts radiation dose based on these parameters. This dose optimization is achieved by two ways. The tube current is modified based on topogram, where the machine compares the actual patient size to "standard-sized" patient. Additionally, AEC also takes into account the body part

under evaluation as different body parts may require different mAs. Therefore a smaller patient receives smaller mAs dose and a heavier patient receives larger mAs dose[48,77]. AEC in majority of equipments irrespective of manufacturer is relatively similar; however the strength of modulation algorithm and the minimum acceptable image quality may differ. These parameters can be adjusted manually in most of the CT scanners[43]. Thus in our study, a combination of AEC and lower tube potential helped to effectively reduce radiation dose (measured in mSv) without affecting image quality.

In the present study, $CTDI_{vol}$ and DLP were used for calculation of radiation dose. DLP refers to the total amount of radiation incident on the patient and is the product of $CTDI_{vol}$ and the scan length. DLP helps to estimate the effective radiation dose received by the patient and therefore evaluate radiation burden on the patient. Estimation of effective radiation dose using $CTDI_{vol}$ and DLP is currently considered as standard evaluation technique[38,48,78]. The CT scanner used in our study displays the $CTDI_{vol}$ for each study which is based on various parameters including pitch of the scan and patient's body habitus. This helps to ensure more accurate data to evaluate radiation dose received by the patient[48].

In our study we classified patients based on the BMI category. The BMI categories 25 to 30 kg/m^2 (n = 41) and 18 to 25 kg/m^2 (n = 36) constituted majority of patients. There was significant reduction in radiation dose received across all the BMI categories and was similar across all the four groups (Table 12) with $P<.0001$. We concluded that dose reduction was consistent across all the BMI groups (Table 13). A

comparison between increase in tube current with both standard and low dose groups was also evaluated. There was increase in the tube current with low-dose protocol in the BMI categories <18 and 18-25 kg/m^2 groups, which was statistically not significant ($P = .59$ and $P = .26$ respectively); whereas the difference in tube current in BMI categories 25-30 and 30-35 kg/m^2groups assumed statistical significance ($P = .03$ and $P = .008$ respectively). This suggests that with increasing BMI, the mean increase in mAs becomes statistically significant with low-dose CT compared with standard dose-CT. However, the overall reduction in radiation dose is similar irrespective of BMI category.

The subgroup analysis was performed to determine if BMI has an impact on dose reduction and efficacy of low-dose CT in our study. It is known that BMI may affect the performance of CT study. A meta-analysis by Neimann et al observed that the effects of CT dose reduction in obese patients may be unclear[4] with some studies showing lower sensitivity of low-dose CT for diagnosis of urolithiasis[16], while some studies have reported no significant differences in terms of calculi detection[15]. A study by Tack et al comparing efficacy of standard- and low-dose CT used additional 60 mAs to supplement the low-dose protocol in obese patients, suggested that use of blanket low-dose CT without considering BMI may be ineffective in obese patients[65]. Additionally, Kalra et al observed a linear correlation between patient size and image quality and suggested that a similar dose reduction in obese and non-obese patients may not be feasible as there may be more image degradation in obese patients[79]. This also highlights the importance of AEC in dose-reduction studies, as a tailor made dose reduction is more effective across different populations. It is widely accepted that with the introduction of AEC technology, the focus in low-dose CT should be on

increase on image noise and not as much on absolute tube current[4]. Furthermore, Huda et al have shown that although the energy imparted by CT increased with patient's size, the corresponding effective radiation dose is smaller in large phantoms compared with small phantoms[80]. Tack et al observed that as pelvic organs constitute for a significant part of radiation dose as they are close to centre of pelvis, the effective dose in obese patients should be lower than underweight patients. The authors therefore concluded that an increase in mAs may not translate to increased effective radiation dose[65]. El-Ghar et al have shown that use of AEC in patients with BMI > 30 kg/m^2 reduces the radiation significantly compared to using fixed dose mAs[12]. In our study, we have demonstrated significant dose reduction with low-dose CT irrespective of BMI status. Moreover the compensatory increase in mAs (more so in the BMI category 25-30 and 30-35 kg/m^2) has not necessarily translated into increased radiation dose.

It may be logical to use a standard-dose protocol for the initial study in patients who have non-specific renal colicky pain in order to evaluate other structures in the abdomen. For subsequent imaging, when the indication is only renal/ureteric calculi, low-dose protocols may be used in order to achieve lower radiation to the patients. Additionally, in a patient with history of previous renal colic, a low-dose CT study may be prudent.

Our study has certain limitations. First, most of the patients in our study were from BMI category 25 to 30 and 18 to 25 kg/m^2. We had comparatively smaller sample size in BMI category 30 to 35 kg/m^2, which probably limited comparison

across other subgroups. Nevertheless, our results have shown uniform reduction of radiation across all the BMI category groups. Future studies in obese patients will help to confirm the efficacy of low-dose CT. Second, we did not evaluate if BMI > 35 kg/m^2 has any impact on radiation dose reduction and image quality. Currently there is sparse data on the same and considering the body weight, it may not be feasible to use low-dose CT protocol in these patients. Third, we also did not evaluate the accuracy of ancillary CT findings at reduced tube potential settings. However, our study was not designed for this purpose, which makes this limitation less relevant. Fourth, although the studies were blinded between the readers, the slight increase in image noise in low-dose group may have inadvertently introduced reporting bias. Lastly, our study design was based on AEC model, which can vary from machine-to-machine and is manufacturer specific. Some old generation machines may not have AEC modulation technology. Nonetheless, most of the scanners employ similar technology and the results can be extrapolated to other machines as well[43,70].

CONCLUSION

We conclude that use of low tube potential setting by tube voltage reduction of 15% significantly reduced radiation dose by approximately 31% in patients undergoing CT for evaluation of urolithiasis, irrespective of their BMI. Although there is increase in the mAs to offset increase in noise at lower tube potential setting, use of AEC helps to achieve optimal dose reduction. AEC also helps to personalize the radiation dose received by each patient based on their BMI, thereby optimizing image quality. Therefore, a combination of reduced tube potential and AEC helps to achieve optimum results for diagnosis of urolithiasis. We strongly support the use of low-dose CT for diagnosis and follow-up of urolithiasis in patients who are not morbidly obese.

SUMMARY

Patients with renal calculi often undergo multiple imaging studies before, during, and after treatment. Additionally, these patients are at high risk of recurrence, with recurrence rates as high as 75% in 20 years. CT is currently the investigation of choice in the diagnosis of urolithiasis, but is associated with risk of radiation. There is need to use low-dose CT study whenever feasible. There are very few studies conducted in Indian subcontinent comparing standard-dose and low-dose CT. It is therefore necessary to obtain data on usefulness of low-dose CT when compared with standard-dose CT in this population.

The objectives of the study are to evaluate the efficacy in terms of sensitivity and specificity with low-dose CT when compared with standard-dose CT for detection of urolithiasis, to understand the potential limitations of using low-dose CT when compared with standard-dose CT for detection of urolithiasis and to help formulate appropriate strategies for diagnosis and follow-up of urolithiasis

Individuals with clinically/sonographically suspected urolithiasis and referred for CT evaluation at Department of Radiology, R. L. Jalappa Hospital and Research Centre were screened for the study. The study was conducted for a period of 18 months from January 2015 to June 2016. All the patients underwent standard-dose CT before entering the study. The addition of low-dose CT protocol to standard-dose protocol is not expected to have any significant impact radiation risk.

The study was conducted in two stages. During the first stage, individuals underwent NCCT scan (SIEMENS® SOMATOM EMOTION® 16) with standard dose protocol as per current management strategy (130 kVp along with mAs as per CARE Dose 4D). Individuals with CT evidence of urolithiasis were included in the second stage of the study. Individuals, who did not demonstrate urolithiasis on standard-dose CT were excluded from Stage 2 and not included in the study. During Stage 2, individuals in whom the standard-dose CT showed presence of urolithiasis, an additional NCCT with low-dose protocol was performed (110 kVp along with mAs per CARE Dose 4D). Both the scans were performed in a single scan setting. Two experienced radiologists reviewed the scans. The radiologists were blinded to the type of the scans (130 kVp and 110 kVp) and assessed the studies independently.

In our study we have compared the diagnostic yield with low-dose CT scan when compared with standard-dose CT scan in the same patient population. We reduced the tube voltage with automated tube current setting based on CARE Dose 4D software (Siemens®), which modulated tube current based on patient's body habitus both in standard-dose and low-dose studies. A total of 837 individuals with clinically suspected urolithiasis who underwent ultrasonography were screened for the study. Finally there were 104 patients who underwent low-dose CT and were included in the study. Majority of the patients were males (>80%). A total of 428 calculi were observed across 104 patients in both the standard- and low-dose groups (range: 1 to 19 calculi/patient). None of the calculi seen in the standard-dose CT were missed on low-dose CT with excellent calculus size agreement. There was an excellent interobserver agreement among both the radiologists.

There was a statistically significant reduction (P<.0001) in mean effective radiation dose in the low-dose group (4.16 ± 1.47 mSv; mean ± SD) (range: 1.84 to 9.86 mSv) compared with the standard-dose group (6.04 ± 2.11 mSv; mean ± SD) (range: 2.63 to 15.39 mSv) with a mean difference of 1.88 ± 0.69 mSv (mean ± SD) (range: 0.71 to 5.53 mSv). There was an overall increase non-significant increase (P = .08) in mean mAs delivered by about 8.83 ± 5.48% (mean ± SD) (range: 3.28% to 53.46%) in the low-dose group (141.9 ± 55.95 mAs; mean ± SD) (range: 63 to 310 mAs) compared with the standard-dose group (129.4 ± 47.15 mAs; mean ± SD) (range: 61 to 244 mAs). We reduced the tube potential by about 15.4% and achieved a mean reduction in radiation dose by 31.21 ± 3.15% (mean ± SD) (range: 22.45% to 41.4%). The dose reduction was similar across all the subgroups studies, irrespective of the BMI status. Use of automated tube current modulation or AEC in our study preserved image quality in low-dose CT study but with non-significant increase in mAs.

We classified patients based on the BMI category. Majority of the patients were in the BMI category of 25 to 30 kg/m^2 (n = 42; 40.4%) and 18 to 25 kg/m^2 (n = 38; 36.5) followed by BMI category 30-35 kg/m^2 (n = 13; 12.5%) and lastly in BMI category 18 to 25 kg/m^2 (n = 11; 10.6%). There was a statistically non-significant increase in the tube current with low-dose protocol in the BMI categories <18 and 18-25 kg/m^2 groups (P = .59 and P = .26 respectively), whereas the difference in tube current in BMI categories 25-30 and 30-35 kg/m^2 groups assumed statistical significance (P = .03 and P = .008 respectively). With increasing BMI, the mean increase in mAs became statistically significant with low-dose CT compared

with standard dose-CT. However, the overall reduction in radiation dose is similar irrespective of BMI category.

We conclude that use of low tube potential setting by tube voltage reduction of 15% significantly reduced radiation dose by approximately 31% in patients undergoing CT for evaluation of urolithiasis, irrespective of their BMI. A combination of reduced tube potential and AEC helps to achieve optimum results for diagnosis of urolithiasis. We strongly support the use of low-dose CT for diagnosis and follow-up of urolithiasis in patients who are not morbidly obese.

BIBLIOGRAPHY

1 Kidney stones in Adults [Internet]. [cited 2016 Oct 05]. Available from: https://www.niddk.nih.gov/health-information/health-topics/urologic-disease/kidney-stones-in-adults/Pages/facts.aspx.

2 Turney BW, Reynard JM, Noble JG, Keoghane SR. Trends in urological stone disease. BJU Int 2012;109:1082-7.

3 Fulgham PF, Assimos DG, Pearle MS, Preminger GM. American Urology Association Guideline. Clinical effectiveness protocols for imaging in the management of ureteral calculous disease: AUA technology assessment. 2012.

4 Niemann T, Kollmann T, Bongartz G. Diagnostic performance of low-dose CT for the detection of urolithiasis: A meta-analysis. AJR Am J Roentgenol 2008; 191:396–401.

5 Sheafor DH, Hertzberg BS, Freed KS, Carroll BA, Keogan MT, Paulson EK, et al. Nonenhanced helical CT and US in the emergency evaluation of patients with renal colic: prospective comparison. Radiology 2000;217:792-7.

6 Brink JA. Radiation dose reduction in renal colic protocol CT: Are we doing enough to ensure adoption of best practices? Radiology 2014;271:323–5.

7 Semelka RC, Armao DM, Elias J Jr, Huda W. Imaging strategies to reduce the risk of radiation in CT studies, including selective substitution with MRI. J Magn Reson Imaging 2007;25:900-9.

8 Frush DP, Donnelly LF, Rosen NS. Computed tomography and radiation risks: what pediatric health care providers should know. Pediatrics 2003;112:951-7.

9 Kim BS, Hwang IK, Choi YW, Namkung S, Kim HC, Hwang WC, et al. Low-dose and standard-dose unenhanced helical computed tomography for the assessment of acute renal colic: prospective comparative study. Acta Radiol 2005;46:756-63.

10 Licheng J, Yidong F, Ping W, Keqiang Y, Xueting W, Yingchen Z, et al. Unenhanced low-dose versus standard-dose CT localization in patients with upper urinary calculi for minimally invasive percutaneous nephrolithotomy (MPCNL). Indian J Med Res Mar 2014;139:386-2.

11 Paulson EK, Weaver C, Ho LM, Martin L, Li J, Darsie J, et al. Conventional and reduced radiation dose of 16-MDCT for detection of nephrolithiasis and ureterolithiasis. AJR Am J Roentgenol 2008; 190:151–7.

12 Abou El-Ghar ME, Shokeir AA, Refaie HF, El-Nahas AR. Low-dose unenhanced computed tomography for diagnosing stone disease in obese patients. Arab J Urol 2012;10:279-83.

13 Zilberman DE, Tsivian M, Lipkin ME, Ferrandino MN, Frush DP, Paulson EK, et al. Low dose computerized tomography for detection of urolithiasis - Its effectiveness in the setting of the urology clinic. J Urol 2011;185:910-4.

14 Heneghan JP, McGuire KA, Leder RA, DeLong DM, Yoshizumi T, Nelson RC. Helical CT for nephrolithiasis and ureterolithiasis: comparison of conventional and reduced radiation-dose techniques. Radiology 2003;229:575-80.

15 Mulkens TH, Daineffe S, De Wijngaert R, Bellinck P, Leonard A, Smet G, et al. Urinary stone disease: comparison of standard-dose and low-dose with 4D MDCT tube current modulation. AJR Am J Roentgenol 2007;188:553-62.

16 Poletti PA, Platon A, Rutschmann OT, Schmidlin FR, Iselin CE, Becker CD. Low-dose versus standard-dose CT protocol in patients with clinically suspected renal colic. AJR Am J Roentgenol 2007;188:927-33.

17 Ciaschini MW, Remer EM, Baker ME, Lieber M, Herts BR. Urinary calculi: radiation dose reduction of 50% and 75% at CT-effect on sensitivity. Radiology 2009;251:105-11.

18 Kidney and ureter. Urogenital system. In: Standring S editor. Gray's Anatomy: The anatomical basis of clinical practice. 40th edition.Chapter 74. Spain: Churchill Livingstone Elsevier.2008. p 1225-44.

19 Tublin M, Thurston W, Wilson SR. The kidney and urinary tract. In: Rumack CM, Wilson SR, Charbonneau JW, Levine D, editors. Diagnostic ultrasound. 4th edition. Chapter 9. Philadelphia: Elsevier Mosby. 2011. p 317-91.

20 Olivetti L, Marchetti G. Urinary system: Normal anatomy and microscopic anatomy. In: Olivetti L, Grazioli L eds. Imaging of urogenital diseases. A color atlas. Chaper 1. Italy: Springer-Verlag Italia. 2009. p 3-10.

21 Allan PL. Kidneys: Anatomy and technique. In: Allan PL, Baxter GM, Weston MJ, editors. Clinical ultrasound. 3rd edition. Churchill Livingstone Elsevier. 2011. p411-27.

22 Bladder, prostate and urethra.In: Standring S editor. Gray's Anatomy: The anatomical basis of clinical practice. 40th edition. Chapter 75. Spain: Churchill Livingstone Elsevier.2008. p 1244-59.

23 Türk C, Knoll T, Petrik A, Sarica K, Skolarikos A, Straub M, et al. Guidelines on urolithiasis [Internet]. 2015 Mar [cited 2016 Jul 21]. Available from: http://uroweb.org/wp-content/uploads/22-Urolithiasis_LR_full.pdf.

24 Kidney Stones. American Urological Association [Internet]. [cited 2016 Jul 21]. Available from: https://www.auanet.org/education/kidney-stones.cfm.

25 Evan A, Lingeman J, Coe FL, Worcester E. Randall's plaque: pathogenesis and role in calcium oxalate nephrolithiasis. Kidney Int 2006;69:1313-8.

26 Smith RC, Coll DM. Helical computed tomography in the diagnosis of ureteric colic. BJU Int 2000;86:33-41.

27 Kambadakone AR, Eisner BH, Catalano OA, Sahani DV. New and evolving concepts in the imaging and management of urolithiasis: urologists' perspective. Radiographics 2010;30:603-23.

28 Gücük A, Üyetürk U. Usefulness of Hounsfield unit and density in the assessment and treatment of urinary stones. World J Nephrol 2014;3:282-6.

29 Shahnani PS, Karami M, Astane B, Janghorbani M. The comparative survey of Hounsfield units of stone composition in urolithiasis patients. J Res Med Sci 2014;19:650-3.

30 García Marchiñena P, Billordo Peres N, Liyo J, Ocantos J, Gonzalez M, Jurado A, et al. CT SCAN as a predictor of composition and fragility of urinary lithiasis treated with extracorporeal shock wave lithotripsy in vitro. Arch Esp Urol 2009;62:215-22.

31 Gupta NP, Ansari MS, Kesarvani P, Kapoor A, Mukhopadhyay S. Role of computed tomography with no contrast medium enhancement in predicting the outcome of extracorporeal shock wave lithotripsy for urinary calculi. BJU Int 2005;95:1285-8.

32 Wah TM. Pelvi-ureteric dilatation.In: Allan PL, Baxter GM, Weston MJ, editors. Clinical ultrasound. 3rd edition. Churchill Livingstone Elsevier. 2011. p 428-44.

33 Masarani M, Dinneen M. Ureteric colic: New trends in diagnosis and treatment. Postgrad Med J 2007;83:469–72.

34 Hobbs DL, Lampignano JP, Martensen KM, Anthony BT. Abdomen. In: Bontrager KL, Lampignano JP, editors. Textbook of radiographic positioning and related anatomy.8th edition. Missouri. Elsevier Mosby. p 102-24.

35 Sameh WM. Value of intravenous urography before shockwave lithotripsy in the treatment of renal calculi: a randomized study. J Endourol. 2007;21:574-7.

36 Sreeram E. Computed tomography: Physical principles, Clinical applications and Quality control. 2nd ed. Philadelphia PA. W B Saunders 2001.p1-28.

37 Goldman LW. Principles of CT and CT technology*. J Nucl Med Technol 2007; 35:115–28.

38 McNitt-Gray MF. AAPM/RSNA Physical tutorial for residents: Topics in CT: Radiation dose in CT. Radiographics 2002; 22:1541–53.

39 Kalra MK, Maher MM, Toth TL, Hamberg LM, Blake MA, Shepard JA, et al. Strategies for CT radiation dose optimization. Radiology 2004;230:619-28.

40 Linet MS, Slovis TL, Miller DL, Kleinerman R, Lee C, Rajaraman P, et al. Cancer risks associated with external radiation from diagnostic imaging procedures. CA Cancer J Clin 2012;62:75-100.

41 McCollough CH, Primak AN, Braun N, Kofler J, Yu L, Christner J. Strategies for reducing radiation dose in CT. Radiol Clin North Am 2009;47:27-40.

42 Rehani MM, Bongartz G, Kalender W, et al. Managing x-ray dose in computed tomography: ICRP Special Task Force report. Ann ICRP 2000; 30:7–45.

43 Raman SP, Johnson PT, Deshmukh S, Mahesh M, Grant KL, Fishman EK. CT dose reduction applications: available tools on the latest generation of CT scanners. J Am Coll Radiol 2013;10:37-41

44 Mahesh M, Scatarige JC, Cooper J, Fishman EK. Dose and pitch relationship for a particular multislice CT scanner. AJR Am J Roentgenol 2001; 177:1273–5.

45 Toth TL. Dose reduction opportunities for CT scanners. Pediatr Radiol 2002;32:261–267.

46 Hu H, Fox SH. The effect of helical pitch and beam collimation on the lesion contrast and slice profile in helical CT imaging. Med Phys 1996; 23:1943–54.

47 Grover SB, Kumar J, Gupta A, Khanna L. Protection against radiation hazards: Regulatory bodies, safety norms, does limits and protection devices. Indian J Radiol Imag 2002;12:157-67.

48 Guide to low dose. Siemens [Internet]. 2010 Nov [cited 2016 Aug 15]. Available from: http://www.siemens.com/press/pool/de/events/healthcare/2010-11-rsna/guide-low-dose-e.pdf.

49 Patient safety: radiation dose in X-ray and CT exams [Internet]. 2014 [updated 2014 Aug 10; cited 2014 Oct 02]. Available from: http://www.radiologyinfo.org/en/safety/?pg=sfty_xray

50 AAPM Response in Regards to CT Radiation Dose and its Effects [Internet]. 2009 Dec 17 [cited 2014 Oct 02]. Available from: http://www.aapm.org/publicgeneral/CTDoseResponse.asp.

51 Computed tomography (CT) scans and cancer [Internet]. [updated 2013 Jul 16; cited 2014 Oct 04]. Available from: http://www.cancer.gov/cancertopics/factsheet/detection/CT.

52 AAPM position statement on radiation risks from medical imaging procedures [Internet]. 2011 Dec 13 [cited 2016 May 15]. Available from: https://www.aapm.org/org/policies/details.asp?id=318&type=PP&current=true.

53 Lund VJ, Lloyd DS, Lloyd G. Imaging for endoscopic sinus surgery in adults. J Laryngol Otol 2000;114:395-7.

54 Som PM. CT of the paranasal sinuses. Neuroradiology 1985;27:189-201.

55 Zammit-Maempel I, Chadwick CL, Willis SP. Radiation dose to the lens of eye and thyroid gland in paranasal sinus Multislice CT. Br J Radiol 2003;76:418-20.

56 Sohaib SA, Peppercorn PD, Horrocks JD, Keene MH, Kenyon GS, Reznek RH. The effect of decreasing mAs on image quality and patient dose in sinus CT. Br J Radiol 2001;74:157-61.

57 Tack D, Widelec J, Maertelaer V, Bailly JM, Delcour C, Gevenois PA. Comparison between low-dose and standard-dose multidetector CT in patients with suspected chronic sinusitis. AJR Am J Roentgenol 2003;181-939-44.

58 Lam S, Bux S, Kumar G, Ng KH, Hussain A. A comparison between low-dose and standard-dose non-contrasted multidetector CT scanning of the paranasal sinuses. Biomed Imaging Interv J 2009;5:e13.

59 Hagtvedt T, Aaløkken TM, Nøtthellen J, Kolbenstvedt A. A new low-dose CT examination compared with standard-dose CT in the diagnosis of acute sinusitis. Eur Radiol 2003;13:976 80.

60 Peck J, Peck A, Peck C, Peck J. The clinical role of noncontrast helical computed tomography in the diagnosis of acute appendicitis. Am J Surg. 2000;180:133-6.

61 Ahn S; LOCAT group. LOCAT (low-dose computed tomography for appendicitis trial) comparing clinical outcomes following low- vs standard-dose computed tomography as the first-line imaging test in adolescents and young adults with suspected acute appendicitis: study protocol for a randomized controlled trial. Trials 2014;15:28.

62 Kim SY, Lee KH, Kim K, Kim TY, Lee HS, Hwang SS, et al. Acute appendicitis in young adults: low- versus standard-radiation-dose contrast-enhanced abdominal CT for diagnosis. Radiology 2011;260:437-45.

63 Kim K, Kim YH, Kim SY, Kim S, Lee YJ, Kim KP, et al. Low-dose abdominal CT for evaluating suspected appendicitis. N Engl J Med 2012;366:1596-605.

64 Karmazyn B, Frush DP, Applegate KE, Maxfield C, Cohen MD, Jones RP. CT with a computer-simulated dose reduction technique for detection of pediatric nephroureterolithiasis: comparison of standard and reduced radiation doses. AJR Am J Roentgenol 2009;192:143-9.

65 Tack D, Sourtzis S, Delpierre I, de Maertelaer V, Gevenois PA. Low-dose unenhanced multidetector CT of patients with suspected renal colic. AJR Am J Roentgenol 2003;180:305-11.

66 Jin DH, Lamberton GR, Broome DR, Saaty HP, Bhattacharya S, Lindler TU, et al. Effect of reduced radiation CT protocols on the detection of renal calculi. Radiology 2010;255:100-7.

67 Ferrandino MN1, Bagrodia A, Pierre SA, Scales CD Jr, Rampersaud E, Pearle MS, et al. Radiation exposure in the acute and short-term management of urolithiasis at 2 academic centers. J Urol 2009;181:668-72.

68 Manohar P, McCahy P. Repeated radiological radiation exposure in patients undergoing surgery for urinary tract stone disease in Victoria, Australia. BJU Int 2011;108:34-7.

69 Hur J, Park SB, Lee JB, Park HJ, Chang IH, Kwon JK, et al. CT for evaluation of urolithiasis: image quality of ultralow-dose (Sub mSv) CT with knowledge-based iterative reconstruction and diagnostic performance of low-dose CT with statistical iterative reconstruction. Abdom Imaging 2015;40:2432-40.

70 Lira D, Padole A, Kalra MK, Singh S. Tube potential and CT radiation dose optimization. AJR Am J Roentgenol 2015;204:W4-10.

71 Winklehner A, Goetti R, Baumueller S, Karlo C, Schmidt B, Raupach R, et al. Automated attenuation-based tube potential selection for thoracoabdominal

computed tomography angiography: improved dose effectiveness. Invest Radiol 2011;46:767-73.

72 Yu L, Fletcher JG, Grant KL, Carter RE, Hough DM, Barlow JM, et al. Automatic selection of tube potential for radiation dose reduction in vascular and contrast-enhanced abdominopelvic CT. AJR Am J Roentgenol 2013;201:W297-306.

73 Eller A, May MS, Scharf M, Schmid A, Kuefner M, Uder M, et al. Attenuation-based automatic kilovolt selection in abdominal computed tomography: effects on radiation exposure and image quality. Invest Radiol 2012;47:559-65.

74 Funama Y, Awai K, Nakayama Y, Kakei K, Nagasue N, Shimamura M, et al. Radiation dose reduction without degradation of low-contrast detectability at abdominal multisection CT with a low-tube voltage technique: phantom study. Radiology 2005;237:905-10.

75 Tang K, Wang L, Li R, Lin J, Zheng X, Cao G. Effect of low tube voltage on image quality, radiation dose, and low-contrast detectability at abdominal multidetector CT: Phantom study. J Biomed Biotechnol 2012; 2012: 130169.

76 Nakayama Y, Awai K, Funama Y, Hatemura M, Imuta M, Nakaura T, Ryu D, et al. Abdominal CT with low tube voltage: preliminary observations about radiation dose, contrast enhancement, image quality, and noise. Radiology 2005;237:945-51.

77 Lee CH, Goo JM, Ye HJ, Ye SJ, Park CM, Chun EJ, et al. Radiation dose modulation techniques in the multidetector CT era: from basics to practice. Radiographics 2008;28:1451-9.

78 Huda W, Mettler FA. Volume CT dose index and dose-length product displayed during CT: what good are they? Radiology 2011;258:236-42.

79 Kalra MK, Prasad S, Saini S, Blake MA, Varghese J, Halpern EF, et al. Clinical comparison of standard-dose and 50% reduced-dose abdominal CT: effect on image quality. AJR Am J Roentgenol 2002;179:1101-6.

80 Huda W, Atherton JV, Ware DE, Cumming WA. An approach for the estimation of effective radiation dose at CT in pediatric patients. Radiology 1997;203:417-22.

ANNEXURE I

Comparison between low-dose and high-dose computed tomography for diagnosis of urolithiasis

Proforma

Patient ID:

CT No:

Demographic details:

Name:

Age:

Sex: ☐**Male** ☐**Female**

BMI: ☐**<18 kgm^{-2}** ☐**18 to 25 kgm^{-2}** ☐**25-30 kgm^{-2}** ☐**30 to 35 kgm^{-2}**

Study details:

Effective Radiation Dose parameters

Standard Dose CT protocol:

Low Dose CT protocol:

Urolithiasis status:

Location of Calculi		**Standard Dose CT**		**Low Dose CT**	
		Presence and no of calculi	**Size (in mm)**	**Presence and no of calculi**	**Size (in mm)**
Right Kidney	**Upper pole**	☐		☐	
	Mid pole	☐		☐	
	Lower pole	☐		☐	
Left Kidney	**Upper pole**	☐		☐	
	Mid pole	☐		☐	
	Lower pole	☐		☐	
Right Ureter	**Upper ureter**	☐		☐	
	Mid ureter	☐		☐	
	Lower ureter	☐		☐	
Left Ureter	**Upper ureter**	☐		☐	
	Mid ureter	☐		☐	
	Lower ureter	☐		☐	
Bladder	**Vesical**	☐		☐	
	Right VUJ	☐		☐	
	Left VUJ	☐		☐	
VUJ = vesicoureteric junction					

Concomitant Findings (if any):

Radiologist 1: ☐ **Radiologist 2:** ☐

ANNEXURE II

Study Title: Comparison between low-dose and high-dose computed tomography for diagnosis of urolithiasis

Principal Investigators: Dr. Shivaprasad Gangadhar Savagave/Dr. Purnima Hegde

INFORMED CONSENT FORM

I, Mr/Miss/Mrs_____, have been provided an opportunity to participate in research project titled "Comparison between low-dose and standard-dose computed tomography for diagnosis of urolithiasis". It has been communicated to me in my vernacular language that this study requires use of computed tomography (CT) imaging twice, once with standard-dose technique and once with low-dose technique. The standard-dose technique will be performed as per part of usual clinical care. An additional scan will be performed with low-dose CT if the standard-dose CT shows presence of urolithiasis. Furthermore, I have been explained about the potential risks involved with radiation resulting from additional scans and that it is very negligible/ nonexistent.

The research investigators wish to determine if low-dose CT (low-radiation exposure) is as helpful as standard dose CT (associated with more radiation exposure) for evaluation of kidney stones, ureteral stones, and/or bladder stones. If study results are positive, this study can help to consciously reduce radiation dose with CT for detection of urolithiasis.

I understand that the medical information produced by this study will become part of institutional record at Sri Devaraj Urs Medical College and will be kept confidential.

I understand that my participation is voluntary. I may refuse to participate or withdraw my consent and discontinue participation at any time without citing any reason whatsoever and without any prejudice to my present or future care at this institution.

I agree not to restrict the use of any data or results that arise from this study provided such a use is only for scientific purpose(s). I will not be paid any financial compensation for participating in this research project. I hereby give consent to participate in this research project.

Name and Signature/thumb impression.

Name and signature of third person (in case the participant is illiterate)

Name and Signature of PI

Comparison between low dose and standard dose computed tomography for diagnosis of urolithiasis

Patient Information Sheet

Principal Investigators: Dr. Shivaprasad Gangadhar Savagave/ Dr. Purnima Hegde

I, Dr. Shivaprasad Gangadhar Savagave, am a post-graduate student in Department of Radio-Diagnosis at Sri Devaraj Urs Medical College. I will be conducting a study titled "Comparison between low dose and high dose computed tomography for diagnosis of urolithiasis" for my dissertation under the guidance of Dr. Purnima Hegde, Prof. and Head, Department of Radio-Diagnosis. In this study, we will assess the efficacy of low-dose computed tomography (CT) scan when compared with the standard-dose CT scan. You would have undergone CT scan of abdominal region for detection of kidney/ureteric stones before entering the study. If the CT scan shows presence of kidney/ureteric stones, an additional CT scan will be performed with lower dose concurrently. There will be no additional expenses incurred by you for the additional scan as it is part of routine scan procedure. CT scan is associated with risk of X-ray exposure. Performing two scans will not cause any adverse health impact on you.

If the study results are positive, it will help to reduce x-ray exposure for CT scan for patients with kidney/ureteric stones.

All of your personal data will be kept confidential and will be used only for research purpose by this institution. You are free to participate in the study. You can also withdraw from the study at any point of time without giving any reasons whatsoever. Your refusal to participate will not prejudice you to any present or future care at this institution

Name and Signature of the Principal Investigator

Date

ANNEXURE III

Key to Master Chart

BMI = Body mass index;

CT = Computed tomography;

F = Female;

HN = Hydronephrosis;

HUN = Hydroureteronephrosis;

M = Male;

mAs = milli Ampere second;

mGy = milliGray;

mSv = milli Sievert;

PUJ = Pelviureteric junction;

R1 = Radiologist 1

R2 = Radiologist 2

VUJ = Vesicoureteric junction;

Y = Yes/Present

Masterchart - Comparison between low-dose and standard-dose computed tomography for diagnosis of urolithiasis

Sl. No	Trial ID	Sex	BMI* group (kg/m^2)	CT Dose received (mGy*cm)			Effective Dose (in mSv)			mean mAs Delivered (mAs)		(R1)				(R2)				Location of calculus										HUN status			
												No of calculi		Size of smallest calculus (in mm)		No of calculi		Size of smallest calculus (in mm)															
				Standard Dose	Low Dose	Total Dose	Effective Dose (Stadnard dose)	Effective Dose (Low dose)	Total Dose	Standard dose	Low dose	High Dose	Low Dose	High dose	Low dose	High Dose	Low Dose	High dose	Low dose	Right renal	Right PUJ	Right ureteric	Right VUJ	Left renal	Left PUJ	Left ureteric	Left VUJ	Vesical	R HUN	L HUN	R HN	L HN
1	98882	M	25-30	467.56	320.09	791.89	7.01	4.80	11.88	154	164	2	2	3	3	2	2	3	3	Y		Y							Y				
2	15409	M	18-25	375.18	255.95	631.13	5.63	3.84	9.47	147	156	1	1	9	9	1	1	9	9							Y				Y			
3	20038	M	25-30	429.05	297.45	726.5	6.44	4.46	10.90	153	165	1	1	4	4	1	1	4	4			Y							Y				
4	34565	M	25-30	482.54	336.06	822.84	7.24	5.04	12.34	156	169	3	3	4	4	3	3	4	4	Y				Y									
5	14210	M	30-35	576.91	402.12	979.03	8.65	6.03	14.69	178	193	5	5	4	4	5	5	4	4					Y	Y								Y
6	22893	M	≤18	246.5	167.10	413.35	3.70	2.51	6.20	108	114	2	2	10	10	2	2	10	10				Y					Y	Y				
7	50368	M	25-30	501.83	350.10	856.17	7.53	5.25	12.84	176	191	3	3	3	3	3	3	3	3	Y						Y		Y		Y			
8	74093	F	25-30	398.5	271.71	670.21	5.98	4.08	10.05	165	175	1	1	2	2	1	1	2	2					Y									
9	13773	M	30-35	597.31	440.02	1053.2	8.96	6.60	15.80	213	251	11	11	2	2	11	11	2	2	Y		Y		Y					Y				
10	11756	M	25-30	470.59	316.10	786.69	7.06	4.74	11.80	156	163	5	5	2	2	5	5	2	2	Y		Y		Y		Y			Y	Y			
11	41864	M	25-30	495.76	351.11	846.87	7.44	5.27	12.70	177	195	3	3	5	5	3	3	5	5	Y													
12	26963	M	25-30	405.3	275.44	684.98	6.08	4.13	10.27	140	148	10	10	2	2	10	10	2	2	Y				Y	Y								Y
13	8552	F	25-30	459.00	293.00	757.00	6.89	4.40	11.36	164	175	2	2	4	4	2	2	4	4		Y			Y								Y	
14	43450	M	25-30	455.80	330.00	798.00	6.84	4.95	11.97	174	196	3	3	2	2	3	3	2	2					Y			Y			Y			
15	57222	M	25-30	540.00	390.00	931.00	8.10	5.85	13.97	172	187	7	7	2	2	7	7	2	2	Y		Y		Y					Y				
16	2231	M	18-25	338.78	236.20	587.00	5.08	3.54	8.81	130	141	9	9	2	2	9	9	2	2	Y				Y									
17	13896	M	18-25	294.00	187.39	509.00	4.41	2.81	7.64	142	159	19	19	2	2	19	19	2	2	Y				Y			Y			Y			
18	84923	M	25-30	499.70	349.50	853.00	7.50	5.24	12.80	193	210	11	11	2	2	11	11	2	2	Y				Y		Y				Y			
19	62983	M	30-35	504.47	346.67	855.00	7.57	5.20	12.83	203	217	14	14	2	2	14	14	2	2	Y				Y									
20	11460	M	25-30	418.98	296.67	715.65	6.28	4.45	10.73	138	152	5	5	2	2	5	5	2	2	Y				Y									
21	17956	M	25-30	427.15	291.05	736.60	6.41	4.37	11.05	158	176	2	2	2	2	2	2	2	2			Y		Y					Y				
22	45770	F	30-35	558.07	386.36	944.40	8.37	5.80	14.17	182	196	1	1	9	9	1	1	9	9						Y								Y
23	70597	M	25-30	444.20	297.71	741.91	6.66	4.47	11.13	141	147	7	7	2	2	7	7	2	2	Y	Y												
24	84235	M	25-30	486.66	337.88	828.78	7.30	5.07	12.43	150	162	1	1	2	2	1	1	2	2	Y													

BMI = body mass index; CT = Computed tomography; F = Female; HN = hydronephrosis; HUN = hydroureteronephrosis; M = male; mAs = milli Ampere second; mGy = milliGray; mSv = milli Sievert; PUJ = pelviureteric junction; R1 = Radiologist 1; R2 = Radiologist 2; VUJ = vesicoureteric junction; Y = Yes/Present

*BMI groups based on the BMI calculated in terms of weight (in kg)/(height (in m))^2 and measured as kg/m^2

Masterchart - Comparison between low-dose and standard-dose computed tomography for diagnosis of urolithiasis

Sl. No	Trial ID	Sex	BMI* group (kg/m^2)	CT Dose received (mGy*cm)			Effective Dose (in mSv)			mean mAs Delivered (mAs)		(R1)				(R2)				Location of calculus										HUN status			
												No of calculi		Size of smallest calculus (in mm)		No of calculi		Size of smallest calculus (in mm)															
				Standard Dose	Low Dose	Total Dose	Effective Dose (Stadnard dose)	Effective Dose (Low dose)	Total Dose	Standard dose	Low dose	High Dose	Low Dose	High dose	Low dose	High Dose	Low Dose	High dose	Low dose	Right renal	Right PUJ	Right ureteric	Right VUJ	Left renal	Left PUJ	Left ureteric	Left VUJ	Vesical	R HUN	L HUN	R HN	L HN
25	11230	F	30-35	1026.0	657.28	1688.7	15.39	9.86	25.33	202	310	4	4	2	2	4	4	2	2	Y		Y		Y					Y				
26	96809	M	18-25	355.43	213.57	590.00	5.33	3.20	8.85	140	149	5	5	2	2	5	5	2	2	Y				Y									
27	89182	M	25-30	495.07	305.51	824.00	7.43	4.58	12.36	195	206	1	1	7	7	1	1	7	7					Y									
28	10073	F	18-25	380.86	278.15	663.25	5.71	4.17	9.95	120	126	3	3	4	4	3	3	4	4			Y		Y			Y		Y	Y			
29	19228	M	30-35	682.71	400.06	1087.0	10.24	6.00	16.31	231	286	2	2	4	4	2	2	4	4	Y				Y									
30	57966	F	18-25	270.93	180.98	456.15	4.06	2.71	6.84	119	128	3	3	4	4	3	3	4	4	Y	Y				Y							Y	Y
31	71870	M	30-35	608.00	381.51	980.20	9.12	5.72	14.70	178	218	4	4	2	2	4	4	2	2	Y		Y		Y					Y				
32	58109	M	18-25	370.96	255.51	630.71	5.56	3.83	9.46	140	150	3	3	2	2	3	3	2	2	Y						Y				Y			
33	80479	F	18-25	318.18	220.50	542.92	4.77	3.31	8.14	141	152	2	2	4	4	2	2	4	4	Y				Y									
34	35657	F	≤18	265.02	183.31	476.83	3.98	2.75	7.15	79	85	3	3	2	2	3	3	2	2	Y				Y			Y			Y			
35	55403	M	25-30	423.05	298.34	725.63	6.35	4.48	10.88	134	147	2	2	2	2	2	2	2	2	Y													
36	3211	M	≤18	261.92	191.05	472.35	3.93	2.87	7.09	120	125	1	1	7	7	1	1	7	7							Y				Y			
37	1458	M	25-30	568.72	414.63	987.59	8.53	6.22	14.81	179	203	11	11	2	2	11	11	2	2	Y				Y									
38	91349	M	25-30	523.47	382.52	926.34	7.85	5.74	13.90	139	158	1	1	11	11	1	1	11	11								Y			Y			
39	55594	M	≤18	231.77	157.27	409.39	3.48	2.36	6.14	72	76	7	7	2	2	7	7	2	2	Y		Y				Y			Y	Y			
40	17058	M	≤18	247.62	165.69	453.54	3.71	2.49	6.80	84	90	2	2	8	8	2	2	8	8								Y	Y		Y			
41	89871	M	25-30	465.11	334.73	804.08	6.98	5.02	12.06	159	178	1	1	6	6	1	1	6	6							Y				Y			
42	24958	M	18-25	297.50	181.75	513.90	4.46	2.73	7.71	84	91	1	1	12	12	1	1	12	12							Y				Y			
43	72376	M	18-25	348.30	217.05	585.70	5.22	3.26	8.79	88	93	1	1	16	16	1	1	16	16		Y										Y		
44	94294	M	18-25	254.00	175.85	463.92	3.81	2.64	6.96	78	84	5	5	2	2	5	5	2	2	Y				Y		Y				Y			
45	10382	M	≤18	211.79	164.24	384.44	3.18	2.46	5.77	69	73	1	1	4	4	1	1	4	4			Y							Y				
46	29020	M	25-30	511.58	360.11	875.93	7.67	5.40	13.14	179	196	6	6	2	2	6	6	2	2	Y		Y		Y					Y				
47	99348	F	25-30	479.41	337.03	836.79	7.19	5.06	12.55	120	132	1	1	7	7	1	1	7	7			Y							Y				
48	88883	M	18-25	368.07	259.27	647.69	5.52	3.89	9.72	94	103	12	12	2	2	12	12	2	2	Y				Y		Y				Y			

BMI = body mass index; CT = Computed tomography; F = Female; HN = hydronephrosis; HUN = hydroureteronephrosis; M = male; mAs = milli Ampere second; mGy = milliGray; mSv = milli Sievert; PUJ = pelviureteric junction; R1 = Radiologist 1; R2 = Radiologist 2; VUJ = vesicoureteric junction; Y = Yes/Present

*BMI groups based on the BMI calculated in terms of weight (in kg)/(height (in m))^2 and measured as kg/m^2

Masterchart - Comparison between low-dose and standard-dose computed tomography for diagnosis of urolithiasis

Sl. No	Trial ID	Sex	BMI* group (kg/m^2)	CT Dose received (mGy*cm)			Effective Dose (in mSv)			mean mAs Delivered (mAs)		(R1)				(R2)				Location of calculus										HUN status			
												No of calculi		Size of smallest calculus (in mm)		No of calculi		Size of smallest calculus (in mm)															
				Standard Dose	Low Dose	Total Dose	Effective Dose (Stadnard dose)	Effective Dose (Low dose)	Total Dose	Standard dose	Low dose	High Dose	Low Dose	High dose	Low dose	High Dose	Low Dose	High dose	Low dose	Right renal	Right PUJ	Right ureteric	Right VUJ	Left renal	Left PUJ	Left ureteric	Left VUJ	Vesical	R HUN	L HUN	R HN	L HN
49	10968	M	18-25	360.67	249.31	649.08	5.41	3.74	9.74	95	100	2	2	4	4	2	2	4	4					Y		Y				Y			
50	53241	M	30-35	650.98	467.61	1122.8	9.76	7.01	16.84	213	238	9	9	4	4	9	9	4	4	Y				Y									
51	61717	M	18-25	246.28	163.32	436.51	3.69	2.45	6.55	70	75	16	16	2	2	16	16	2	2	Y		Y		Y		Y			Y	Y		
52	87161	F	18-25	292.26	207.66	520.27	4.38	3.11	7.80	76	84	4	4	2	2	4	4	2	2				Y	Y					Y			
53	14307	M	25-30	449.64	315.82	785.81	6.74	4.74	11.79	108	118	1	1	6	6	1	1	6	6							Y				Y		
54	79100	M	18-25	345.54	242.56	608.45	5.18	3.64	9.13	87	95	2	2	7	7	2	2	7	7							Y		Y		Y		
55	18819	M	18-25	286.57	191.70	511.83	4.30	2.88	7.68	88	94	1	1	12	12	1	1	12	12		Y										Y	
56	84780	F	18-25	314.83	217.39	536.46	4.72	3.26	8.05	108	116	1	1	8	8	1	1	8	8	Y												
57	27402	M	18-25	283.48	180.39	491.57	4.25	2.71	7.37	79	84	1	1	10	10	1	1	10	10			Y							Y			
58	75957	M	25-30	446.25	308.45	758.94	6.69	4.63	11.38	133	143	2	2	9	9	2	2	9	9	Y						Y				Y		
59	53174	F	18-25	349.61	248.66	618.62	5.24	3.73	9.28	94	104	7	7	2	2	7	7	2	2	Y		Y		Y					Y			
60	52587	M	25-30	409.29	297.43	710.64	6.14	4.46	10.66	161	180	1	1	5	5	1	1	5	5			Y							Y			
61	54990	M	25-30	408.93	273.55	686.72	6.13	4.10	10.30	146	161	1	1	10	10	1	1	10	10							Y				Y		
62	52674	F	18-25	240.03	181.84	448.58	3.60	2.73	6.73	76	86	1	1	11	11	1	1	11	11					Y								
63	95462	M	30-35	662.03	484.29	1150.6	9.93	7.26	17.26	203	231	3	3	6	6	3	3	6	6							Y				Y		
64	27528	M	25-30	444.87	310.94	760.05	6.67	4.66	11.40	149	162	4	4	3	3	4	4	3	3	Y				Y								
65	81067	M	30-35	767.86	550.27	1322.4	11.52	8.25	19.84	244	272	5	5	2	2	5	5	2	2	Y		Y							Y			
66	20811	F	18-25	330.78	226.70	561.72	4.96	3.40	8.43	121	129	4	4	3	3	4	4	3	3	Y												
67	46450	M	18-25	234.47	152.46	419.40	3.52	2.29	6.29	67	72	10	10	2	2	10	10	2	2	Y				Y				Y				
68	7816	M	25-30	411.09	286.71	718.15	6.17	4.30	10.77	106	115	1	1	5	5	1	1	5	5								Y			Y		
69	44651	M	18-25	244.48	147.58	418.67	3.67	2.21	6.28	71	74	1	1	8	8	1	1	8	8	Y												
70	57425	M	25-30	371.65	256.16	637.92	5.57	3.84	9.57	97	104	1	1	7	7	1	1	7	7			Y							Y			
71	56051	M	≤18	221.41	152.12	393.88	3.32	2.28	5.91	66	69	14	14	2	2	14	14	2	2	Y				Y								
72	94309	M	18-25	271.49	186.65	485.15	4.07	2.80	7.28	72	77	3	3	5	5	3	3	5	5	Y			Y						Y			

BMI = body mass index; CT = Computed tomography; F = Female; HN = hydronephrosis; HUN = hydroureteronephrosis; M = male; mAs = milli Ampere second; mGy = milliGray; mSv = milli Sievert; PUJ = pelviureteric junction; R1 = Radiologist 1; R2 = Radiologist 2; VUJ = vesicoureteric junction; Y = Yes/Present

*BMI groups based on the BMI calculated in terms of weight (in kg)/(height (in m))^2 and measured as kg/m^2

Masterchart - Comparison between low-dose and standard-dose computed tomography for diagnosis of urolithiasis

Sl. No	Trial ID	Sex	BMI* group (kg/m^2)	CT Dose received (mGy*cm)			Effective Dose (in mSv)			mean mAs Delivered (mAs)		(R1)				(R2)				Location of calculus										HUN status			
												No of calculi		Size of smallest calculus (in mm)		No of calculi		Size of smallest calculus (in mm)															
				Standard Dose	Low Dose	Total Dose	Effective Dose (Stadnard dose)	Effective Dose (Low dose)	Total Dose	Standard dose	Low dose	High Dose	Low Dose	High dose	Low dose	High Dose	Low Dose	High dose	Low dose	Right renal	Right PUJ	Right ureteric	Right VUJ	Left renal	Left PUJ	Left ureteric	Left VUJ	Vesical	R HUN	L HUN	R HN	L HN
73	39492	M	18-25	263.07	178.65	462.07	3.95	2.68	6.93	71	75	2	2	9	9	2	2	9	9					Y		Y				Y			
74	70323	M	25-30	412.46	290.89	723.70	6.19	4.36	10.86	103	113	2	2	1.5	1.5	2	2	1.5	1.5	Y							Y			Y			
75	73388	M	25-30	527.97	375.77	924.09	7.92	5.64	13.86	135	147	5	5	2	2	5	5	2	2	Y		Y							Y				
76	52380	F	≤18	175.26	122.99	329.33	2.63	1.84	4.94	61	63	2	2	25	25	2	2	25	25	Y	Y										Y		
77	89532	M	25-30	417.47	290.95	728.77	6.26	4.36	10.93	107	116	3	3	9	9	3	3	9	9			Y				Y			Y	Y			
78	734	F	18-25	270.24	184.58	481.03	4.05	2.77	7.22	80	85	1	1	16	16	1	1	16	16					Y									
79	87398	M	18-25	250.98	175.85	462.38	3.76	2.64	6.94	79	84	1	1	8	8	1	1	8	8							Y				Y			
80	52157	M	30-35	697.36	494.23	1195.8	10.46	7.41	17.94	244	269	1	1	2.5	2.5	1	1	2.5	2.5								Y			Y			
81	73679	M	25-30	432.58	296.03	732.85	6.49	4.44	10.99	155	165	11	11	2	2	11	11	2	2	Y				Y		Y				Y			
82	47861	M	18-25	268.95	181.77	477.73	4.03	2.73	7.17	78	82	5	5	2	2	5	5	2	2	Y		Y		Y		Y			Y	Y			
83	23836	F	18-25	272.33	187.14	479.82	4.08	2.81	7.20	87	93	2	2	4	4	2	2	4	4	Y	Y										Y		
84	50604	F	25-30	428.56	302.86	735.66	6.43	4.54	11.03	141	155	2	2	2	2	2	2	2	2	Y		Y							Y				
85	62261	M	25-30	546.17	390.72	941.13	8.19	5.86	14.12	195	217	3	3	2	2	3	3	2	2	Y				Y									
86	73019	M	18-25	252.17	173.69	446.21	3.78	2.61	6.69	70	75	7	7	2	2	7	7	2	2	Y				Y		Y	Y			Y			
87	86119	M	30-35	640.52	455.88	1100.6	9.61	6.84	16.51	196	217	3	3	5	5	3	3	5	5	Y					Y								Y
88	72604	M	≤18	235.67	158.50	414.52	3.54	2.38	6.22	65	68	1	1	12	12	1	1	12	12							Y				Y			
89	8122	M	≤18	227.99	160.75	406.41	3.42	2.41	6.10	62	68	15	15	2	2	15	15	2	2	Y		Y		Y					Y				
90	9539	F	18-25	245.34	162.03	433.18	3.68	2.43	6.50	69	74	1	1	9	9	1	1	9	9							Y				Y			
91	15853	M	18-25	318.92	219.48	543.80	4.78	3.29	8.16	85	91	1	1	10	10	1	1	10	10							Y				Y			
92	20618	M	18-25	364.61	250.01	634.97	5.47	3.75	9.52	90	96	4	4	2	2	4	4	2	2			Y		Y					Y				
93	13883	M	18-25	236.66	163.49	420.50	3.55	2.45	6.31	67	72	2	2	11	11	2	2	11	11	Y	Y										Y		
94	98899	M	25-30	515.27	360.14	878.35	7.73	5.40	13.18	172	187	2	2	8	8	2	2	8	8	Y		Y							Y				
95	85492	M	18-25	289.92	194.63	488.79	4.35	2.92	7.33	113	118	1	1	12	12	1	1	12	12							Y				Y			
96	44638	M	25-30	439.29	304.99	748.52	6.59	4.57	11.23	150	162	3	3	2	2	3	3	2	2					Y									

BMI = body mass index; CT = Computed tomography; F = Female; HN = hydronephrosis; HUN = hydroureteronephrosis; M = male; mAs = milli Ampere second; mGy = milliGray; mSv = milli Sievert; PUJ = pelviureteric junction; R1 = Radiologist 1; R2 = Radiologist 2; VUJ = vesicoureteric junction; Y = Yes/Present

*BMI groups based on the BMI calculated in terms of weight (in kg)/(height (in m))^2 and measured as kg/m^2

Masterchart - Comparison between low-dose and standard-dose computed tomography for diagnosis of urolithiasis

Sl. No	Trial ID	Sex	BMI* group (kg/m^2)	CT Dose received (mGy*cm)			Effective Dose (in mSv)			mean mAs Delivered (mAs)		(R1)				(R2)				Location of calculus										HUN status			
												No of calculi		Size of smallest calculus (in mm)		No of calculi		Size of smallest calculus (in mm)															
				Standard Dose	Low Dose	Total Dose	Effective Dose (Stadnard dose)	Effective Dose (Low dose)	Total Dose	Standard dose	Low dose	High Dose	Low Dose	High dose	Low dose	High Dose	Low Dose	High dose	Low dose	Right renal	Right PUJ	Right ureteric	Right VUJ	Left renal	Left PUJ	Left ureteric	Left VUJ	Vesical	R HUN	L HUN	R HN	L HN
97	63890	M	25-30	402.59	260.83	676.13	6.04	3.91	10.14	164	179	1	1	23	23	1	1	23	23			Y							Y				
98	89989	M	25-30	482.40	335.5	822.14	7.24	5.03	12.33	171	185	2	2	3	3	2	2	3	3				Y	Y					Y				
99	58559	M	≤18	234.78	168.48	436.03	3.52	2.53	6.54	67	71	6	6	3	3	6	6	3	3	Y		Y		Y		Y			Y	Y			
100	64279	M	25-30	434.58	292.8	741.16	6.52	4.39	11.12	158	175	4	4	4	4	4	4	4	4	Y			Y	Y					Y				
101	10474	M	18-25	362.88	245.11	612.23	5.44	3.68	9.18	138	145	2	2	2	2	2	2	2	2	Y							Y			Y			
102	13109	M	30-35	591.59	421.2	1017.0	8.87	6.32	15.26	186	206	6	6	3	3	6	6	3	3	Y		Y		Y	Y				Y				Y
103	67364	M	18-25	305.49	204.2	514.00	4.58	3.06	7.71	69	72	6	6	3	3	6	6	3	3	Y				Y		Y				Y			
104	93436	M	25-30	429.03	282.24	715.00	6.44	4.23	10.73	87	93	16	16	3	3	16	16	3	3	Y		Y	Y	Y		Y			Y	Y			

BMI = body mass index; CT = Computed tomography; F = Female; HN = hydronephrosis; HUN = hydroureteronephrosis; M = male; mAs = milli Ampere second; mGy = milliGray; mSv = milli Sievert; PUJ = pelviureteric junction; R1 = Radiologist 1; R2 = Radiologist 2; VUJ = vesicoureteric junction; Y = Yes/Present

*BMI groups based on the BMI calculated in terms of weight (in kg)/(height (in m))^2 and measured as kg/m^2